UNIVERSITY OF OKLAHOMA

GRADUATE COLLEGE

INTEGRATED PETROPHYSICAL-SEISMIC SEQUENCE STRATIGRAPHY OF THE MIXED CARBONATE CLASTIC SEDIMENT GRAVITY FLOWS OF THE BONE SPRING FORMATION, NEW MEXICO

A THESIS

SUBMITTED TO THE GRADUATE FACULTY

in partial fulfillment of the requirements for the

Degree of

MASTER OF SCIENCE

By

MATTHEW PEYTON LYNCH
Norman, Oklahoma
2020

Downloaded from SHAREOK. Persistent Handle URL: https://hdl.handle.net/11244/325617

INTEGRATED PETROPHYSICAL-SEISMIC SEQUENCE STRATIGRAPHY OF THE MIXED CARBONATE CLASTIC SEDIMENT GRAVITY FLOWS OF THE BONE SPRING FORMATION, NEW MEXICO

A THESIS APPROVED FOR THE
SCHOOL OF GEOSCIENCES

BY THE COMMITTEE CONSISTING OF

Dr. John D. Pigott, Chair

Dr. Heather Bedle

Dr. Matthew Pranter

© Copyright by MATTHEW PEYTON LYNCH 2020
All Rights Reserved.

This work is dedicated to God and my supportive family

Acknowledgements

First, I want to thank my advisor Dr. John D. Pigott for giving me the opportunity to further my education and study with the incredible group of students that he assembled. His relentless and enthusiastic support has been invaluable through the entirety of this study and I cannot thank him enough for his help.

I would also like to thank my committee members, Dr. Heather Bedle and Dr. Matthew Pranter for offering their guidance and time to help me. I am greatly appreciative for their revisions and assistance.

Thank you to the Oklahoma School of Geoscience for the resources provided to allow me to conduct my study.

This research would not have been possible without Schlumberger for providing the 3D seismic survey and Mewbourne Oil Company for providing well logs, both of which comprise the majority of the study.

Finally, I would like to thank my friends, including Andrew Layden, Andrew Brown, Travis Plemons, Travis Moreland, and Sam Berg that were extremely helpful and have made my time in Oklahoma so much more enjoyable.

Table of Contents

Acknowledgements v

Table of Contents vi

List of Figures viii

Abstract xix

Chapter 1: Introduction 1

Study Location 1

Previous Work 3

Problem Definition and Objectives 7

Chapter 2: Geologic Background 11

Tectonic History 13

Depositional History 17

Late Cambrian - Wolfcampian Deposition 17

Leonardian Bone Spring Formation Deposition 19

Guadalupian - Ochoan Deposition 23

Chapter 3: Stratigraphy Introduction 25

Reciprocal Sedimentation 29

Permian Sequence Stratigraphy 31

Wolfcampian 32

Leonardian 33

Chapter 4: Data Availability 35

Log Data 36

Seismic Data 36
Chapter 5: Methods 39
Well Log Analysis 39
Seismic Analysis 42
Chapter 6: Results 45
Well Log Analysis 45
Depositional Dip and Strike Cross Sections 51
Well Log Sequence Stratigraphy 46
Seismic Analysis 54
Structure Maps 54
Isopach Maps 66
Seismic Sequence Stratigraphy 73
Discussion 91
Chapter 7: Conclusions 98
Conclusions 98
Recommendations for Future Work 100
Coda… 101
References 103

List of Figures

Figure 1: Overview of play trends in the Permian Basin. Highlights the overlapping Bone Spring Formation, Wolfcamp, and Avalon trends in the Delaware Basin. From Drillinginfo.com 1

Figure 2: Generalized map of the Delaware and Midland Basins, with the CBP dividing the two. Dark green ring around the Delaware Basin denotes the location of carbonate reef build up. The study area is approximately located by the red box. Modified from Murchisonoil.com 3

Figure 3: Evolution of the Bone Spring Formation deposition with 3rd order sea level changes, where highstands correspond with carbonate intervals while lowstands correspond with siliciclastic intervals. (Crosby, 2015). 5

Figure 4: Seismic map of the 3rd Bone Spring Formation Carbonate and Sand surfaces showing sediment bypass canyons, depositional centers, and submarine channels. (Frazier, 2019) 7

Figure 5: Cross section showing hypothetical correlation between wells by lithostratic correlation alone. Compare this interpretation with Figure 50. 8

Figure 6: Model displaying the evolution of a channel complex from the continental shelf down the slope to the submarine plane. (Huang, 2018) 10

Figure 7: Simplified map showing the outline of the Permian Basin, with the Delaware and Midland Basins split by the CBP with San Simon Channel connecting the two. (Modified from Wright et al., 1962) 12

Figure 8: Major tectonic phases of the Delaware Basin taken from the type well Reeves Jake Hamon Gillespie #1. From Pigott et al. (2016). 13

Figure 9: Map outlining the ancestral Tobosa Basin and its bounding features in relation to the Delaware, Midland, and Val Verde Basins. (Adams, 1965). 15

Figure 10: Simplified model of the breakup of the Central Basin Platform into the Ft. Stockton and Andector blocks. Transform stresses rotates the blocks clockwise and created an uplift, which also cause rapid subsidence of the Delaware Basin. (Schumaker, 1992) 16

Figure 11: Stratigraphic column of the Delaware Basin incorporating the nomenclature of Hardage et al., (1998). Bone Spring Formation intervals and lithologies are enlarged, red boundary denotes intervals of interest. Oil and gas producing targets are annotated to the right. (Core Laboratory, 2014) ; (Bickley, 2019). Note that for the Bone Spring Formation there are twelve members.....22

Figure 12: Model of sea level change showing Lowstand Systems Tract (LST), Transgressive Systems Tract (TST), Highstand Systems Tract (HST), and Regressive Systems Tract (RST) on a sea level curve on the right side, and their corresponding depositional models on the left (Slatt, 2013).....28

Figure 13: Diagram showing one complete relative sea level cycle starting with the falling limb and then rising limb and the corresponding stratigraphic systems tracts associated with, as well as the expected depositions at each stage (Slatt, 2006; Slatt, 2013; Crosby, 2015).....29

Figure 14: Summary of relationships of shelf and basin cyclic sedimentation. Letters A, B, and C represent different sea levels with A being the lowest relative sea level,

C the middle, and B the highest. It highlights the processes and the sedimentation in the basin as well as the shelf during one cycle. Modified from (Wilson, 1967). 30

Figure 15: Simplified reciprocal sedimentation model of the Bone Spring Formation visualizing the deposition of siliciclastic turbidite fans and channel systems at relative lowstands and carbonate apron deposition at relative highstands (Crosby, 2015; Scholle, 2002).....31

Figure 16: Geologic time scale through the Permian period which marks where the Leonardian lies in the Lower Absaroka II with respect to supercycles on the North American Craton that is introduced by Sloss (1963). (Haq and Schutter, 2008; Crosby, 2015). The six third order cycles of the Bone Spring Formation intervals are indicated in blue.....32

Figure 17: Type log from the study area defining the internal Bone Spring Formation tops picked over the study area. These tops agree with the oil and gas industry accepted, lithologically based standards. Also shown at the left are the 3rd order sequences identified which, due to reciprocal sedimentation, drive this alternation in lithology from highstand carbonates to lowstand siliciclastics. This log is centrally located in the study area and will be discussed in more detail later.....34

Figure 18: Map showing the available data used in this study. Shows the relationship of the approximate size and shape of the locations of a few key wells. 35

Figure 19: Seismic cross section displaying a large pocket where seismic reflectors are lacking continuity, highlighted inside the red square. While some reflectors are evident across the seismic, many cannot be followed through the survey.....37

Figure 20: Example of the high-quality seismic survey used in this study. The figure offers a look from a shelf vantage point to the basin a crossline and tying inline with the pre-Bone Spring underlying Wolfcamp top mapped showing subsurface depth. 38

Figure 21: Workflow diagram illustrating the process of producing an integrated interpretating from well logs and 3D seismic.....39

Figure 22: Simplified model of adapted Galloway sequence stratigraphic motifs using GR logs. The models contain a method for clastic and carbonate depositions. The clastic model adopts from the Vail approach and places sequence boundaries at the top of HSTs (Vail, 1987). For carbonates the motifs are flipped to depict clean, blocky carbonates at HSTs (Galloway, 1989; Pigott and Bradley, 2016; Bickley, 2019) 41

Figure 23: An example of the seismic well ties that were generated on every well used in the study and the cross correlation coefficient of the well tie. A phase rotation of -180 degrees was used to achieve the maximum coefficient between the logs synthetic seismic and the seismic data. 43

Figure 24: Cross section locator map showing the path of depositional strike cross section, A-A', and depositional dip cross section B-B' which are shown in Figures 25 through 28.....45

Figure 25: Cross section A – A' breaking out 3rd order sequence boundaries with orange lines across the logs. Small arrows break out the 4th order sequences. 49

Figure 26: Cross section B - B' breaking out 3rd order sequence boundaries with orange lines across the logs. Small arrows break out the 4th order sequences. 50

Figure 27: Cross section A – A' showing depositional strike. Highlighting the Bone Spring intervals, color coordinated for yellow to represent sand intervals and blue for carbonates. This figure illustrates the difference in interval thicknesses across the depositional strike. 52

Figure 28: Cross section B – B' showing depositional dip, with the same color coordination as cross section A – A'. This figure illustrates the difference in interval thicknesses across the depositional dip. 53

Figure 29: Seismic map view below the Wolfcamp top displaying a large fault zone passing through the entirety of study area. The East side is the downthrown block and provides significant accommodation space. The color scale was clipped to highlight contrast. 55

Figure 30: Cross section view of large compressional fault zone that continues into the Wolfcamp Formation. The fault on the eastern section has significantly more displacement. Three reflectors have been colored to highlight the fault displacement. 56

Figure 31: TWT structure map of the top of the Wolfcamp showing structure and deepening to the South-Southeast. TWT values range from -1040 to -1475 across the study area. This surface importantly reveals the effect of inherited topography for the overlying Bone Spring deposition. The arrows represent paths of possible sediment transportation trajectories as curved contours which point shelfward and broaden basinward. The average shelf slope angle is 18°. The different sections of the shelf are also labeled. 57

Figure 32: TWT structure map of the top of the 3rd Bone Spring Sand top with values ranging from -1000 to -1460. Displays a slight steepening compared to the Wolfcamp top. The arrows represent paths of possible sediment transportation trajectories as curved contours which point shelfward and broaden basinward. The average shelf slope angle is 19°. The different sections of the shelf are also labeled.....58

Figure 33: TWT structure map of the top of the 3rd Bone Spring Carbonate top with values ranging from -900 to -1450. The arrows represent paths of possible sediment transportation trajectories as curved contours which point shelfward broaden basinward. The average shelf slope angle is 19°. The different sections of the shelf are also labeled.....59

Figure 34: TWT structure map of the top of the 2nd Bone Spring Sand top with values ranging from -860 to -1360. The arrows represent paths of possible sediment transportation trajectories as curved contours which point shelfward broaden basinward. The average shelf slope angle is 21°. The different sections of the shelf are also labeled. 60

Figure 35: TWT structure maps of the top of the 2nd Bone Spring Carbonate top with values ranging from -810 to -1320. The arrows represent paths of possible sediment transportation trajectories as curved contours which point shelfward broaden basinward. The average shelf slope angle is 20°. The different sections of the shelf are also labeled.....61

Figure 36: TWT structure maps of the top of the 1st Bone Spring Sand top with values ranging from -790 to -1270. The arrows represent paths of possible sediment

transportation trajectories as curved contours which point shelfward broaden basinward. The average shelf slope angle is 22°. The different sections of the shelf are also labeled. 62
Figure 37: TWT structure maps of the top of the 1st Bone Spring Carbonate top with values ranging from -640 to -1060. The arrows represent paths of possible sediment transportation trajectories as curved contours which point shelfward broaden basinward. The average shelf slope angle is 20°. The different sections of the shelf are also labeled.....63
Figure 38: TWT structure maps of the top of the 1st Bone Spring Carbonate top with values ranging from -640 to -1060. The arrows represent paths of possible sediment transportation trajectories as curved contours which point shelfward broaden basinward. The average shelf slope angle is 20°. 64
Figure 39: A crossline in the seismic that shows the filling and flattening of an incised valley of a feeder channel from the top of the 3rd Bone Spring Sand top to the 1st Bone Spring Sand top. Red horizon represents the 3rd Bone Spring Sand, cyan the 2nd Bone Spring sand, and pink the 1st Bone Spring Sand. Note the dramatic truncation of the reflectors beneath each sand top which represents an LST (see text for explanation). 65
Figure 40: Model of incised valley creation and resulting deposition of submarine fan caused by a change of sea level in the Permian basin. Li et al. (2015), Bickley (2019). 65

Figure 41: Gross Isopach map of the entire Bone Spring Formation interval from the top of the Bone Spring to the top of the Wolfcamp. Thickness is greatest over the faulted area seen on the Wolfcamp and thins drastically to the southern edge. 67

Figure 42: Gross Isopach maps of the 3rd Bone Spring Sand. Thickest areas are proximal to the slope in the basin with depths ranging from ~50 to ~600 feet. 68

Figure 43: Gross Isopach maps of the 3rd Bone Spring Carbonate. Thickest areas are on top of the shelf with thicknesses ranging from ~100 to ~900 feet. 69

Figure 44: Gross Isopach maps of the 2nd Bone Spring Sand. Thickest areas are proximal to the shelf in the basin with thicknesses ranging from ~100 to ~1100 feet and the 2nd Bone Spring Sand is by far the thickest sand interval. 70

Figure 45: Gross Isopach maps of the 2nd Bone Spring Carbonate. Thickest sections are on top of the shelf with thicknesses ranging from ~100 to ~1000 feet. 71

Figure 46: Gross Isopach maps of the 1st Bone Spring Sand. Thickest areas are proximal to the shelf in the basin with thicknesses ranging from ~100 to ~700 feet. 72

Figure 47: Gross Isopach maps of the 1st Bone Spring Carbonate. Thickest sections are on top of the shelf with thicknesses ranging from ~1100 to ~2200 feet and is the thickest carbonate interval in the Bone Springs. 73

Figure 48: Seismic cross section number 1 going through the Mitchell 1 well with terminations displayed. 75

Figure 49: Seismic cross section number 2 going through the Pearsall 6 well with terminations displayed. 76

Figure 50: Seismic cross section 1 going through the Mitchell 1 well but showing the Bone Spring Sand tops and Galloway motifs superimposed, where blue arrows

represent HST's, orange RST's, red LST's and green TST's (see text for explanation). 78
Figure 51: Seismic cross section 2 going through the Pearsall 6 well showing the Bone Spring Sand tops and Galloway motifs superimposed where blue arrows represent HST's, orange RST's, red LST's, and green TST's (see text for explanation).....79
Figure 52: Seismic cross section in strike direction through Love Federal well, displaying formations, HST and LST systems tracts, terminations in yellow and red, and faults designated by dashed black lines. 81
Figure 53: Seismic cross section 1 going through the Mitchell 2, Love and MC Federal wells and displaying seismic stratigraphic parasequence sets. 83
Figure 54: Seismic cross section 2 passing through the Pearsall and displaying the seismic the stratigraphic parasequence sets. 84
Figure 55: Seismic cross section of 3rd Bone Spring Carbonate Highstand Systems Tract (HST) highlighted in blue. 85
Figure 56: Seismic horizon of 3rd Bone Spring Carbonate Highstand Systems Tract (HST). The dark red area shows the carbonate apron fan deposit and the blue lines show interpreted channel paths. 86
Figure 57: Seismic cross section of 3rd Bone Spring Sand Lowstand Systems Tract (LST) highlighted in red. 86
Figure 58: Seismic horizon of 3rd Bone Spring Sand Lowstand Systems Tract (LST). The dark red area shows the deposition of the sand fan deposits and the blue lines show interpreted channel paths. 87

Figure 59: Seismic cross section of 3rd Bone Spring Carbonate Transgressive Systems Tract (TST) highlighted in green. 87
Figure 60: Seismic horizon of 2nd Bone Spring Carbonate Transgressive Systems Tract (TST). The dark red area shows the carbonate apron fan deposits and the blue lines show interpreted channel paths. 88
Figure 61: Seismic cross section of 2nd Bone Spring Sand Regressive Systems Tract (RST) highlighted in yellow. 88
Figure 62: Seismic horizon of 1st Bone Spring Sand Regressive Systems Tract (RST) or Falling Stage Systems Tract (FSST). The dark red area represents sand fan deposits and the blue lines show interpreted channel paths. 89
Figure 63: Seismic cross section of Highstand Systems Tract (HST) showing maximum slope angle of 27°. 90
Figure 64: Seismic cross section of Lowstand Systems Tract (LST) showing maximum slope angle of 28°. 90
Figure 65: Seismic cross section of Transgressive Systems Tract (TST) showing maximum slope angle of 19°. 90
Figure 66: Seismic cross section of Regressive Systems Tract (RST) or Falling Stage Systems Tract (FSST) showing maximum slope angle of 40°. This high angle produces a slump to form at the top of the slope. 91
Figure 67: Love 3 well with 3rd and 4th order sequences correlated to global sea level curve for the Permian from Haq and Schutter (2008). 92

Figure 68: 3rd Bone Spring Sand isopach map with channel interpretations from TWT structure map of top of the 3rd Bone Spring Sand. Displays higher correlations of the channels and thicknesses in the Southeast area of the study. 93

Figure 69: 2nd Bone Spring Sand isopach map with channel interpretations from TWT structure map of top of the 2nd Bone Spring Sand. Higher correlations of channel deposits and greater thicknesses are displayed in the Southwest area of the study. 94

Figure 70: 1st Bone Spring Sand isopach map with channel interpretations from TWT structure map of top of the 1st Bone Spring Sand. Higher area of channel deposits and greater thicknesses are displayed in the Southwest area of the study.....95

Abstract

The Bone Spring Formation is one of the dominant oil and gas producing formations in the Permian Basin today. It is Leonardian in age and lies just below the Guadeloupian Brushy Canyon Formation in the Delaware Basin. Traditional production from these units comes from upslope carbonates on the slope and shelf margins of the Delaware Basin and the Northwest Shelf equivalents of the Bone Spring Formation, the Abo and Yeso Formations, along with up dip clastic pinch-outs. The majority of the production came from diagenetic, secondary porosity developed in carbonate debris flows and slump deposits derived from the shelf margin. New developments in drilling, production, and development technologies have allowed for a shift in primary target focus down dip into the basin. The Bone Spring Formation is presently the most active unconventional play in the Permian Basin today. Therefore, optimizing the sweet spots where extractable oil occurs by preservation in anoxic environments and where it is most brittle is critical to its economic exploitation.

The sources and mechanics that drive the deposition in this environment are dynamic, switching between clastic and carbonate systems. This produces a heterogeneous deposit in the basin, both vertically and horizontally that makes it difficult to interpret in seismic away from core control. Global and regional sea-level changes also increase the complexity of the stratigraphy by vastly changing the shoreline and accommodation space, so the effects of this control must be interpreted to identify depositional trends. In-depth integrated analysis of well logs and seismic data reveals

sequence stratigraphy that provides understanding of seismic data between wells that has significant implications for exploration.

Chapter 1: Introduction

Study Location

The approximate location of the study area is shown in Figure 1 and is edited from Murchison Oil and Gas, Inc. The 3-D seismic survey was shot in southeast New Mexico and geologically it is located at the shelf to slope break to basin floor of the Capitan Reef Trend of the Northwestern Shelf, of the northernmost Delaware basin.

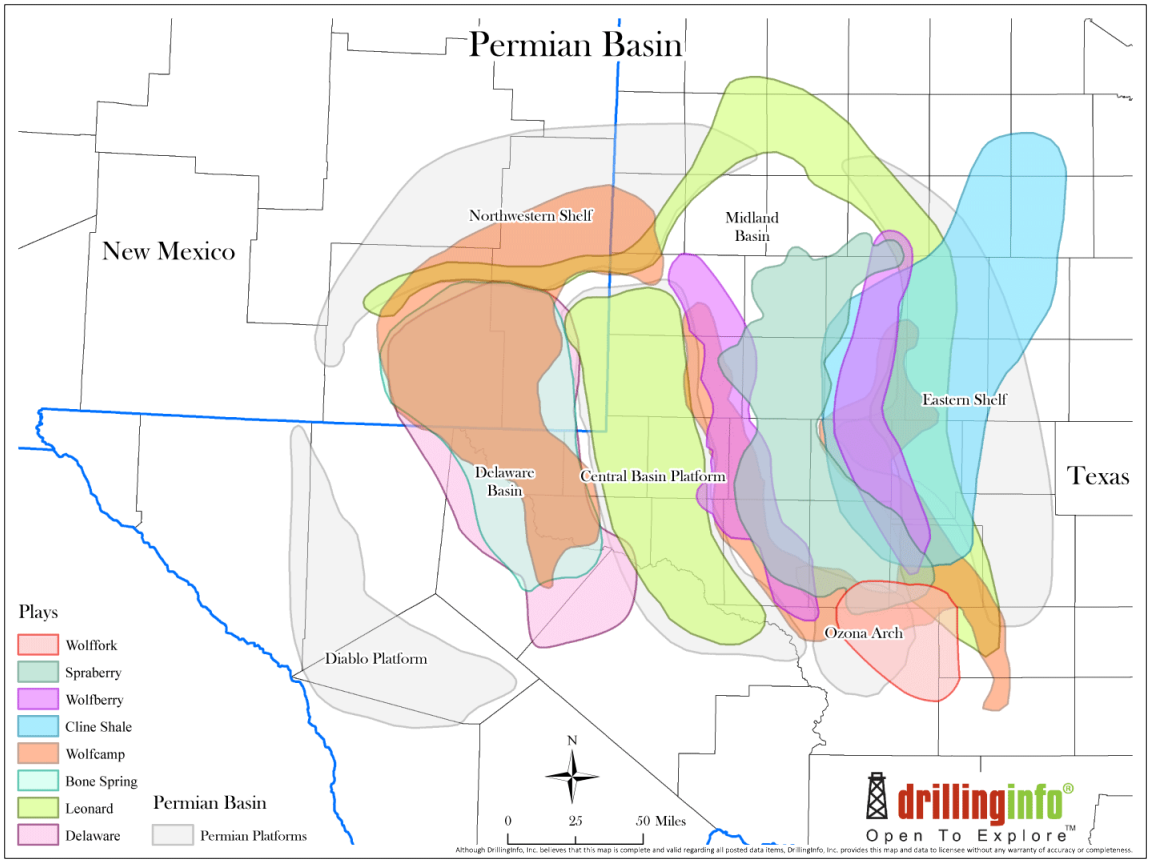

Figure 1: Overview of play trends in the Permian Basin. Highlights the overlapping Bone Spring Formation, Wolfcamp, and Avalon trends in the Delaware Basin. From Drillinginfo.com

The seismic data provided by Schlumberger are proprietary, consequently the specific locations of the survey and wells will be withheld. Most of the wells used in this study were found through the New Mexico Oil Conservation Division (NMOCD) and the other wells used were generously provided by Mewbourne Oil Company. The survey is approximately 100 square miles with a N-S length of ~10 miles, E-W width of ~10 miles. This data set provides an opportunity to map the subsurface shelf to basin origination of the Bone Spring Formation, as the source, migration, and deposition can all be seen in one survey. This will provide a more holistic understanding to the geomechanics involved in the deposition.

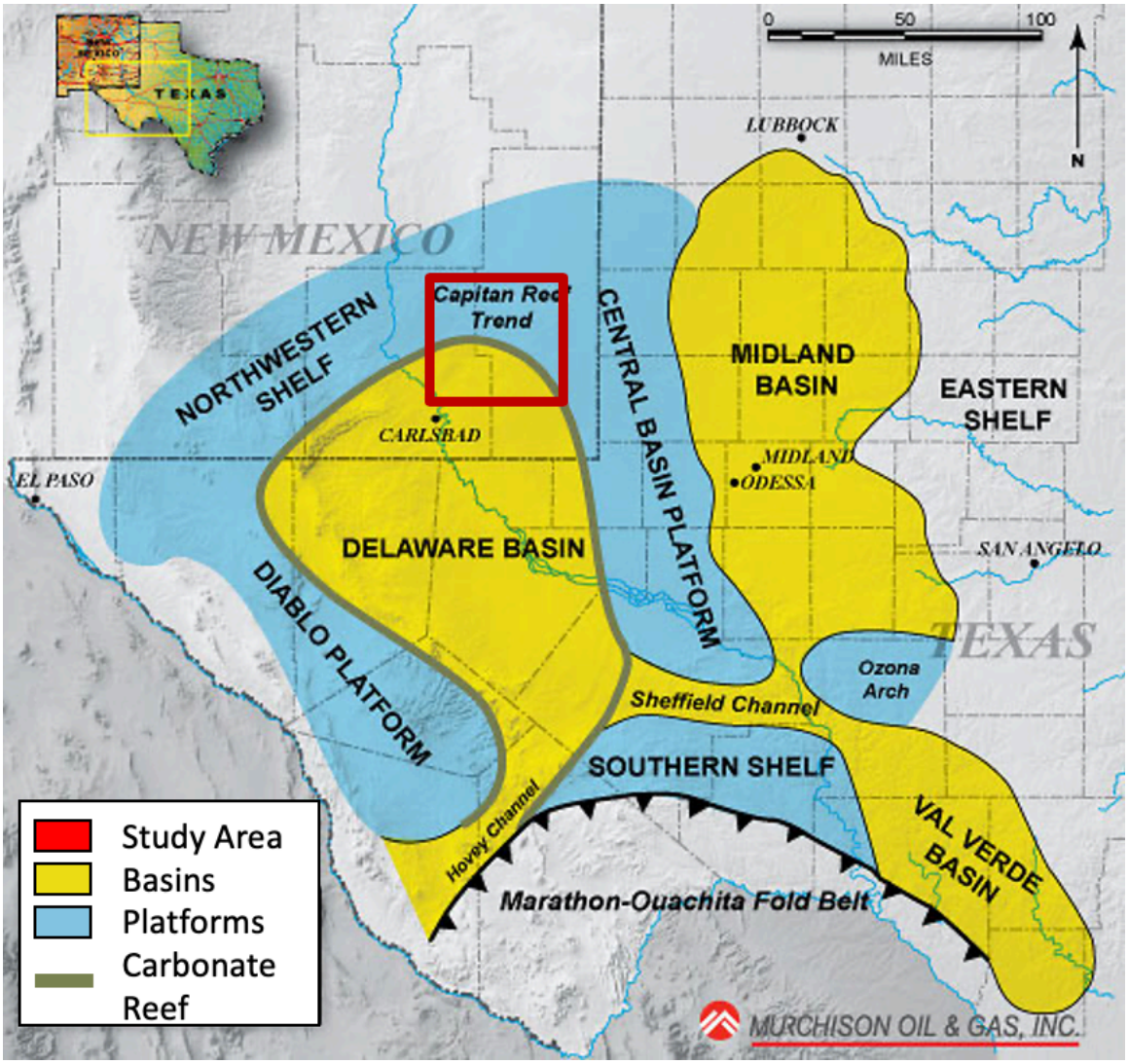

Figure 2: Generalized map of the Delaware and Midland Basins, with the CBP dividing the two. Dark green ring around the Delaware Basin denotes the location of carbonate reef build up. The study area is approximately located by the red box. Modified from Murchisonoil.com

Previous Work

Since the reevaluation of previously deemed uneconomical Permian deep-water sandstone reservoirs in the 1990s (Montgomery et al., 1999), this New Mexico-Texas area has been vastly researched by many (Adams, 1965; Hardage, 1998; Hart, 1997; Montgomery, 1998; Hills, 1984 to name a few). These studies have proven to be invaluable resources and as a building block for this study. The economic impact of the

Bone Spring Formation has driven more recent studies to be focused on the basinal facies using deep well logs and seismic surveys. The work of these studies has given insight into the depositional processes, stratigraphy, as well as the structural extent of the formations that are integral to further studies of the area. There are three main papers that are directly pertinent because of the proximity of the study location and the scope, that this study will build off of.

The first is a thesis by Charlie Crosby (2015) titled, “Depositional History and High-Resolution Sequence Stratigraphy of the Leonardian Bone Spring Formation, Northern Delaware Basin, Eddy and Lea Counties, New Mexico”. Crosby constructed a sequence stratigraphic framework and depositional history using well logs, chemostratigraphy, and is one of the first authors to break out parasequence sets in the Bone Spring Formations using petrophysical logs to relate their motifs to inferred changes in sea level (Figure 3).

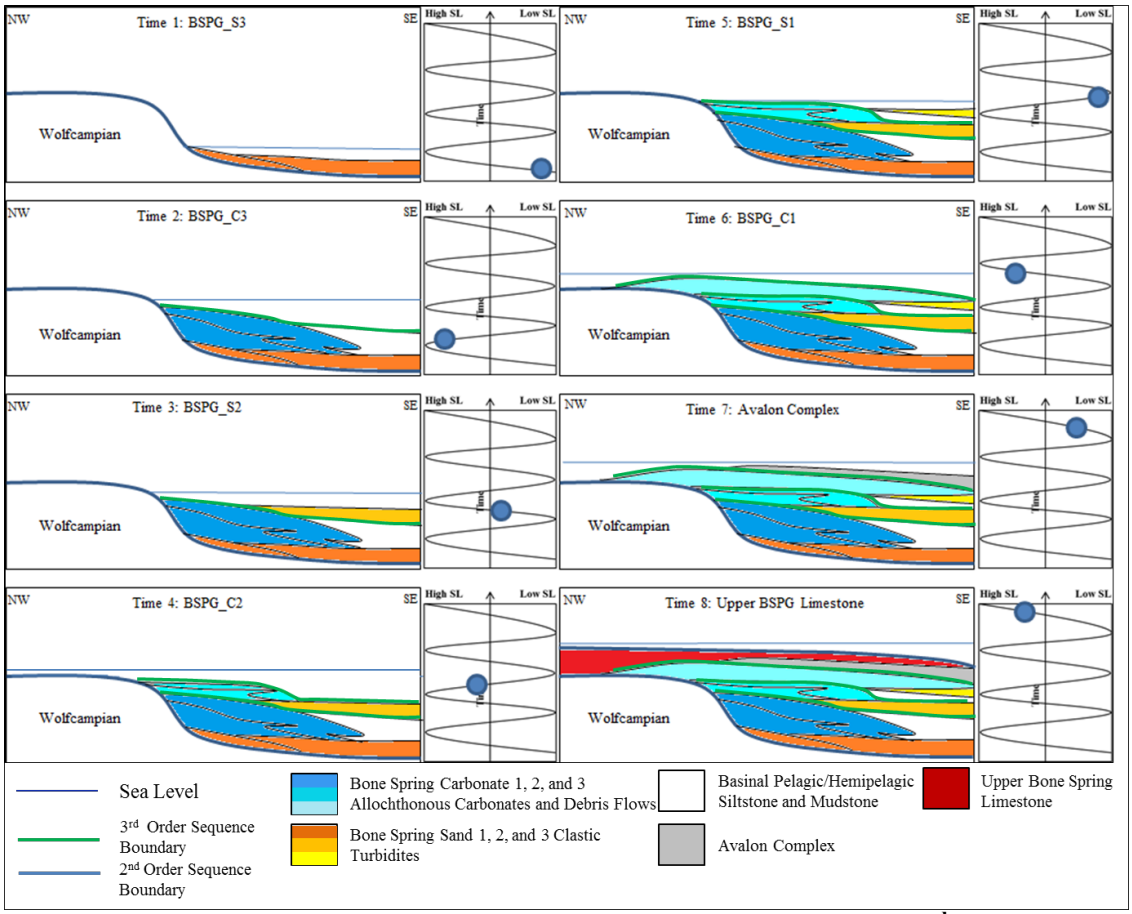

Figure 3: Evolution of the Bone Spring Formation deposition with 3rd order sea level changes, where highstands correspond with carbonate intervals while lowstands correspond with siliciclastic intervals. (Crosby, 2015).

The second is a thesis by Tyler Bickley (2019) titled, "High Resolution Sequence Stratigraphy and Seismic Stratigraphy of the Leonardian Bone Spring Formation, Delaware Basin, Southeast New Mexico". In this study Bickley expanded on Crosby's sequence stratigraphy model of the Bone Spring using Galloway motifs and then constructed a seismic stratigraphic model using the Vail method (Galloway, 1989; Pigott and Bradley, 2014; Vail, 1987)

The third source is a thesis by Cyril Frazier (2019) titled, " High Resolution Integrated Vail-Galloway Sequence Stratigraphy of the Leonardian Bone Spring Fm., N. Delaware Basin, Southeast New Mexico". In this study Frazier applied sequence

stratigraphy on the same 3D seismic volume investigated here in order to derive insights into relative sea level changes. However though not shown in the thesis, in the thesis defense Frazier includes three graphics showing sediment bypass canyons and submarine channels moving down the slope. Figure 4 from the defense illustrates both the 3rd Bone Spring Formation Carbonate and Sand surfaces (see Figure 11 for stratigraphic position which will be detailed later). In the thesis, Frazier explains the method of producing these surfaces was executed by autotracking in Petrel. Unfortunately, such a procedure resulted in abnormally smooth surfaces for an area, which in reality (as will be pointed out) is much more intricate and convoluted.

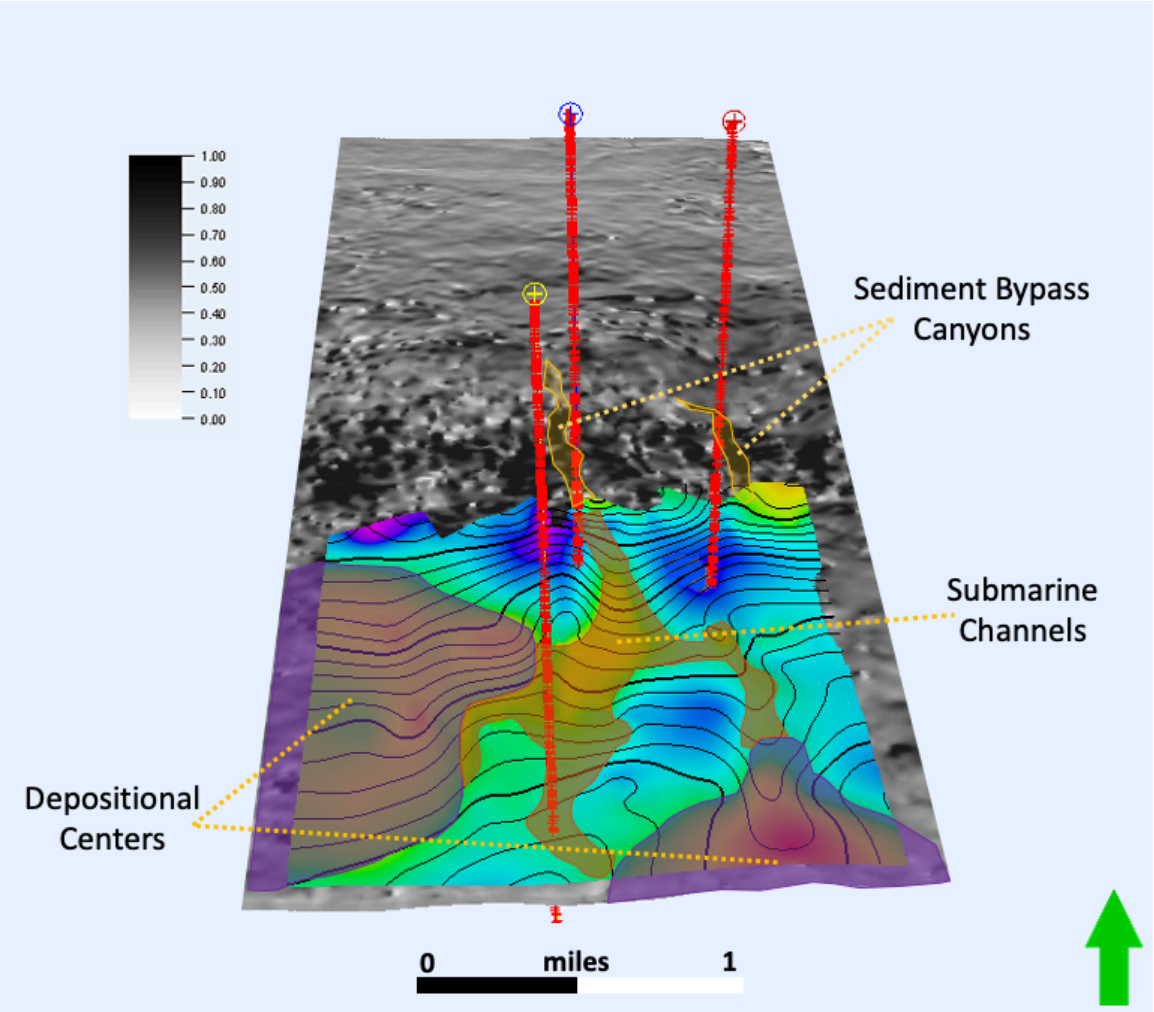

Figure 4: Seismic map of the 3rd Bone Spring Formation Carbonate and Sand surfaces showing sediment bypass canyons, depositional centers, and submarine channels. (Frazier, 2019)

Consequently, this study will take a more detailed look into the channeling deposits in the Bone Spring Formation.

Problem Definition and Objectives

Despite the numerous studies of the Bone Spring Formation, the combination of Leonardian sea level changes, inherited topography, tectonics, and paleoenvironmental factors which contribute to a complex nature of its deposition, focused studies are

instrumental to understand the entirety of the formation. Mass Transport Deposits (MTD), and non-continuous strata add to the confusion in the study area. While all of these factors complicate the area, differences in nomenclature can also be problematic. For example, some workers (Montgomery, 1997) name the sand layer in the 1st Bone Spring Carbonate the Avalon Shale, while others (Hurd, 2016) call it the Cutoff Formation. Adding to the problem of nomenclature, many of the correlations between wells are done by lithostratigraphy correlation alone, an example of which can be seen in Figure 5.

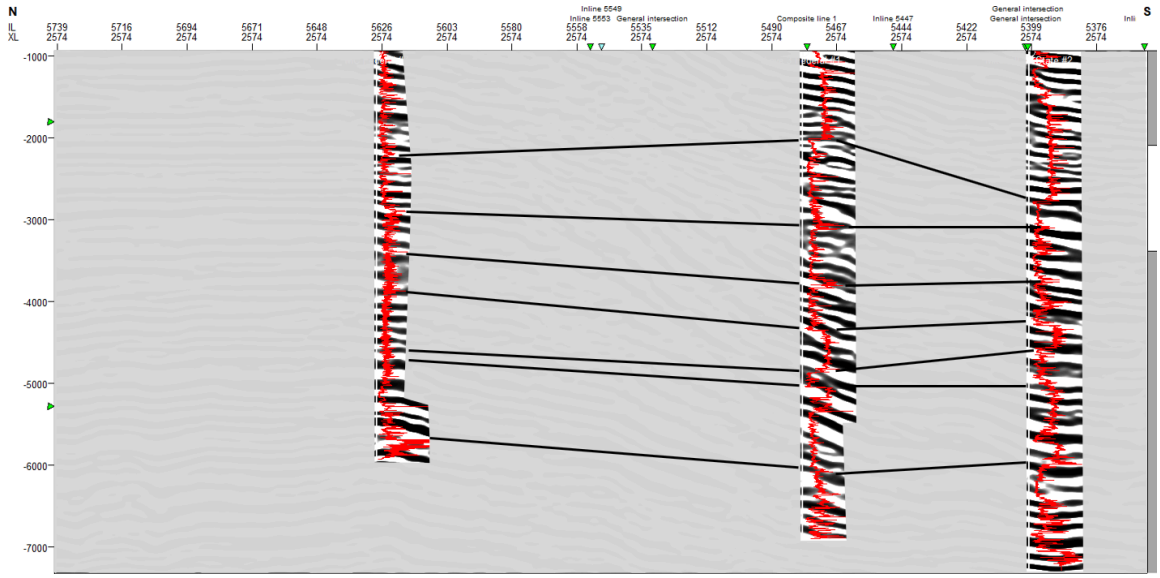

Figure 5: Cross section showing hypothetical correlation between wells by lithostratic correlation alone. Compare this interpretation with Figure 50.

While lithosratic correlations can be very useful in many cases, with the insight of chronostratigraphically significant surfaces as will be incorporated in this area on this 3D seismic volume, lithostratigraphic correlations can often be time transgressive and thus fraught we error.

The objective of this study is to expand upon the previous works, in further defining the sequence stratigraphy and depositional history of the Bone Spring Formation. Through the integration of well log sequence stratigraphic analysis and 3-D seismic stratigraphic analysis together will yield a more accurate result than either could by itself. The four principal questions to be answered are:

1. What is the three dimensional geometry of sediment gravity flows as a function of sea level and predominant lithological makeup?
2. What is the nature of channeling, abandonment, and fill?
3. How did the Mass Transport Complexes respond? And
4. How can this information be used for exploration?

An adapted Galloway motif will be applied to the well logs. This approach allows for a more accurate depiction of the carbonate intervals by flipping the Galloway motifs for carbonate dominated intervals and then applying these to Vail approach (Galloway, 1989; Pigott and Bradley, 2014; Vail, 1897). This adapted approach uses the locally confined detail found in well logs and applies it across the expansive seismic, and also correlates this information with the other available well logs in the study.

The well log and seismic analysis will help to break out sequence systems tracts across the seismic and also to illustrate the channeling associated with the transportation and deposition of clastic (in this case, both terrigenous clastic and carbonate clastic) materials. Figure 6 shows the evolution of a channel as it cuts through the continental slope.

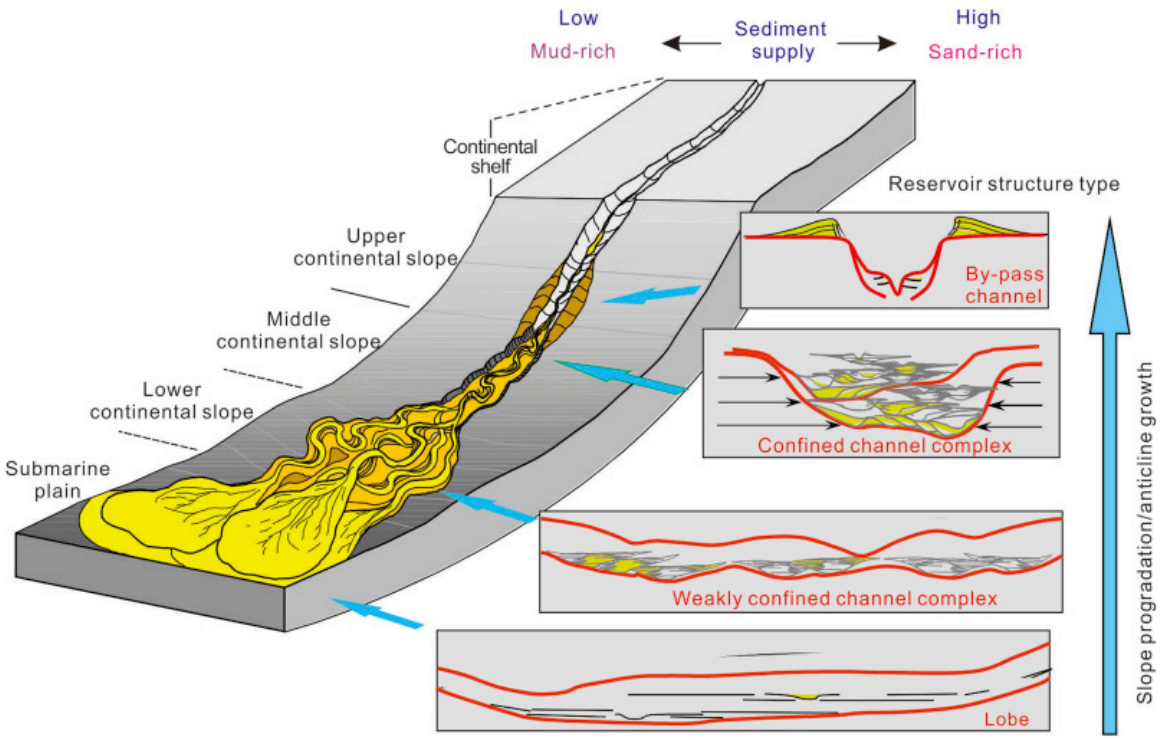

Figure 6: Model displaying the evolution of a channel complex from the continental shelf down the slope to the submarine plane. (Huang, 2018)

Chapter 2: Geologic Background

The Delaware Basin is the westernmost structural subdivision of the larger Permian Basin with an area of more than 13,000 square miles of west Texas and south New Mexico (Hills, 1984). It encloses four significant features; the Central Basin Platform to the East, the Marathon-Ouachita fold and thrust belt to the South, the Diablo platform to the West, and the Northwest Shelf to the North. The Midland Basin (that is to the East of the Central Basin Platform) was connected to the Delaware Basin by the San Simon channel at the northeast and by the Sheffield Channel at the southeast during Leonardian time. The Delaware Basin was to the Panthalassa Sea by a restricted southwestern opening named the Hovey Channel (King, 1942) (Figure 7).

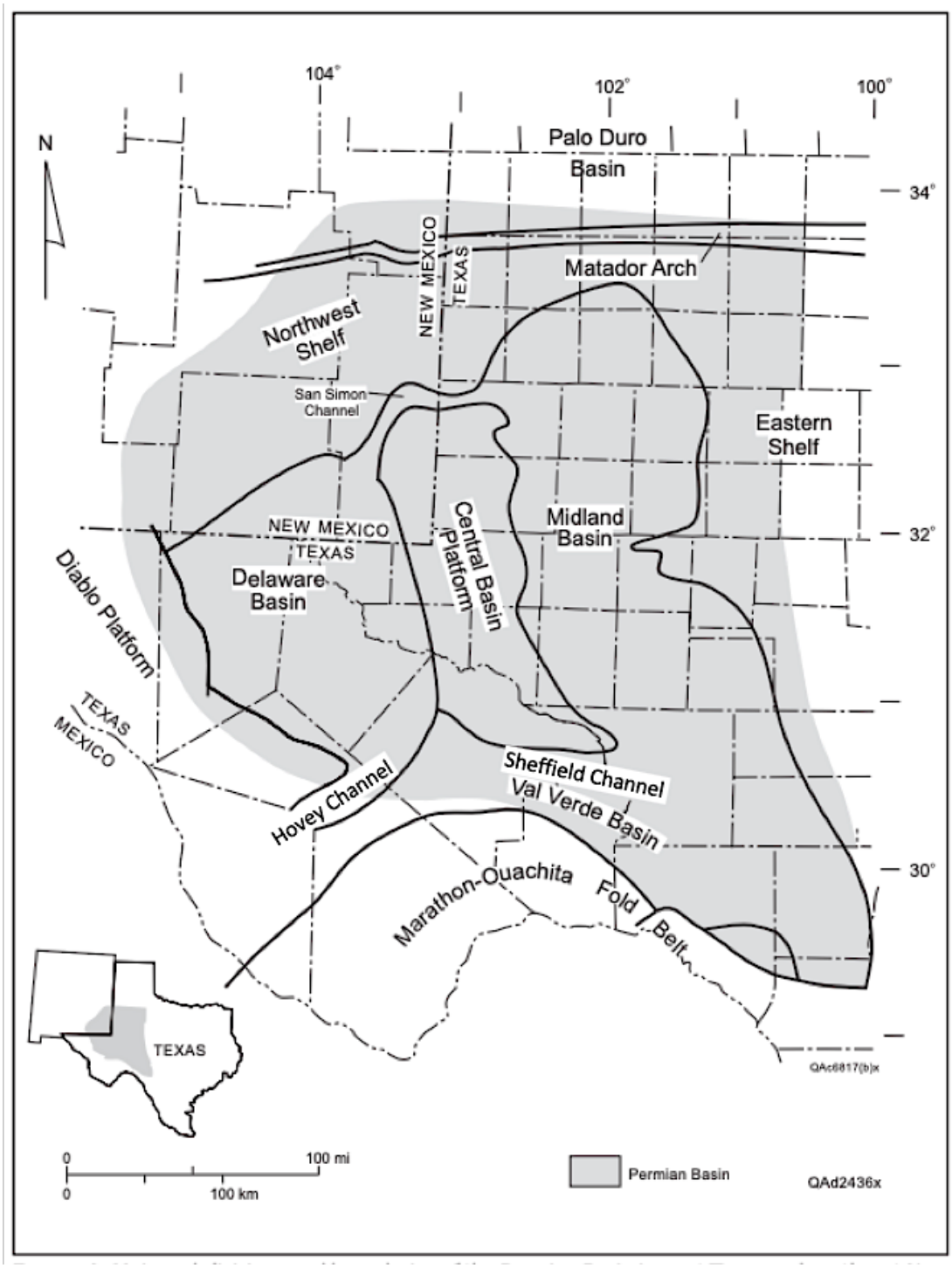

Figure 7: Simplified map showing the outline of the Permian Basin, with the Delaware and Midland Basins split by the CBP with San Simon Channel connecting the two. (Modified from Wright et al., 1962)

Tectonic History

It remains vital for any endeavor aimed at establishing depositional and stratigraphic frameworks to embark from a comprehensive understanding of the effect deformation from tectonic evolution has upon the stratigraphic sequences (Yang and Dorobek, 1995). The tectonic structure controls almost every aspect of a basin, it is useful to systematically construct a timeline of events. The tectonic thermal evolution of the Delaware Basin has been summarized by Williams et al. (2014) and Pigott et al. (2016) and with respect to tectonic episodes is shown in Figure 8.

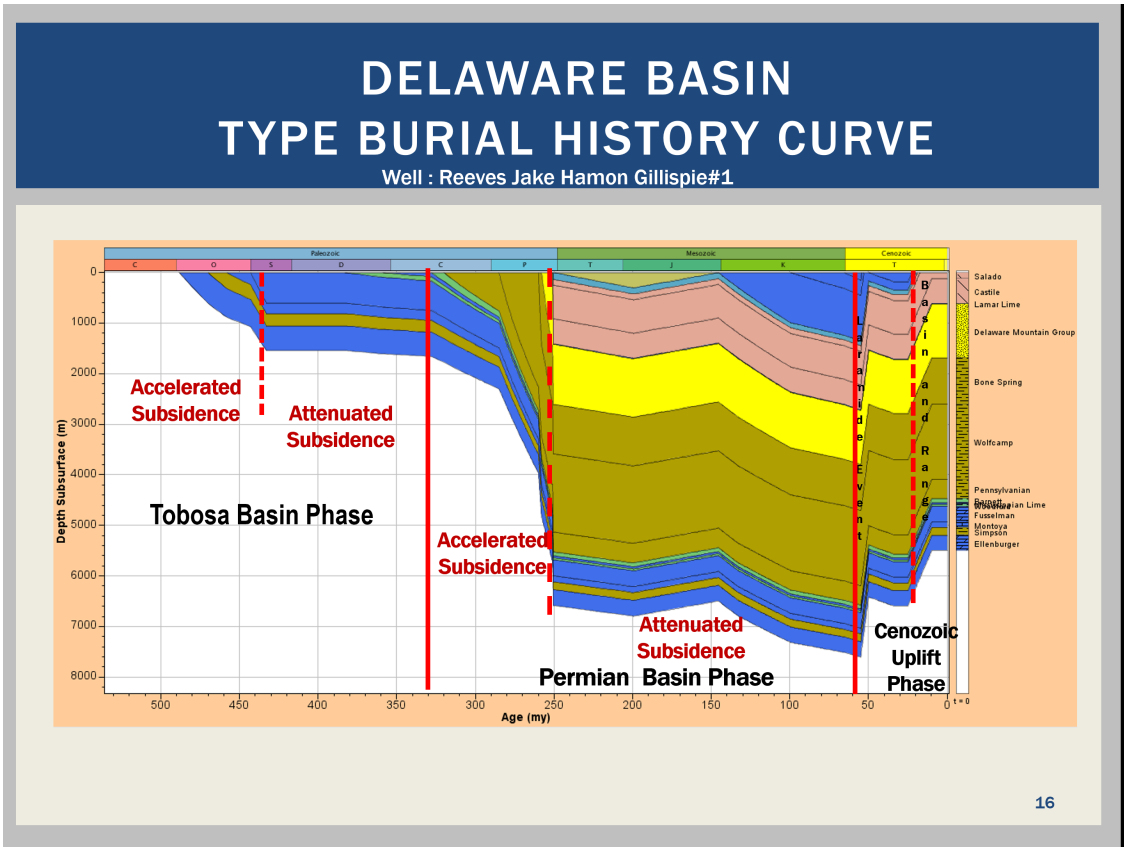

Figure 8: Major tectonic phases of the Delaware Basin taken from the type well Reeves Jake Hamon Gillespie #1. From Pigott et al. (2016).

The origination of the Permian Basin, as well as smaller subdivisions (Delaware Basin, Central Basin Platform, Midland Basin) are believed to be traced back to the

Grenville orogeny, which is associated with the creation and subsequent breakup of Rodinia. The rifting from the Grenville Orogeny caused a zone with lines of weakness that later defined the location of the Central Basin Platform (Shumaker, 1992).

After the Grenville orogeny the late Precambrian to Devonian the tectonic development is tied to a passive margin, during which a peninsular spur off of the Transcontinental arch that spanned through southeast New Mexico and West Texas started to collapse. This spur likely subsided owing to the cooling of mantle rocks below, which flattened out the area in the Early Ordovician (Figure 9). This allowed the Ellenburger sea to transgress northwestward in order fill the negative depression, the area now known as the Delaware Basin (Adams, 1965).

In the Middle Ordovician, crustal warping created a series of sags and arches and created the Tobosa Basin, as well as the Diablo Arch to the west and the Texas Arch to the east (Figure 9)(Adams, 1965). The Tobosa Basin then provided a southern opening that enabled the sea to transgress.

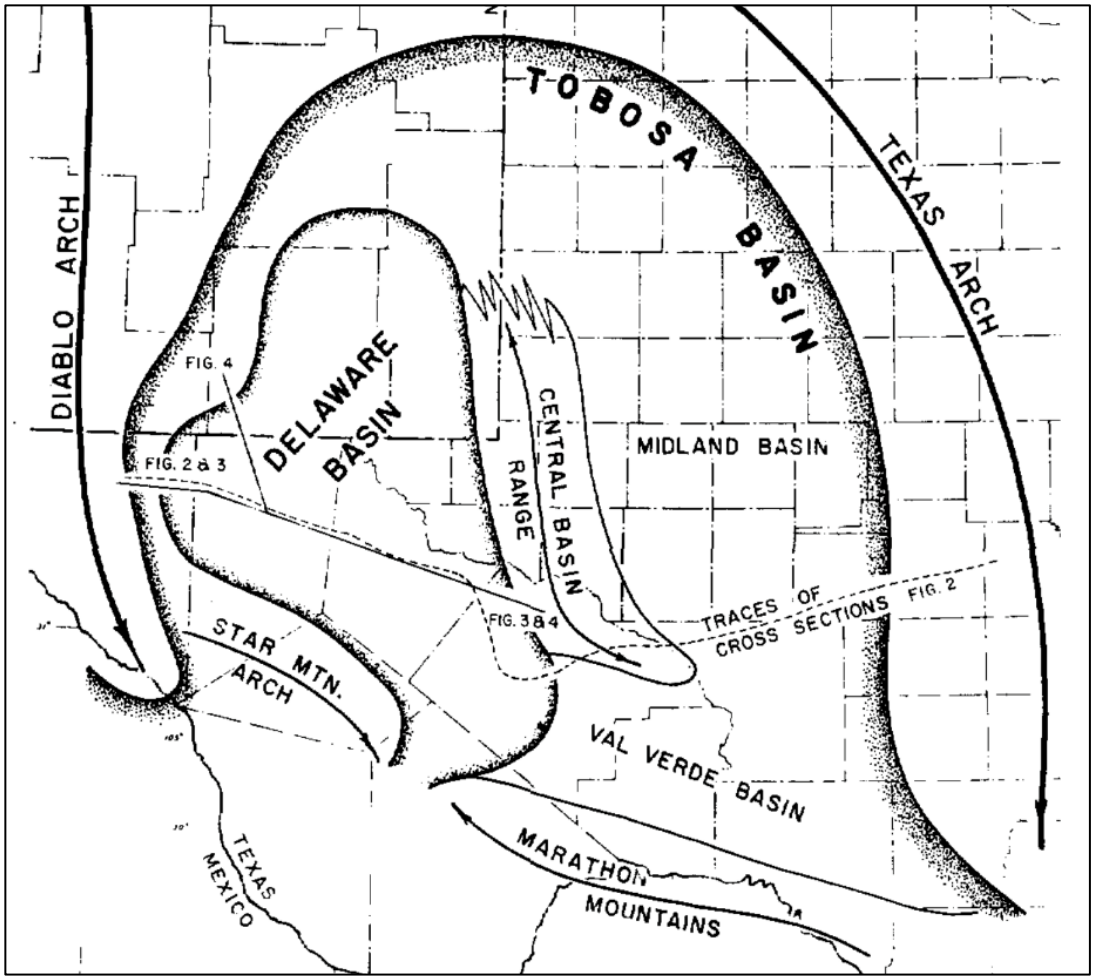

Figure 9: Map outlining the ancestral Tobosa Basin and its bounding features in relation to the Delaware, Midland, and Val Verde Basins. (Adams, 1965).

After the formation of the Tobosa basin, tectonic activity was relatively dormant until the Variscan Orogeny in the Mississippian (Hills, 1984) and crustal thermal cooling occurred (Pigott et al., 2016). The compressional forces from the Variscan Orogeny reactivated the Proterozoic lines of weakness around the Central Basin Platform. The Central Basin Platform is comprised of several asymmetric blocks that can be viewed as two groups of blocks, the Fort Stockton and Andector Blocks (Shumaker, 1992). These two blocks were subjected to right lateral shear through the Mississippian and in the Pennsylvanian caused a clockwise rotation on the blocks (Figure 10). This clockwise

rotation may have been the cause of the deformation and uplift of the Central Basin Platform (Yang and Dorobek, 1995) and accompanied flexural uplift (Pigott et al., 2016). This uplift caused the separation of the Midland and Delaware Basins and rapid subsidence in both basins that continued until the Early Permian (Yang and Dorobek, 1995).

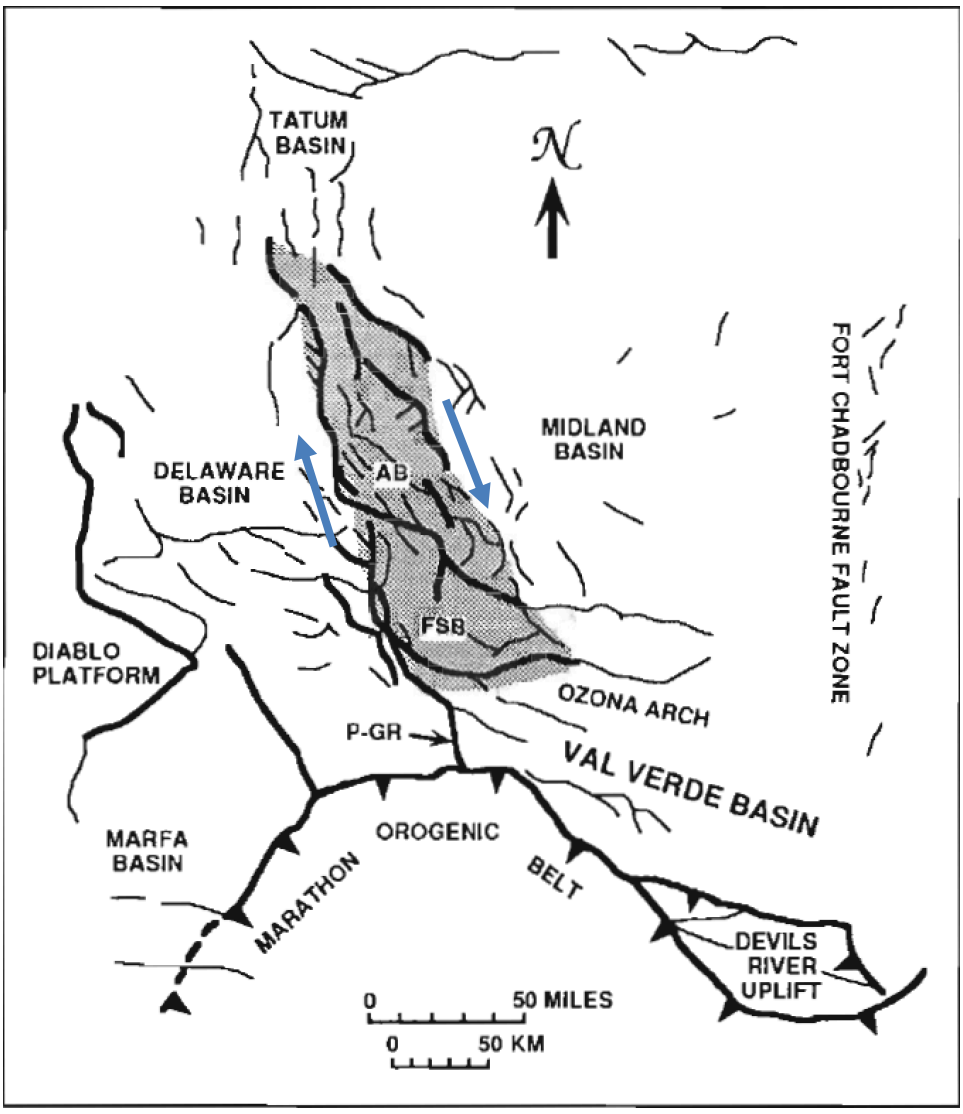

Figure 10: Simplified model of the breakup of the Central Basin Platform into the Ft. Stockton and Andector blocks. Transform stresses rotates the blocks clockwise and created an uplift, which also cause rapid subsidence of the Delaware Basin. (Schumaker, 1992)

During the Permian there was continuously abating effects of the Variscan Orogeny that produced short intervals of tectonic pulses. The culmination of these tectonic pulses and rapid sedimentation in the Delaware Basin into the accommodation caused accelerated subsidence. This subsidence caused considerably more uplift to the Central Basin Platform of several thousand feet and this caused a greater divide between the Delaware Basin and the Midland Basin (Adams, 1965). Towards the Middle to Late Permian tectonic activity greatly reduced, and the eastward deepening and tilting in the Delaware Basin was all that remained (Keller, et al., 1980) caused by crustal flexure (Pigott et al., 2016)

Since the end of the Late Paleozoic the Permian Basin had undergone minimal deformation; thus, the major structures have remained unaltered until today (Yang and Dorobek, 1995) with the exception of crustal uplift (Figure 8) as described by Pigott et al., (2016).

Depositional History

Late Cambrian - Wolfcampian Deposition

In the Delaware Basin, the Late Cambrian Dagger Flat Sandstone represents the earliest transgression over heavily weathered granitic rocks prior to the formation of the Tobosa Basin (Hills, 1984). This widespread sea in the Late Cambrian through the Early Ordovician brought on the deposition of the Ellenburger carbonates on broad shelfs (Hills, 1984). These carbonates were evenly bedded and covered near shore thin deposits

of clastics that were sources from weathering of the underlying basement (Adams, 1965). During the Middle Ordovician the Tobosa Basin commenced to subside, providing accommodation for the interbedded Simpson Sandstone, Shale, and Limestone to accumulate in the lower areas of the sag (Adams, 1965).

From the Late Ordovician through the Devonian there was predominately carbonates being deposited. In the Middle Devonian there was significant siliceous material interbedded in the carbonates, deposited during lowstand times (Hills, 1984). During the Late Devonian the sedimentation could not keep up with the subsidence of the Tobosa basin, causing the carbonate shelfs to prograde (Adams, 1965). The shallow sea that covered not only this area, but much of North America was poorly ventilated, and during the late Devonian to Mississippian, widespread organic rich shales were deposited and preserved as a carbonaceous residue known as the Woodford Formation (Hills, 1984).

The Middle Mississippian deposition was primarily carbonate intervals, but the uplift of the Central Basin Platform provided a clastic source that was deposited in basinal black organic rich shales (Hills, 1984). This tectonic activity increased into the Pennsylvanian, causing rapid subsidence and increasing accommodation that was progressively filled with deltaic sediments from the concomitant northwest uplift in New Mexico (Hills, 1984). Carbonate shelfs started to from in the Early Pennsylvanian covering the recently deposited clastics, however much of the deep basin Pennsylvanian deposits were likely eroded by bottom currents or Early Permian turbidity flows (Adams, 1965). The carbonate banks that developed around the ridge also trapped clastic material behind it and aided to the starving of the basin during this time (Hills, 1984).

In the early Wolfcampian the final thrust of the Marathon orogeny provided a source from southern rocks and deposited muds in the southern and central portion of the Delaware basin, and intermittently deposited many thin carbonate beds during times of inactivity. (Hills, 1984). The early Wolfcampian sediments mainly consist of clastics, and most of them were sourced from the newly forming mountains on the northwest, west, and southwest sides of the basin and were likely transported by turbidity flows (Adams, 1965). These turbidity flows kept the water column mixed and provided the necessary nutrients for hydrocarbon source material. (Adams, 1965). Carbonate shelf production increased throughout the Wolfcampian caused basinal circulation to be more limited. However, through the Hovey channel, Val Verde basin, and channels in the carbonate shelves the seawater was able to remain filled with the necessary nutrients to support organic production (Hills, 1984).

Leonardian Bone Spring Formation Deposition

In the Leonardian, the Delaware Basin experienced various stages of fluctuating sea level, where during relative lowstands clastics were deposited and in relative highstands carbonates were produced and deposited. This oscillating deposition, known as reciprocal sedimentation after Wilson (1965), is responsible for the alternating beds of carbonates and clastics that make up the Bone Spring Formation. The controls on Leonardian deposition were a combination of basinal subsidence and cyclic sea level fluctuations (Montgomery, 1997), though Saller (et al., 1989) suggested the rapid subsidence was the larger factor of the two. This investigation will show that actually

there is a third mechanism, that of autocyclic control which governed the basinal channel downcutting, abandonment, and fill.

Through the Leonardian, the carbonate shelf was expanded by reef buildup on the shelf edge which contributed to the basinal circulation to become restricted, but the Hovey, Sheffield, and nearby San Simon Channels allowed enough circulation to keep the shallow waters productive (Hills, 1984). The productive shallow waters allowed for organisms, like phytoplankton to be produced while the anoxic underlying waters caused a high amount of the material to be preserved until subsequentially buried (Hills, 1984). The Bone Spring is such a prominent oil and gas play, because the well-preserved organic material was buried in stratigraphic units that roughly total an average between 3,000 and 4,5000 feet in thickness (Hart, 1997; Crosby, 2015). The deposition and preservation of these deepwater organics are a direct consequence of oscillating anoxic-oxic zone (Crosby et al., 2017)

The actual control of the siliciclastic deposition in basins has been problematic. Commonly stratigraphers have used the word “bypass” to simply say that using well control fence diagrams the material in some manner “bypasses” the shelf and ends up in the basin. Stevenson et al. (2017) write concerning sediment gravity flows: “Despite its importance, sediment bypass is poorly understood in terms of flow processes and the associated stratigraphic expression. Indeed, Pray (1998) theorized that the sediment was funneled through channel systems that cut through the shelf and transported by debris flows during lowstands, and during highstands sediment gravity flows transported carbonates from the shelf (Pray, 1988; Plemons et al., 2019). This investigation will not only show the channeling predicted from outcrop studies, but also reveal where the

channels developed, how the channels developed, and not only when they developed, but when they were abandoned.

At the beginning of the Leonardian the sea level fell from the prior highstand at the end of the Wolfcampian, and subsequently yielded the lowstand deposition of the 3rd Bone Spring Sand (Hart, 1998). This sand deposition is interpreted to be a widespread submarine-fan deposit (Montgomery, 1997). Although named the 3rd Bone Spring Sand, it is important to understand the nomenclature. While counted the 3rd Bone Spring Sand from the top, this is the first and oldest stratigraphic unit of the Bone Spring Formation, which is split up into three major groups numbered third (oldest) through first (youngest). Each of these three groups contain a carbonate unit and a sand unit, thus bringing the total number of units in the Bone Spring to six. As seen on the more detailed stratigraphic column in Figure 11, the main members of focus for this study of the Bone Spring in depositional and chronologic order are 3rd Bone Spring Sand, 3rd Bone Spring Carbonate, 2nd Bone Spring Sand, 2nd Bone Spring Carbonate, 1st Bone Spring Sand, and 1st Bone Spring Carbonate. A further complication in nomenclature is that the 1st Bone Spring Carbonate is split into upper and lower divisions and encompass the Avalon complex (Hart, 1998; Crosby 2015).

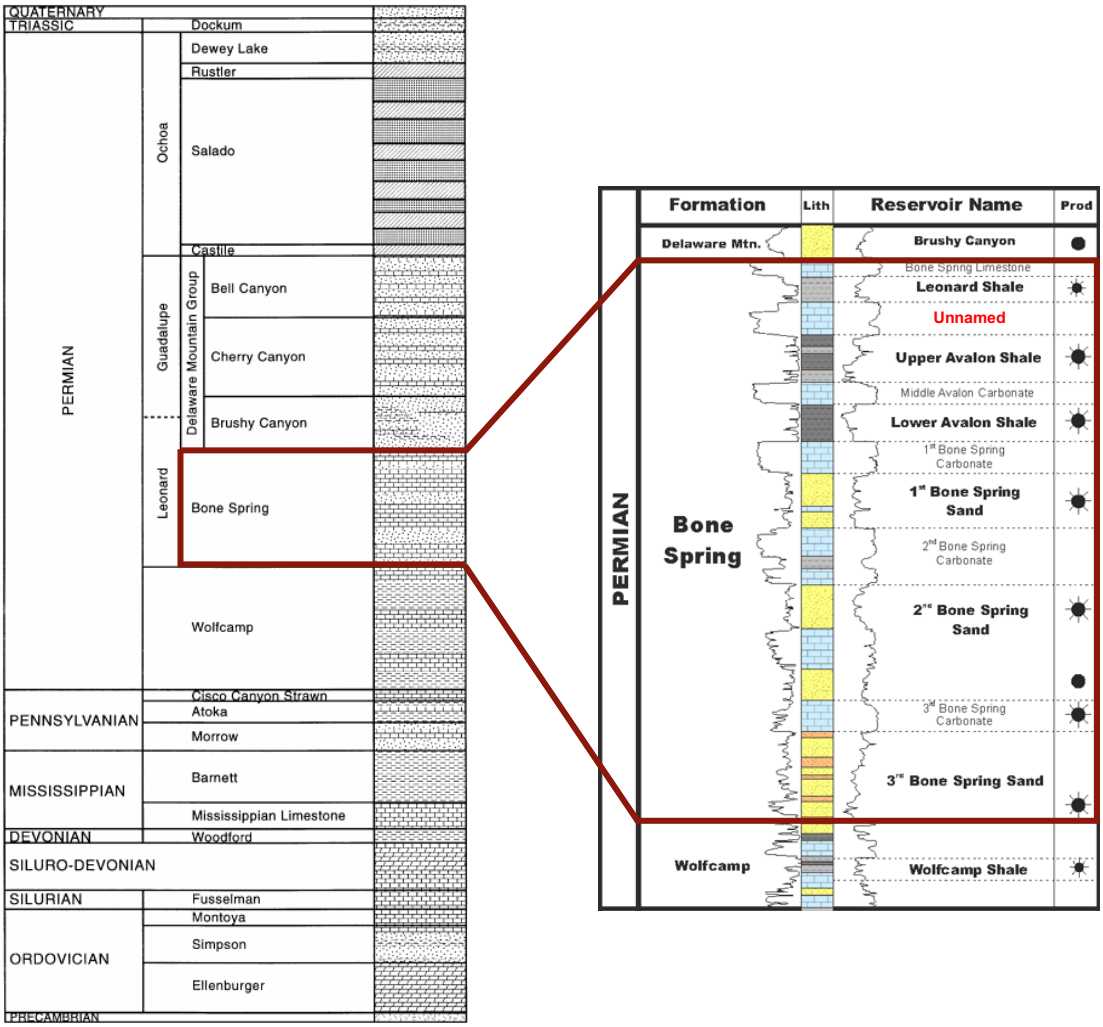

Figure 11: Stratigraphic column of the Delaware Basin incorporating the nomenclature of Hardage et al., (1998). Bone Spring Formation intervals and lithologies are enlarged, red boundary denotes intervals of interest. Oil and gas producing targets are annotated to the right. (Core Laboratory, 2014) ; (Bickley, 2019). Note that for the Bone Spring Formation there are twelve members.

Both Hart (1998) and Silver and Todd's (1969) studies suggest the inherited Wolfcampian topography had substantial impact upon the deposition of the Bone Spring. The two studies conclude the steep depositional topography of the Wolfcamp shelf is responsible for the progradational depositional style of the Bone Spring (Silver and Todd, 1969). As the Bone Spring was broadly deposited over the Wolfcamp, differential

compaction played an important factor in influencing the shelf to basin relief. The carbonate shelf deposits experienced significantly less compaction than the clastic material that was distributed in the basin, and this difference greatly enhanced the relief from shelf to basin (Silver and Todd, 1969).

Another important controlling factor to the deposition of the Bone Spring was the eustatic sea-level fluctuations. Silver and Todd (1969) argue that the cyclic depositional nature of the Wolfcampian through Guadalupian strata was caused by the eustatic sea-level change that was concurrent with basinal subsidence. The sea-level changes are believed to be predominantly controlled by global eustatic effects, such as glaciation; however, tectonics and varying rates of subsidence also play an important role in more regional changes (Silver and Todd, 1969). Nonetheless, as is shown in Figures 16, 25, and 26 the six cycles or twelve subcycles of HST zeniths and LST nadirs correspond exactly to the twelve members of the Bone Spring, suggesting that local tectonic subsidence and uplift pulses during this time were not powerful enough to overprint the global signal.

Guadalupian - Ochoan Deposition

After the Bone Spring deposition, the reciprocal sedimentation that had prevailed through the Leonardian drew to a close as the sea level fell and siliciclastics became the prevalent deposition in the Delaware basin. This dramatic change in lithology accompanying a regional unconformity marks the beginning of the Guadalupian sediment (Ross and Ross, 1995) The Guadalupian strata in order of deposition consist of the Brushy Canyon, Cherry Canyon, and Bell Canyon formations (Silver and Todd, 1969). During this time reefs flourished around the margins of the basin developed limestone

shelves, while the deposits in the center of the basin were mostly sandstone and siltstone (Adams, 1965). These central basinal deposits were transported through channels in the reef shelves, and broadly spread over the basin floor as turbidity flows (Adams, 1965). Reciprocal sedimentation once again prevailed but with especially notable changes in oxic anoxia as the Hovie channel opened and closed (Xu et al., 2018).

Towards the end of the Guadalupian the burgeoning carbonate reefs further restricted sediment from passing through, thus greatly reducing the sedimentation in the central area of the basin (Hills, 1984). The sea level fell again, and basin restriction continued causing the deposition of the Castile evaporites (Hills, 1984). This change in deposition is what creates the division between the Guadalupian and the Ochoan (Adams, 1965). The two main deposits of the Ochoan are the Castile Anhydrite and Salado Salt (Keller et al., 1980). These evaporites produced a widespread seal around 2,000 ft thick over the Delaware basin (Hills, 1984). By the end of the Permian the Delaware basin was largely the same that it is today with the exception of terrestrial red beds that prograded over the evaporites, and subaerial erosion through the early Mesozoic (Hills, 1984).

Chapter 3: Stratigraphy Introduction

In order to provide a more holistic approach to the stratigraphy, this study will combine both well log sequence stratigraphy and sequence stratigraphy. Sequence stratigraphy grants a way to subdivide, correlate and map sedimentary rocks observed in seismic data (Vail and Posamentier, 1988). It is a useful tool that will help to build a model to understand the controls that influence deposition such as; eustatic sea level fluctuations, sedimentation rates, and tectonic subsidence by using correlative time surfaces or unconformities to tie events in the rock record (Slatt, 2006). The primary surfaces that are used for correlation are sequence boundaries and maximum flooding surfaces, which are used to break the sedimentary record into sequences and parasequences, which indicate the depositional environment (Slatt, 2006).

In sequence stratigraphy there are many different approaches and disciplines, so it is crucially important to provide a glossary of terms that will be used through this study in order to provide a unified understanding of how these terms will be used through interpretations and further discussion. Most of the important stratigraphic terms that will be used are listed below and have been previously compiled in Bickley's (2019) thesis (Cosby, 2015; Catuneanu et al., 2011; McCullough, 2014; Zhou, 2014):

- Parasequence – A genetically related, conformable succession of beds or bedsets bounded by sub-regional correlative surfaces
- Sequence – A succession of genetically related strata during a full cycle of change in accommodation or sediment supply bounded by sequence boundaries

- Sequence Boundary – A regional surface that denotes the transition from one sequence to another. Vail and Galloway define sequence boundaries differently based on what is easily correlative on seismic or well logs respectively. This study attempts to compare well log and seismic stratigraphy and it is therefore essential to use a common definition of the sequence boundary. This investigation adopts the Vail sequence boundary which places sequence boundaries on the top of highstand systems tracts (Vail, 1987; Galloway, 1989).
- Maximum Flooding Surface – Interpretation of highest relative sea level. Marked by widespread silt/shale deposition in clastic sediments and can also be marked by blocky carbonate deposition in carbonates (May 2018).
- Lowstand Systems Tract (LST) – A systems tract deposited at a relative lowstand in sea level usually associated with increased process energy and progradation of coarser grained sediments into the basin. In the Bone Spring Formation, 3rd order LSTs correlate with the dominantly siliciclastic 1st, 2nd, and 3rd Bone Spring Sands as well as the Avalon Sand/Shale.
- Highstand Systems Tract (HST) – A systems tract associated with a relative highstand in sea level usually marked by progradation onto the maximum flooding surface. The HST is capped by the Vail sequence boundary (Vail, 1987). In the Bone Spring Formation, HSTs are associated with the dominantly carbonate deposition of the 1st, 2nd, and 3rd Bone Spring Carbonates.

- Transgressive Systems Tract (TST) – Sediments deposited during the onset of sea level rise usually following an LST. The TST is then caped by the maximum flooding surface.
- Falling Stage Systems Tract (FSST or RST) – Sediments associated with the onset of a drop in sea level deposited on top of the HST. In the Bone Spring this is associated with incision and erosion and the beginning of siliciclastic sediments being transported into the basin. At a higher order within relative LSTs, FSSTs can also be associated with carbonate erosion and slumping moving more carbonate sediment into the basin (Li, 2015; Pigott and Bradley, 2014).

Figure 12 shows provides a visual representation on a sea level curve for the systems tracts as well as a respective depositional model for each, showing shoreline movement and the erosion and or deposition that would be expected for each systems tract.

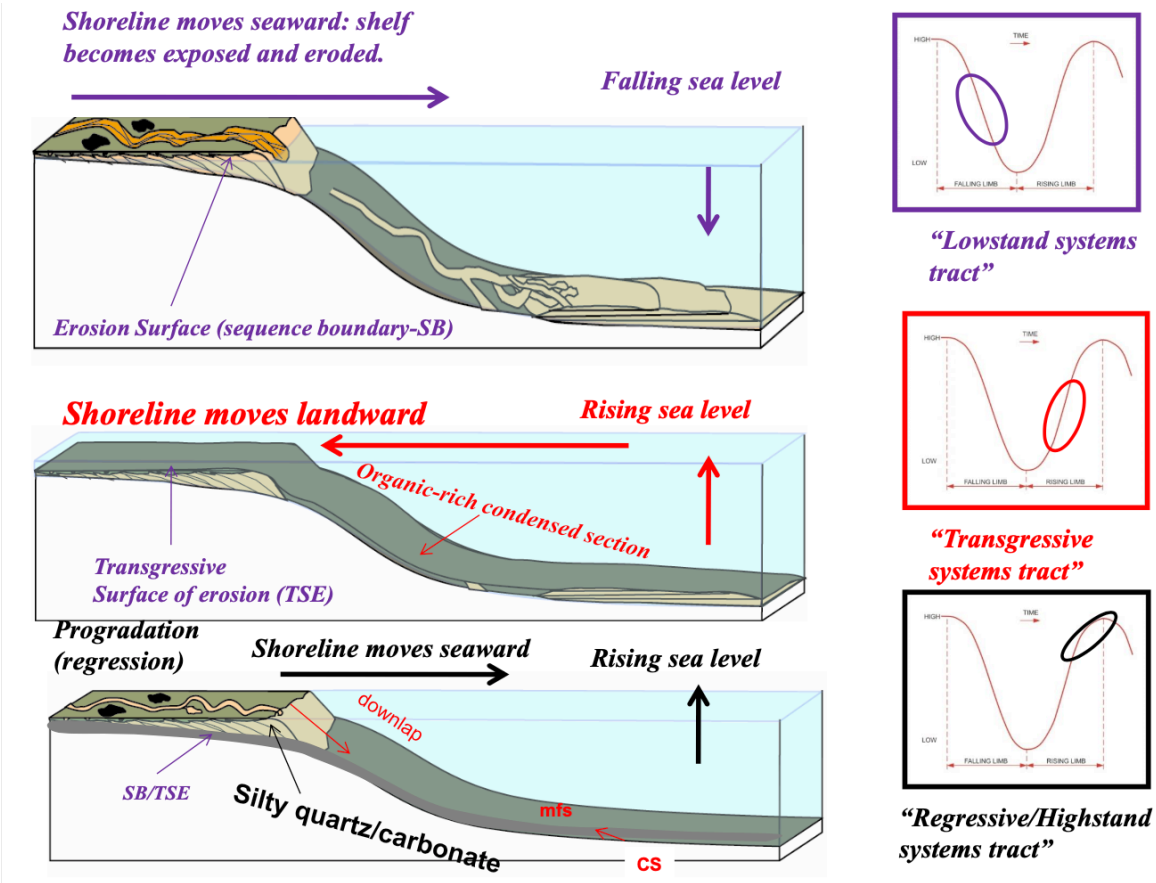

Figure 12: Model of sea level change showing Lowstand Systems Tract (LST), Transgressive Systems Tract (TST), Highstand Systems Tract (HST), and Regressive Systems Tract (RST) on a sea level curve on the right side, and their corresponding depositional models on the left (Slatt, 2013)

Figure 13 shows a more detailed sea level curve over a full period, showing all of the systems tracts and where they occur in the on the relative sea level curve. It also shows the type of depositions that would be expected during each systems tract.

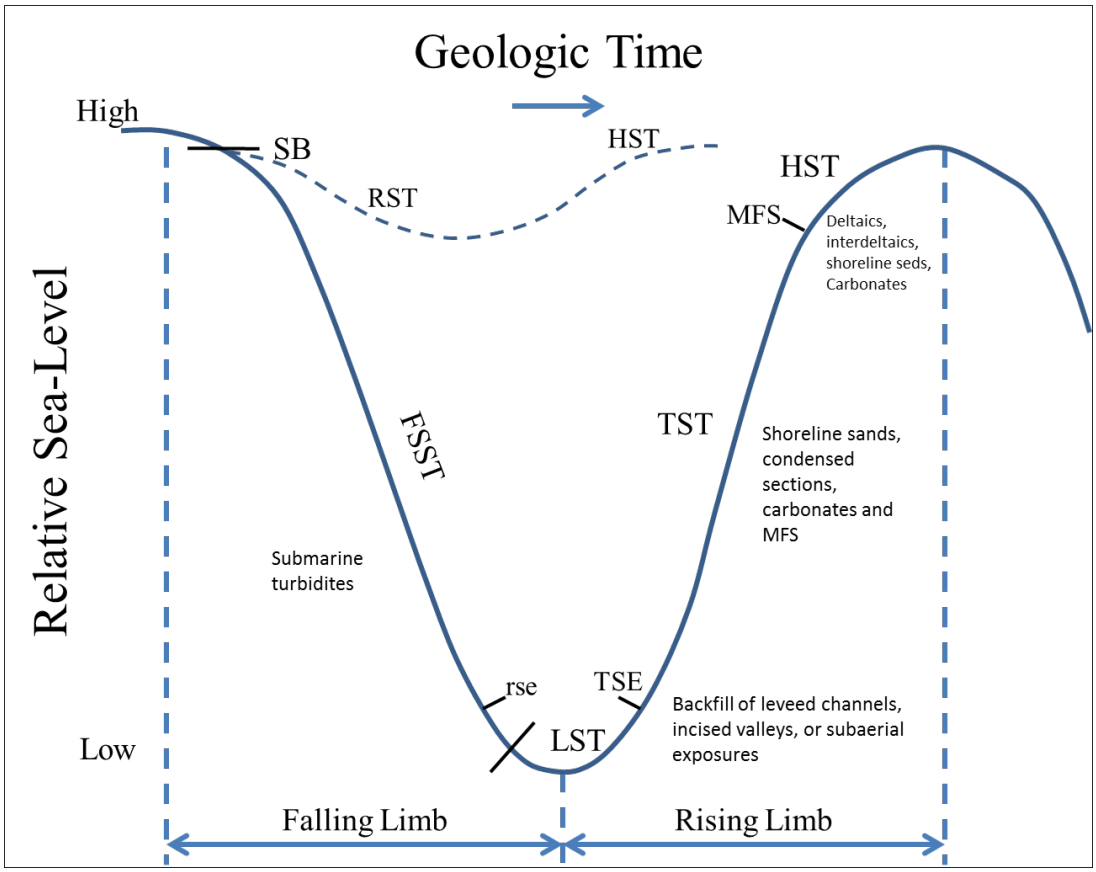

Figure 13: Diagram showing one complete relative sea level cycle starting with the falling limb and then rising limb and the corresponding stratigraphic systems tracts associated with, as well as the expected depositions at each stage (Slatt, 2006; Slatt, 2013; Crosby, 2015).

Reciprocal Sedimentation

The Bone Spring Formation is the prototypical model for reciprocal sedimentation, with distinct alternating beds of carbonates and siliciclastics. Wilson (1967) used the term reciprocal sedimentation while studying the Pennsylvanian in New Mexico, and produced Figure 14 showing processes, basin and shelf sedimentation at different sea levels.

Time	Process	Basin sedimentation	Shelf sedimentation
(4) *C*	Regression or stabilized low stand of sea level	Euxinic tidal flat limestone or gypsum	Exposure
(3) *B*	Shoaling possibly beginning	Dark shale or possibly little deposition in starved basin	Shoal limestone building out and up from shelf
(2)	Maximum inundation, water clearing	Dark shale but diminishing sedimentation	Normal marine limestone
	Maximum inundation	Dark shale	Calcareous shale with abundant normal marine fauna
	Deepening	Dark shale	Lower terrigenous member; either a transgressive sequence of channel fill or coarse gravel beach grading up to lagoonal sand and shale; or a regressive sequence of lagoonal shale grading up to bedded sands and conglomerate-filled channels
	Shallowing or stabilized sea level due to clastic infill		
(1) *A*	Transgression or sea level stabilized at a low stand	Cross-bedded lithic quartz sandstone	Exposure and downcutting of channels

Figure 14: Summary of relationships of shelf and basin cyclic sedimentation. Letters A, B, and C represent different sea levels with A being the lowest relative sea level, C the middle, and B the highest. It highlights the processes and the sedimentation in the basin as well as the shelf during one cycle. Modified from (Wilson, 1967).

Mullins and Cook (1986) describe reciprocal sedimentation as highstand systems tracts producing carbonate aprons and lowstand systems tracts as producing turbidite sand deposits. Since these two deposits are dependent on the sea level, and alternating sea level between relative high and low produce the reciprocal sedimentation. Scholle (2002) produced a model of reciprocal sedimentation of the Delaware basin (Figure 15) that shows platform sandstones and basin turbidites cut through the shelf and are deposited during the lowstand. The model also shows during a highstand that carbonates are formed on the shelf and dolomitized bioclastic packstones and mud-supported debris flows that are deposited in the basin. The model shows only one lowstand and highstand, but this model shows the depositions that repeat back and forth during cyclic sea level changes.

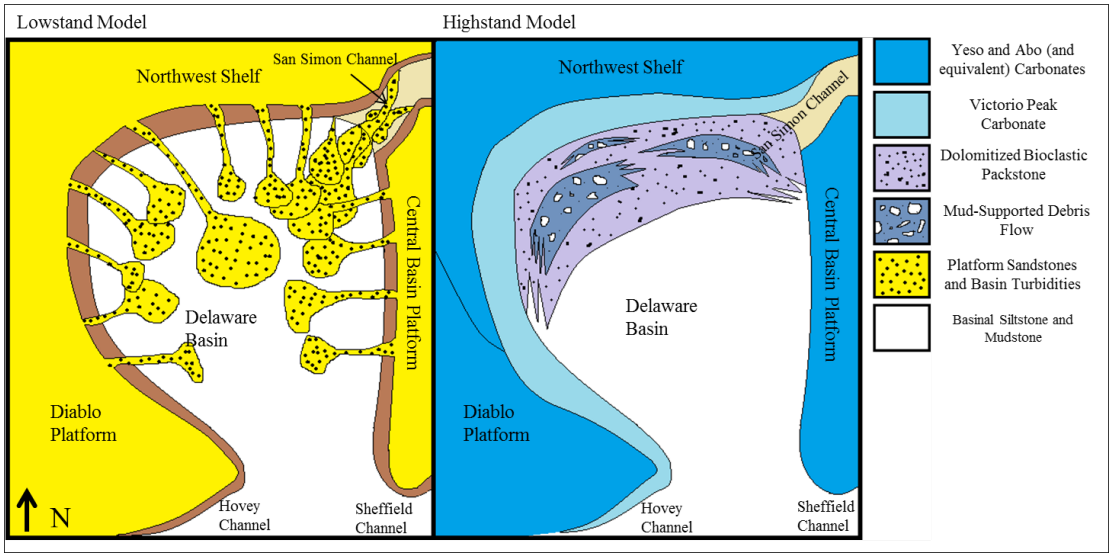

Figure 15: Simplified reciprocal sedimentation model of the Bone Spring Formation visualizing the deposition of siliciclastic turbidite fans and channel systems at relative lowstands and carbonate apron deposition at relative highstands (Crosby, 2015; Scholle, 2002).

Permian Sequence Stratigraphy

The Permian age units of the Delaware Basin are classified in the 1st order Absaroka Sequence or Supercycle of the North American Craton, this is considered to contain strata from the Latest Mississippian to the Early Jurassic (Sloss, 1963). In a later study, Sloss (1988) further divided the Absaroka Sequence into three subsequences and the Leonardian lies in the Lower Absaroka II. The Absaroka II has been designated to be a 2nd order eustatic regression that features lower sea level fluctuations than the underlying Absaroka I (Pennsylvanian – Earliest Permian), both in frequency and amplitude. However, the Absaroka II has higher fluctuations than the overlying Absaroka III (Triassic to Earliest Jurassic (Ross and Ross, 1995).

The Wolfcampian, Leonardian, Guadalupian, and Ochoan times of the Permian delineate cyclic sea level fluctuations within the 1st or 2nd order regression, while the Leonardian is discordant showing a stasis or very minor transgression. Each of these series have 3rd and higher order sequences within that have direct control on the deposition on each stratigraphic unit within. Figure 16 shows other controls to sedimentation, such as glacial intervals, onlap curve and sea level changes through the Permian.

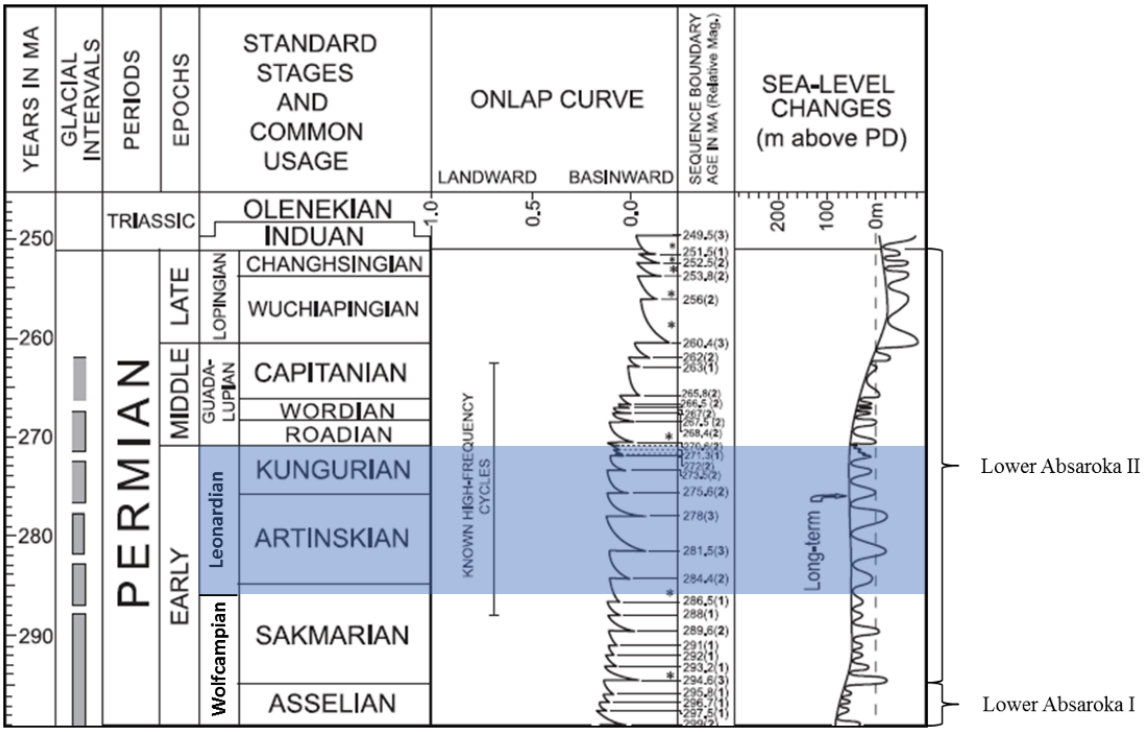

Figure 16: Geologic time scale through the Permian period which marks where the Leonardian lies in the Lower Absaroka II with respect to supercycles on the North American Craton that is introduced by Sloss (1963). (Haq and Schutter, 2008; Crosby, 2015). The six third order cycles of the Bone Spring Formation intervals are indicated in blue.

Wolfcampian

The Wolfcampian is comprised of the first five 3rd order sequence stratigraphic depositions of the Permian, while the first four of these are a continuation of the types of

short-term changes in sea level that are seen in the underlying latest Carboniferous (Ross and Ross, 1994). Both Veevers and Powell (1987) and Silver and Todd (1969) convey the significant impact that glacioeustacy had on the formation of the Early Permian by its influence on sea level fluctuations, however Silver and Todd (1969) also say that the still active tectonics and varying rates of subsidence are also considerable controls. The

Leonardian

The Leonardian is characterized to be deposited during a continued sea level rise and is lapped over the unconformable surface of the upper Wolfcampian (Silver and Todd, 1969). The Leonardian is estimated to contain from four to eight 3rd order sequences (Ross and Ross, 1994; Sarg, 1988; Ye and Kerans, 1996; Montgomery, 1998; Crosby, 2015), and the number is debated among all of these studies. This investigation will show that there are five 3rd order sequences, and sixteen 4th order sequences within the Bone Spring Formation. This series is internally complex, as increased carbonate production is theorized to cause the periods of cycles to be longer than the Wolfcampian series (Ross and Ross, 1995). Figure 17 shows a type log of the Leonardian deposited Bone Spring Formation in the study area.

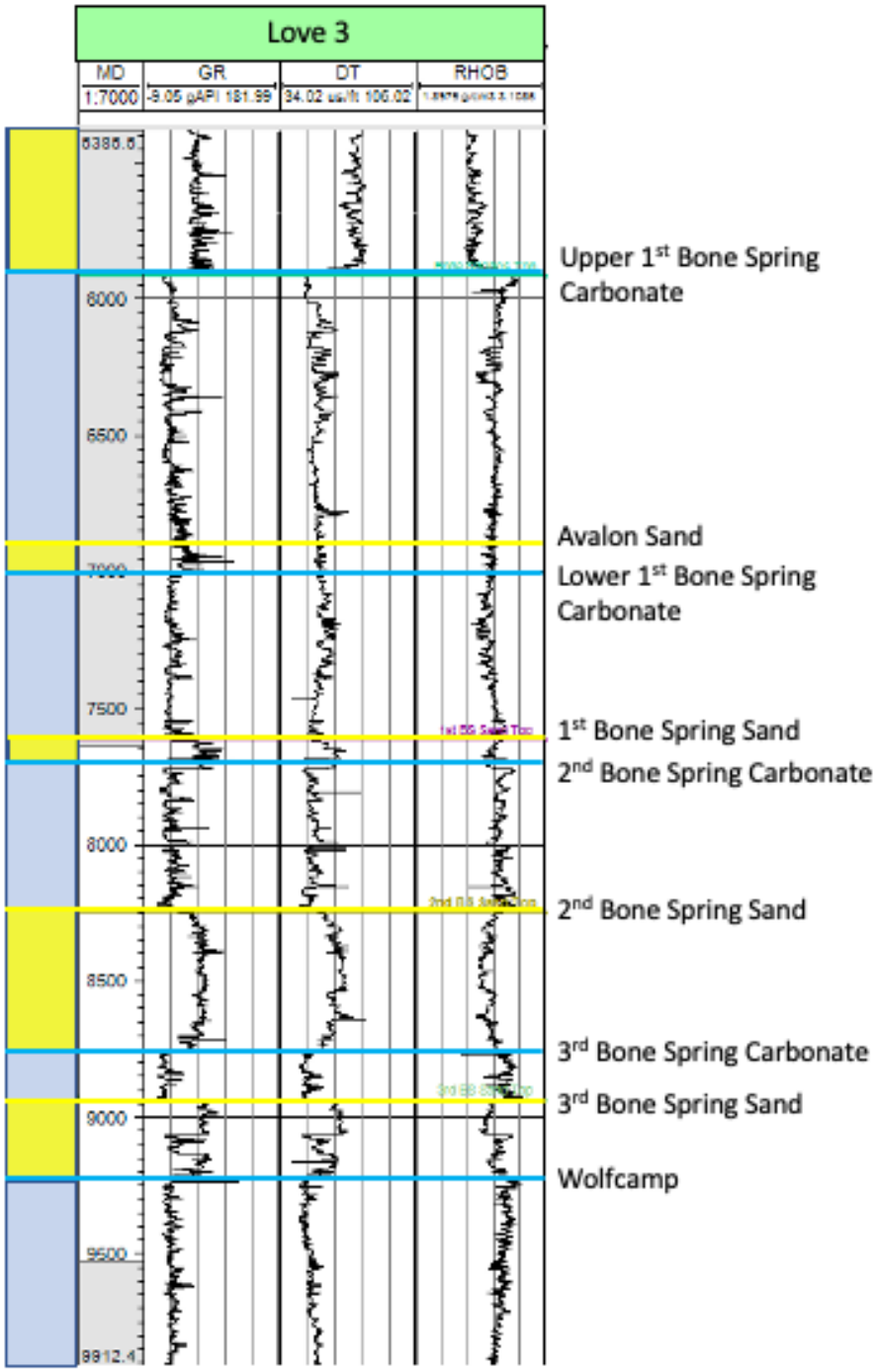

Figure 17: Type log from the study area defining the internal Bone Spring Formation tops picked over the study area. These tops agree with the oil and gas industry accepted, lithologically based standards. Also shown at the left are the 3rd order sequences identified which, due to reciprocal sedimentation, drive this alternation in lithology from highstand carbonates to lowstand siliciclastics. This log is centrally located in the study area and will be discussed in more detail later.

Chapter 4: Data Availability

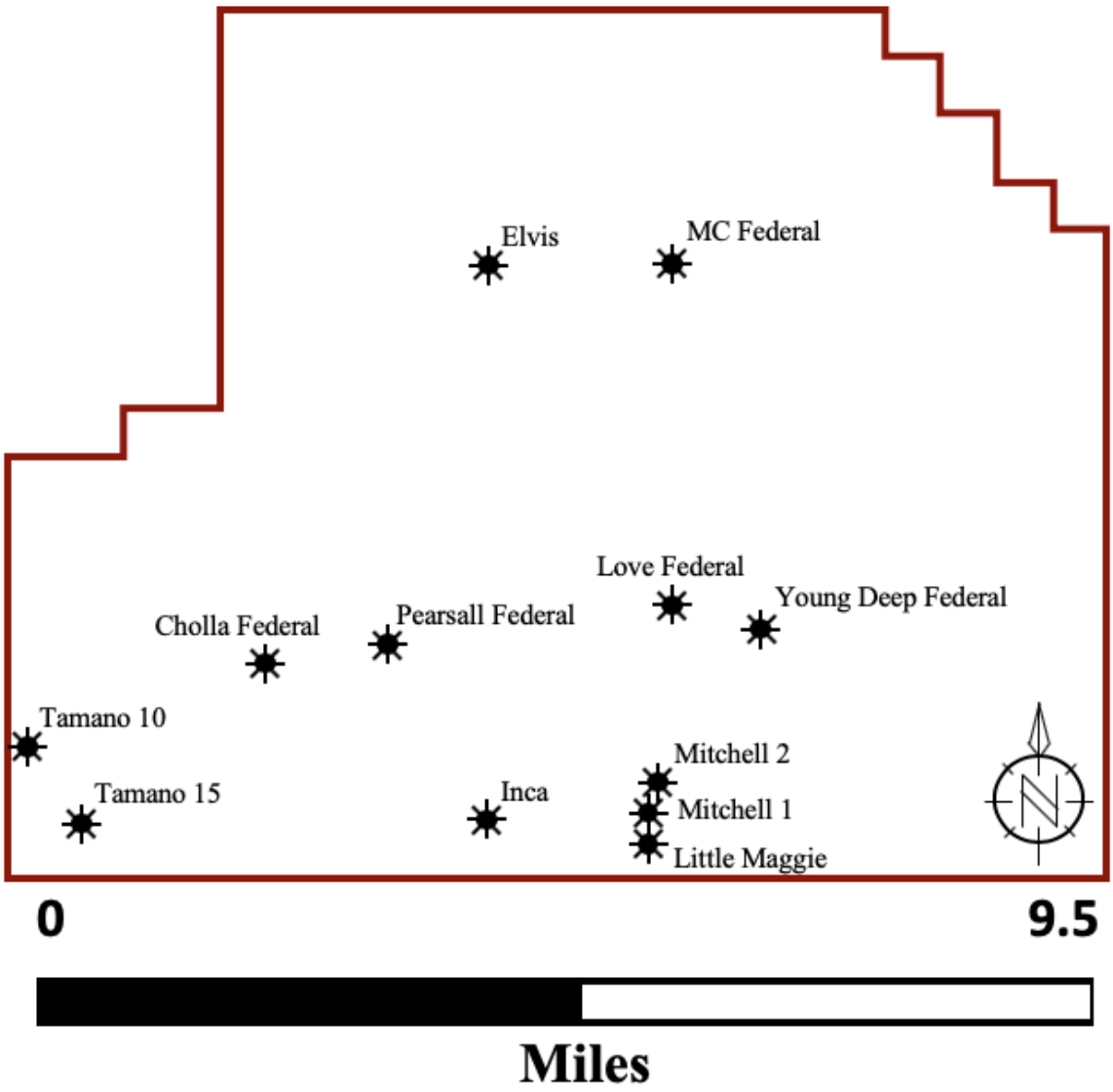

Figure 18: Map showing the available data used in this study. Shows the relationship of the approximate size and shape of the locations of a few key wells.

The 3D seismic survey used in this study is proprietary data that were generously provided by Schlumberger. Digitized well data from 21 wells were also generously provided by Mewbourne Oil Company, and the other 72 wells were collected from New Mexico Oil Conservation Division (NMOCD) and then digitized by a third-party. The

exact names and locations of the survey and wells other than a few key ones will be withheld to preserve confidentiality, since this area is actively being explored and developed by both Mewbourne Oil Company and Schlumberger. Figure 2 provides an approximate outline of the study location and Figure 18 shows the relative well locations and the shape of the seismic survey.

Log Data

Digital well logs were obtained for 93 of the wells within the study area, and then narrowed down to twelve that had sufficiently penetrated the Bone Spring and had gamma ray, sonic, and bulk density or neutron porosity logs.

Seismic Data

The 3D seismic data volume that was provided covers an area of ~100 square miles and was shot and processed by Schlumberger. In the past overlying evaporitic sediments in the Delaware Basin have caused acquisition problems because they obstruct seismic reflector data from the underlying strata. Newer methods afford much greater resolution by having a better bin size and higher CDP fold than previous methods. The higher resolution data is vitally important because it allows for more accurate interpretations, especially for finer intricacies that were not visible through older methods (Catuneanu, 2009). Since much of the Bone Spring was deposited through mass transport deposits and deep water fans with rapidly switching lobes, many of the internal reflectors appear to lack continuity (Figure 19), however some of the major reflectors can be distinguished. In the studied area the well log data are available which offers greater detail and permit more accurate seismic interpretations of chronostratigraphic surface continuity and correlation.

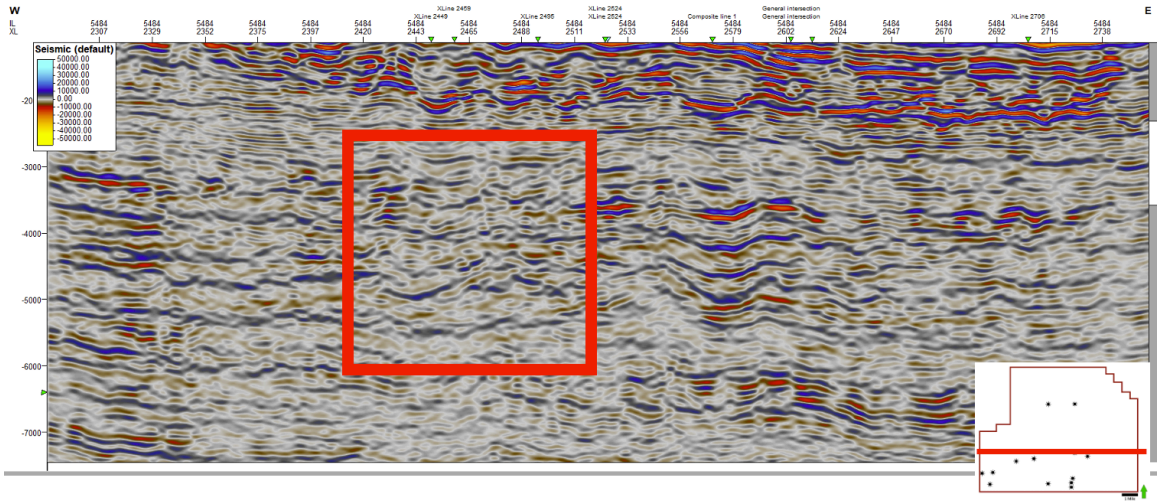

Figure 19: Seismic cross section displaying a large pocket where seismic reflectors are lacking continuity, highlighted inside the red square. While some reflectors are evident across the seismic, many cannot be followed through the survey.

The polarity of the data is SEG normal polarity, North American standard convention with peaks which reveal positive acoustic impedance reflections displayed in red and troughs in blue (Brown, 2011). Processing parameters are unknown. However, an example of the excellent seismic data quality can be seen in Figure 19 which displays the top of the Wolfcamp, which is the base of the Leonardian Bone Spring.

Important acquisition parameters for the survey are as follows:

- Record Length: 4000 ms
- Sample Rate: 2 ms
- Square Bin Size: 110ft
- CDP fold up to 420
- Inlines: 5399 - 5799
- Xlines: 2284 – 2765

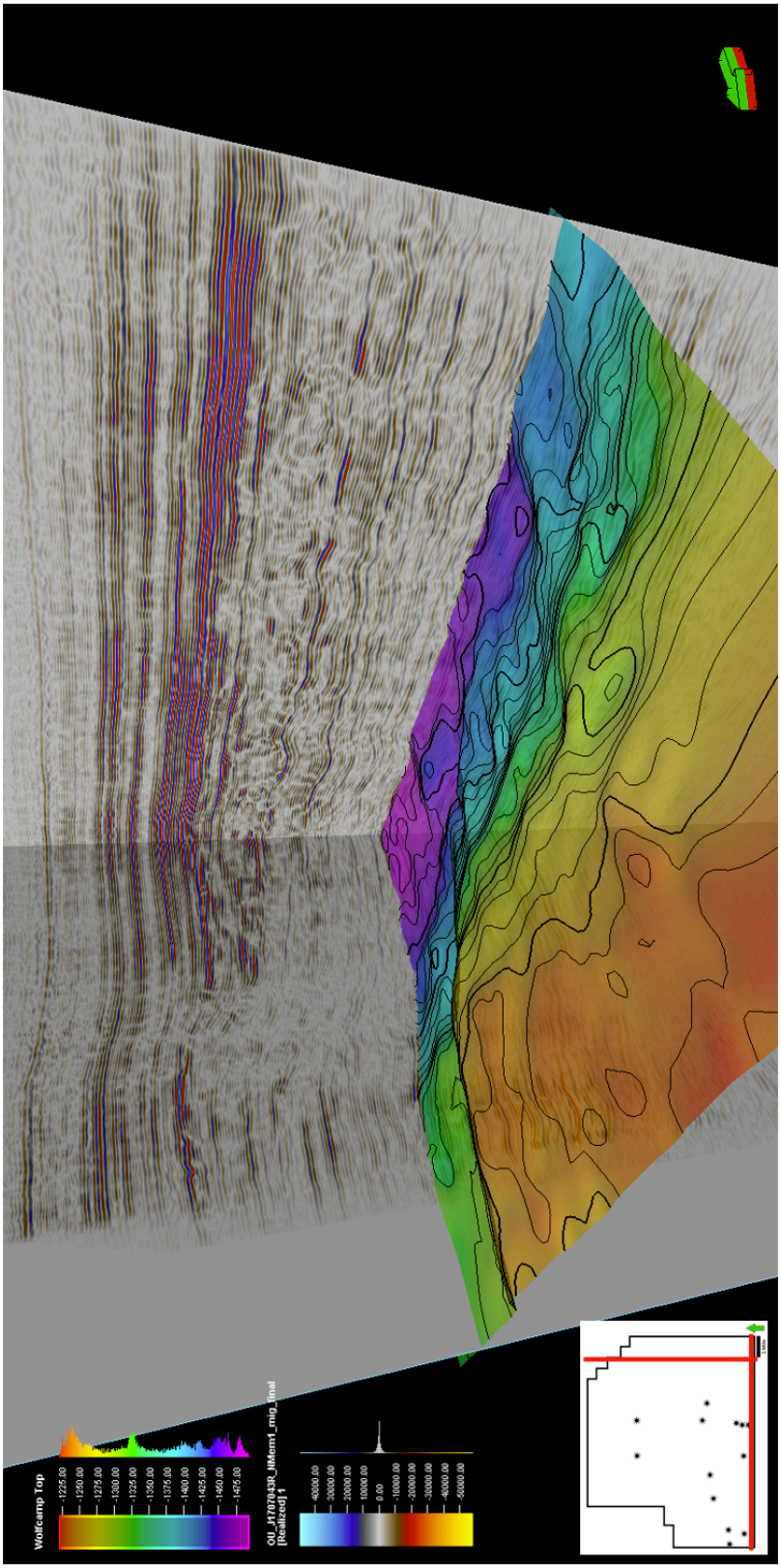

Figure 20: Example of the high-quality seismic survey used in this study. The figure offers a look from a shelf vantage point to the basin a crossline and tying inline with the pre-Bone Spring underlying Wolfcamp top mapped showing subsurface depth.

Chapter 5: Methods

Both well log sequence stratigraphy, herein termed using "Galloway motifs", which has a vertical resolution of centimeters but horizontal resolution of usually one meter or less and seismic stratigraphy, herein termed the "Vail procedure" which has a vertical resolution more than a decameter and a lateral resolution of hundreds of meters, each have their own merits and limits (Vail, 1987; Galloway, 1989). However, by incorporating both techniques which uses all of the available data a more holistic synthesis is possible with more accurate results (Pigott and Bradley, 2014). In other words, the use of both well log sequence stratigraphy and seismic stratigraphy in conjunction provides a higher resolution of understanding by filling in the figurative resolution gaps of each method alone.

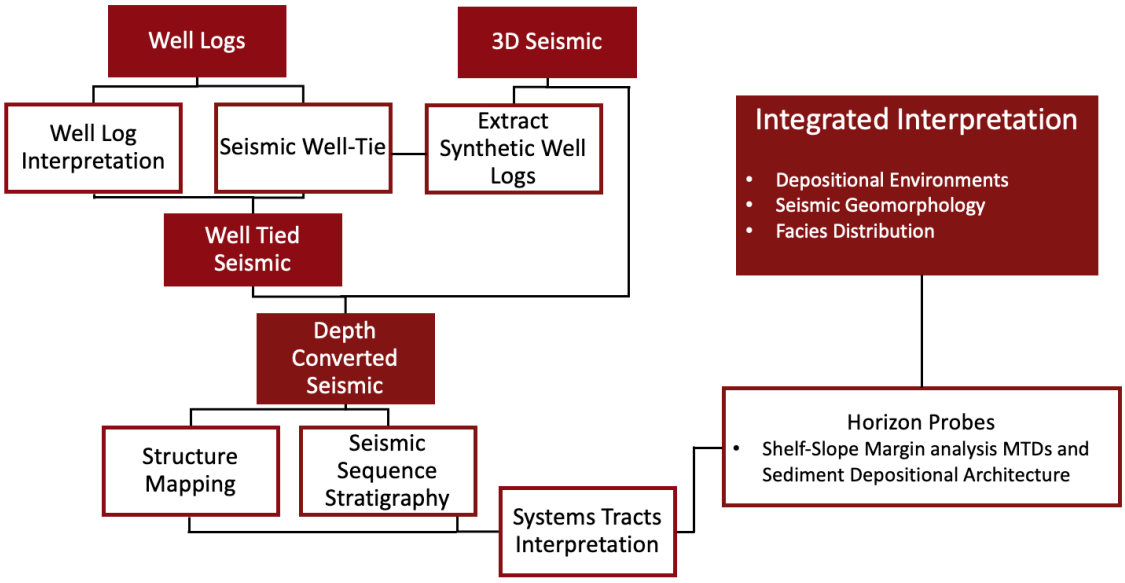

Figure 21: Workflow diagram illustrating the process of producing an integrated interpretating from well logs and 3D seismic.

Well Log Analysis

In this study the first objective of the well log analysis was to break out the major formation boundaries in each well and then correlate these boundaries across all of the wells. Many of the wells had public well reports that included industry produced well tops, however significant quality control was necessary, because not all of these tops were accurate and required more work to produce consistent tops across all wells. The major boundaries of importance from oldest to youngest include Wolfcamp top, 3rd Bone Spring Sand, 3rd Bone Spring Carbonate, 2nd Bone Spring Sand, 2nd Bone Spring Carbonate, 1st Bone Spring Sand, 1st Bone Spring Carbonate, Avalon, and Brushy Canyon. Although many of these named tops are associated with lithological changes, the reciprocal nature of deposition causes these changes to have sequence stratigraphic implications.

An adapted Galloway method (Figure 22) of sequence stratigraphy (Pigott and Bradley, 2014) was used to interpret and correlate wells through the Bone Spring.

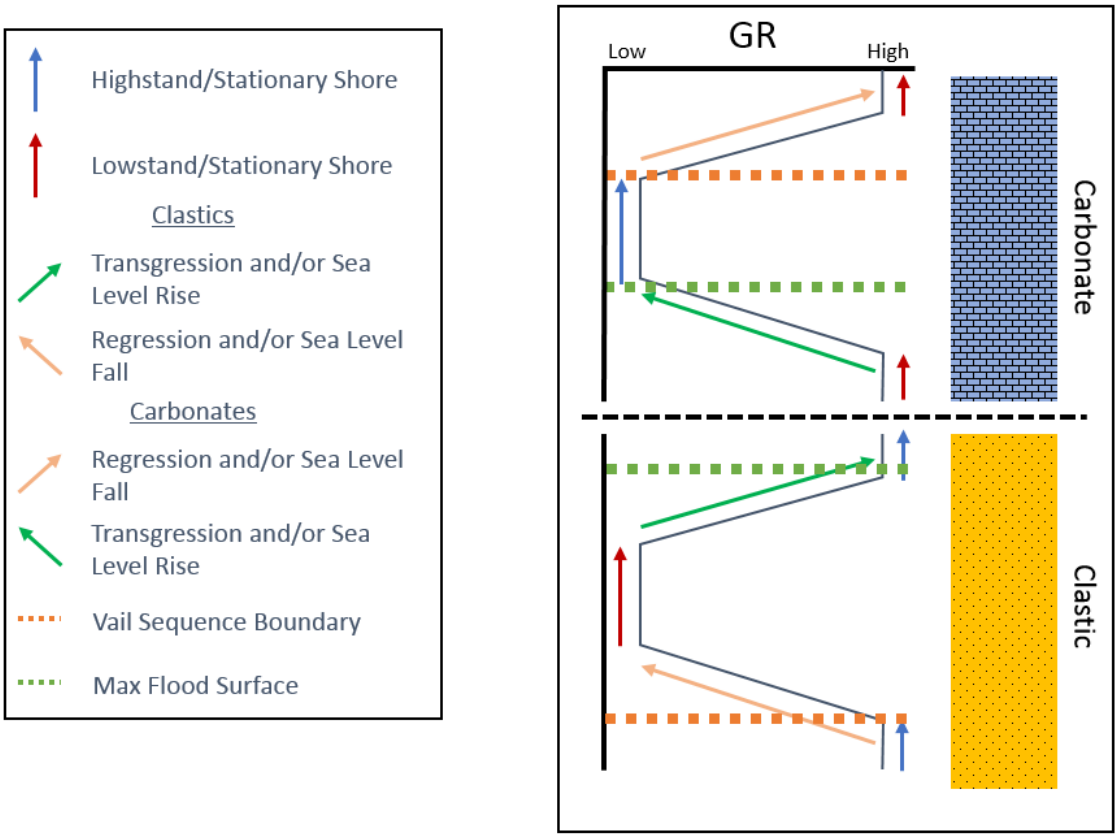

Figure 22: Simplified model of adapted Galloway sequence stratigraphic motifs using GR logs. The models contain a method for clastic and carbonate depositions. The clastic model adopts from the Vail approach and places sequence boundaries at the top of HSTs (Vail, 1987). For carbonates the motifs are flipped to depict clean, blocky carbonates at HSTs (Galloway, 1989; Pigott and Bradley, 2016; Bickley, 2019)

This adapted clastic carbonate Galloway approach (Pigott, unpublished Sequence Stratigraphy class notes) is conducive for sequence stratigraphy in mixed carbonate and clastic systems because it allocates a process for both sedimentation types into one approach. It uses the conventional Galloway approach, besides placing sequence boundaries at the top of Highstand Systems Tracts (HSTs) like is used in the Vail approach. It also flips the motifs when in carbonate depositions to better depict clean, blocky carbonates at HSTs. The primary log curve used in this method of analysis is the gamma ray (GR), which links itself to process energy of deposition and conjointly

lithology. Sonic, bulk density, and neutron porosity logs were also aided GR to corroborate lithologies, and also to integrate the well log data with the seismic. For example, increased carbonate content was observed to correlate with well patterns utilized in this study with increasing formation velocities and bulk densities, while decreasing porosity readings.

Seismic Analysis

The initial objective was to create synthetic well ties using sonic and density logs convolved with an extracted wavelet using HampsonRussell's (HRS) Geoview; synthetic seismic logs were then created and used to implement a seismic well-tie in HSR. An example of the synthetic well ties is displayed in Figure 23. These ties were then moved over to Schlumberger's Petrel software, where horizons of importance that were consistent with parasequence set boundaries were manually mapped through the seismic survey. Horizons that were mapped include the top Wolfcamp, and each of the Bone Spring intervals (Figures 31 through 37). Each of these horizons give valuable information that can only be inferred when using correlations between well logs alone, such formation thicknesses, depositional topography, channeling or other pathways of transportation, and stacking patterns that all influence the deposition of the Bone Spring.

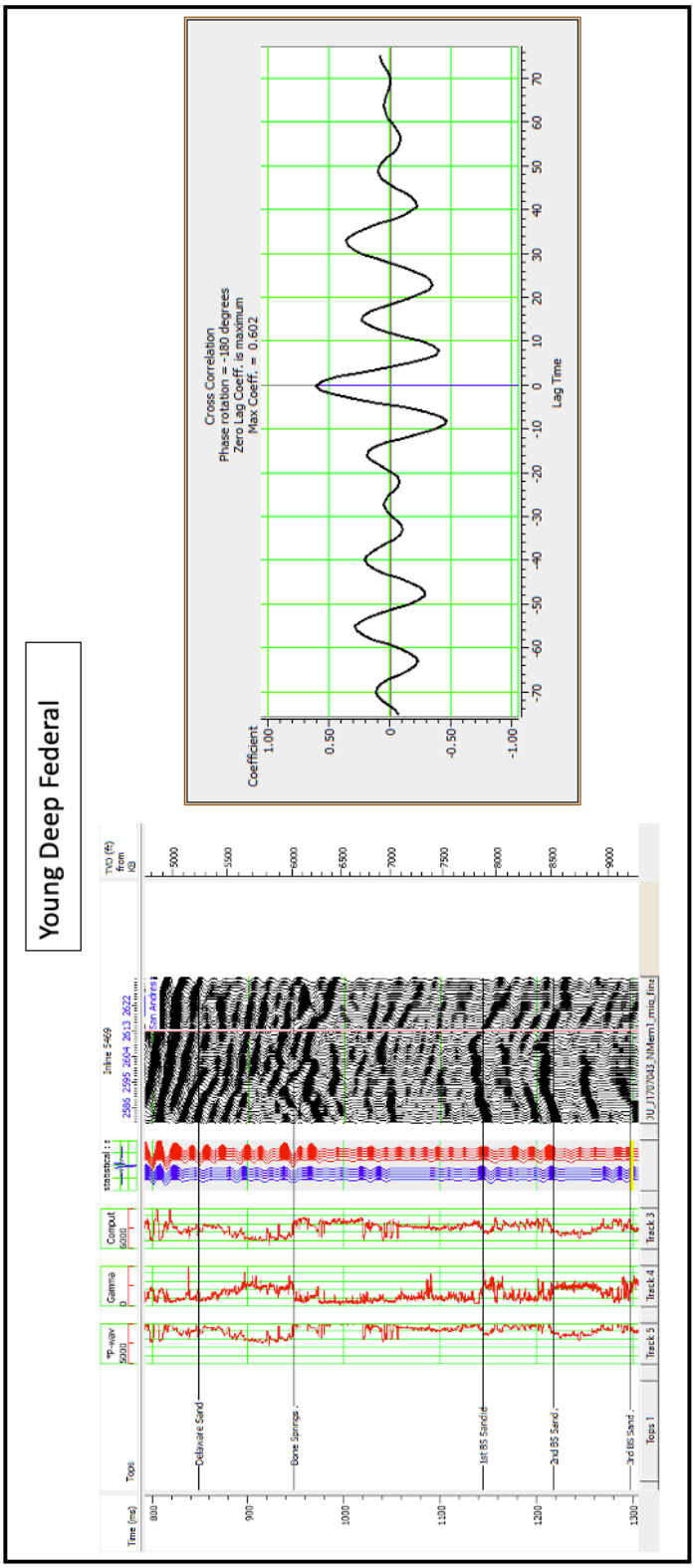

Figure 23: An example of the seismic well ties that were generated on every well used in the study and the cross correlation coefficient of the well tie. A phase rotation of -180 degrees was used to achieve the maximum coefficient between the logs synthetic seismic and the seismic data.

The Vail approach was then used to pick seismic terminations on seismic slices that intersected well positions (Vail, 1987). These terminations represent 3rd order sequence boundaries, which were then used to subdivide the Bone Spring into five operational sequence sets (procedure of Radivojevic and Pigott, 2010; Bradley and Pigott, 2014). This study aims to interpret the stratigraphic significance of the internal reflectors by integrating 4th order adapted Galloway motifs with the seismic (Galloway, 1989).

Many of the seismic reflectors within the Bone Spring are severely of limited continuity, which causes interpretations to be problematic. This is likely owing to the turbulent nature of the sediment gravity flows and mass transport deposits that comprise the Bone Spring.

Chapter 6: Results

Well Log Analysis

This section will demonstrate the results through the mapping process and display the created maps in an attempt to illustrate the process as well as the results. Since the primary focus of this study is the 1st, 2nd, and 3rd sand intervals of the Bone Spring, the 1st Bone Spring Carbonate will be considered one cohesive unit throughout, rather than splitting out the 1st Bone Spring Carbonate into upper and lower units around the imbedded Avalon unit like is seen in many studies.

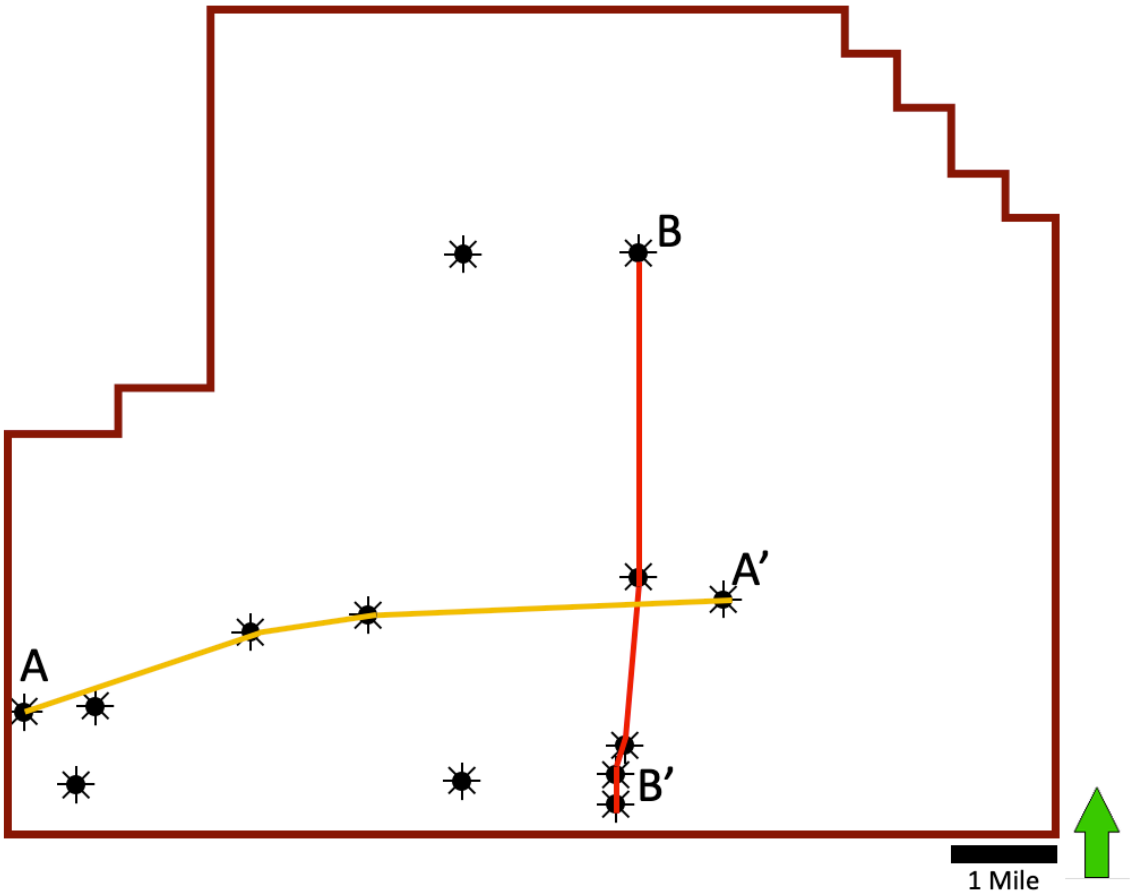

Figure 24: Cross section locator map showing the path of depositional strike cross section, A-A', and depositional dip cross section B-B' which are shown in Figures 25 through 28.

Well Log Sequence Stratigraphy

Through the sequence stratigraphy it is important to contextualize the relationship to the Permian age sea level curve (previously seen in Figure 16), more specifically the Lower Absaroka II 1st order regression. The Leonardian Bone Spring Formation being bounded by 2nd order sequences boundaries or unconformities gives definable boundaries to the interval of interest.

3rd and 4th order sequences were broken displayed on Figure 25 (A-A') and Figure 26 (B-B'). To do this, the adapted Galloway motifs were applied to the entirety of the Bone Spring Formation starting at the Wolfcamp Formation top to the top of the upper 1st Bone Spring Carbonate. Owing to the reciprocal nature of the sedimentation in the Bone Spring, the large shifts in the gamma ray make for obvious sequence boundaries and also make for less complicated correlations between wells.

A total of five 3rd order sequences were mapped out through the Bone Spring and were correlated across each well. These 3rd order sequence boundaries were used as a framework to correlate wells as they are consistent and discernible in each well.

Higher 4th order sequences are less consistent from well to well than aforementioned 3rd order, and while this makes correlation more challenging it offers valuable insight into the subtle discrepancies across the study area. Starting from the bottom of the section, most of the wells that display the 3rd Bone Spring Sand and Carbonate both exhibit two full 4th order sequences. The 3rd Bone Spring Sand displays two spikes across wells that are likely interbedded shales indicative of relatively brief sea

level regression. The subsequent carbonate interval is relatively ephemeral compared to the other carbonate intervals.

The 2nd Bone Spring Sand has a slightly lower gamma ray profile than the 3rd, which could be indicative of the increased amounts of intraformational carbonates and greater carbonate production at the time of deposition. The 2nd Bone Spring Sand shows three complete 4th order cycles through the interval, with one well showing a fourth cycle and does not exhibit similar gamma ray spikes that are seen in the 3rd Bone Spring Sand. The top of the sand gradually transitions to the carbonate interval as opposed to the sharp boundaries that are present in the other intervals. The overlying carbonate shows two 4th order cycles and demonstrates a large spike in the gamma ray reading, that is similar to what is observed in the 3rd Bone Spring Sand.

The 1st Bone Spring Sand shows more variance from well to well than the other sand intervals. The wells on the western side of the study exhibit a thick gamma ray profile with two 4th order cycles, while the wells on the eastern half of the study show a much thinner interval and are comprised of only one 4th order sequence. This variation appears to correlate to the thinner underlying 2nd Bone Spring Carbonate interval in these wells so conceivably the wells on the west side of the study area benefited from increased available accommodation space. The 1st Bone Spring Sand also has several spikes in the gamma ray, again likely to be from organic rich shales that are interbedded.

The lower 1st Bone Spring Carbonate has two 4th order cycles that are mostly contained to the bottom of the interval and capped with a clean, blocky carbonate section indicative of a highstand systems tract that is makes way to a sharp contact of that Avalon Sand, which acts as the division between the upper and lower 1st Bone Spring Carbonate.

The Avalon is a relatively thinner sand interval, that is initiated by a 4th order sea level regression, marking an abbreviated lowstand and contains a similar gamma ray spike as mentioned before in some wells, so is presumably from channel migrations. The Avalon deposition is ended with a 3rd order transgression where carbonate production begins again and deposits the upper 1st Bone Spring Carbonate, which is continues the clean, blocky carbonates that are seen just before the Avalon deposition. Two brief 3rd order cycles break up the otherwise clean carbonate deposition.

In terms of 3rd order cycles, examination of the clastic stratigraphic column of Figure 25 with that of the global sea level curve, Figure 26, shows a remarkable correlation of six major cycles. For example, the six HST's and six LST's correspond to the six zeniths and six nadirs of sea level rise and fall, respectively. If this correspondence is not accidental, then this strongly suggests the third order cycles represent allocyclic global eustasy and the fourth and higher order cycles indicate autocyclic changes in local deposition. The ensuing seismic sequence data interpretation will further support this hypothesis.

As mentioned in the previous chapter, the adapted Galloway requires the carbonate sections to have the motifs flipped to denote clean, blocky carbonates to be accurately accounted and has been applied accordingly.

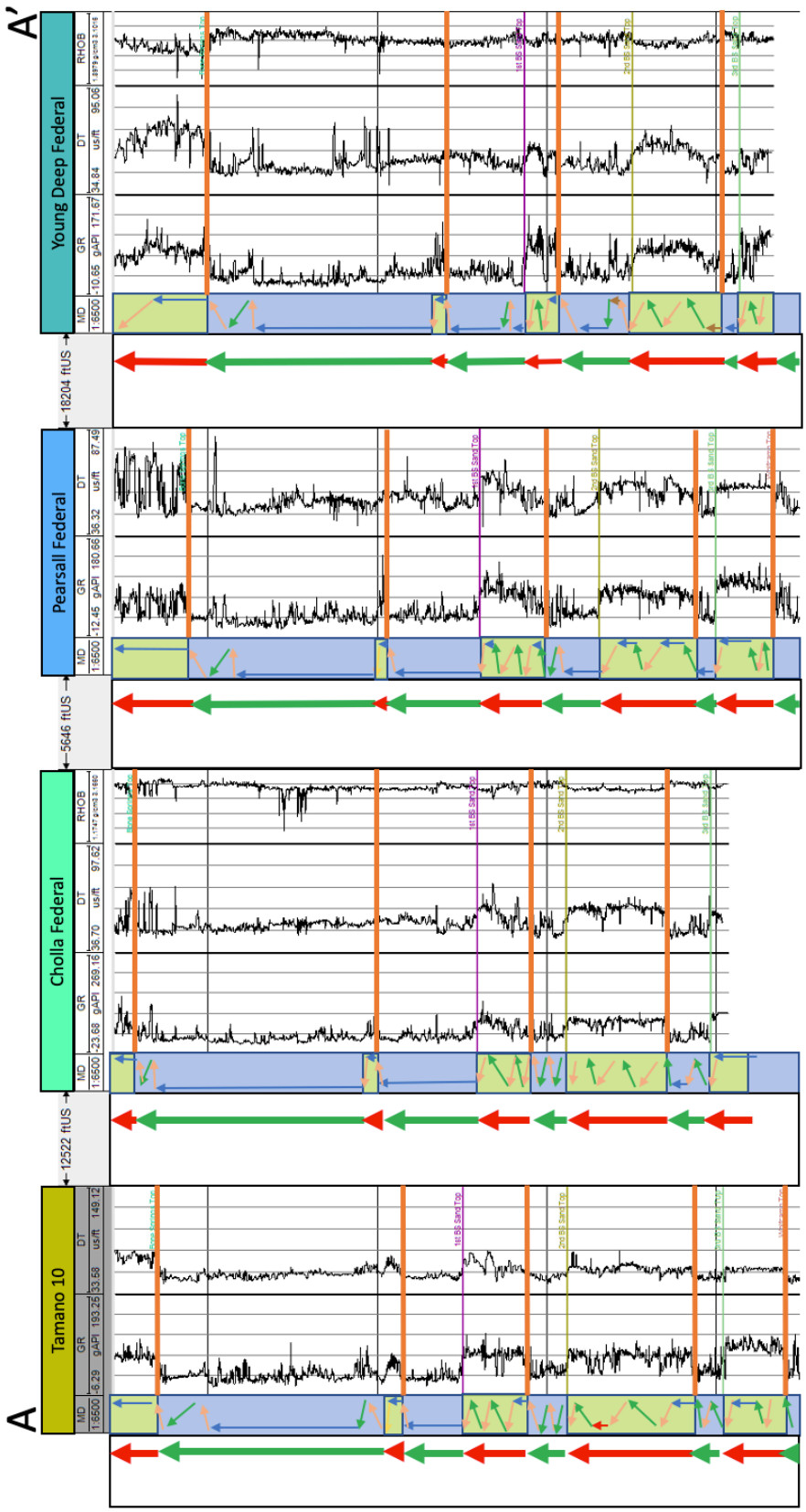

Figure 25: Cross section A – A' breaking out 3rd order sequence boundaries with orange lines across the logs. Small arrows break out the 4th order sequences.

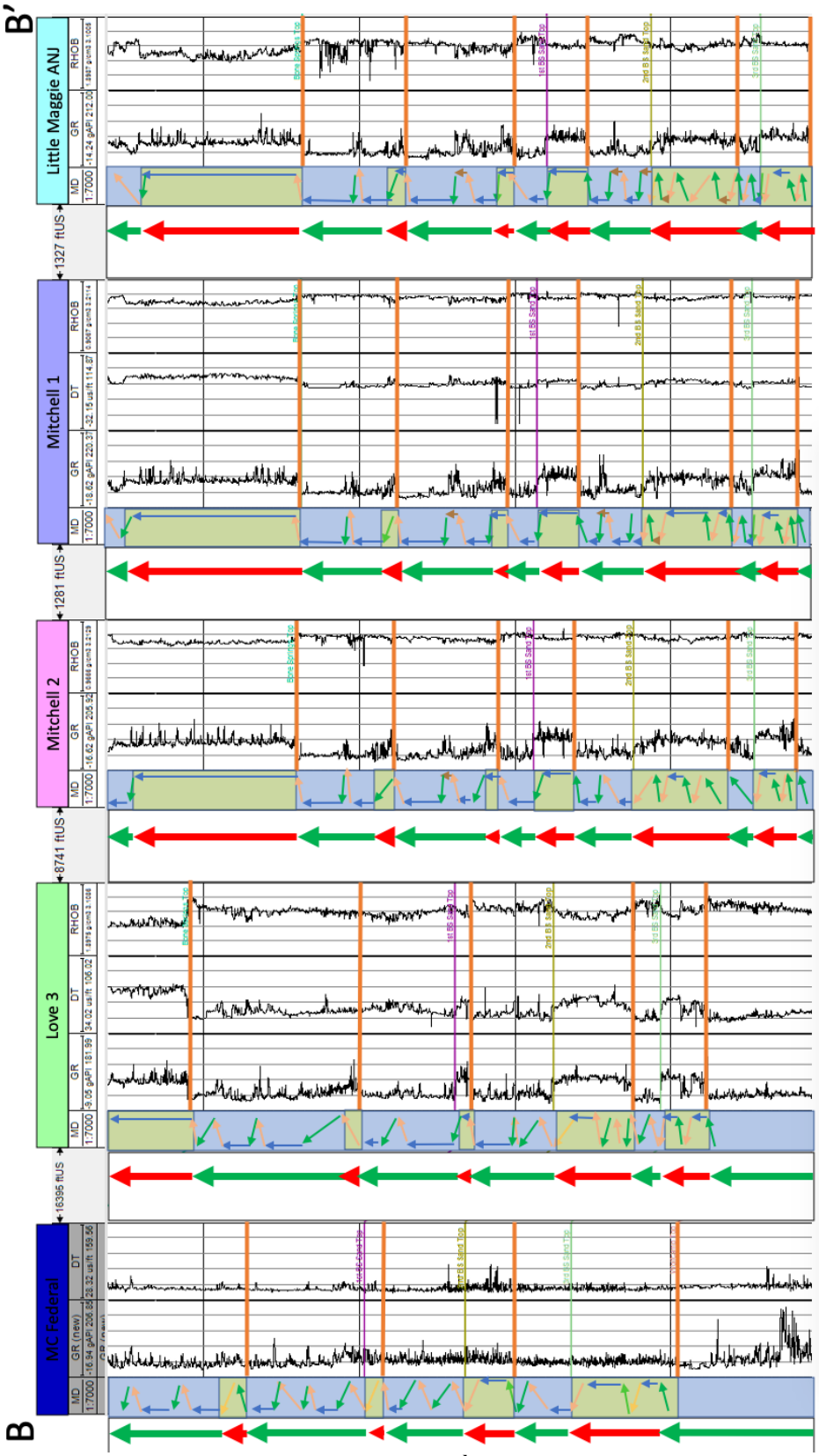

Figure 26: Cross section B - B' breaking out 3rd order sequence boundaries with orange lines across the logs. Small arrows break out the 4th order sequences.

Depositional Dip and Strike Cross Sections

To begin the well log analysis a depositional dip and strike cross section were determined to give the best coverage over the study area using the available wells. Figure 24 illustrates the two cross section lines that were selected, A to A' contains four wells that trend east to west along the depositional strike of the area, and B to B' contains five wells and is oriented north to south down depositional dip and offer a view of the from the shelf to the basin. Figure 27 (A–A') and Figure 28 (B–B') display these two cross sections in a fence diagram correlating the Bone Spring sand dominated intervals denoted by yellow and carbonate dominated intervals with blue across the wells. In the cross sections on Figure 27 and 28 the dominate lithology color coded, yellow for siliciclastic intervals and blue for carbonates.

The depositional strike cross section reveals the variability in the thickness of the Bone Spring intervals, especially the 1st Bone Spring Sand and 3rd Bone Spring Carbonate. Such variations are likely owing to the differing accommodation and transportation pathways, such as channels that were available at the time of deposition. In general, a thinner underlying interval appears to lead to a thicker interval being deposited above. Such compensational stacking (term after Mutti and Sonnino, 1981) is especially evident in the second well where a thin 1st Bone Spring Sand allows for a thicker carbonate section to be deposited on top. In contrast, the depositional dip cross section appears less affected by these channels therefore shows much more consistent thicknesses down the slope. As these cross sections are all displayed at the same scale and are hung on the same measured depth of 5,000ft as a consistent datum, paleo basin deepening of the intervals increases southward.

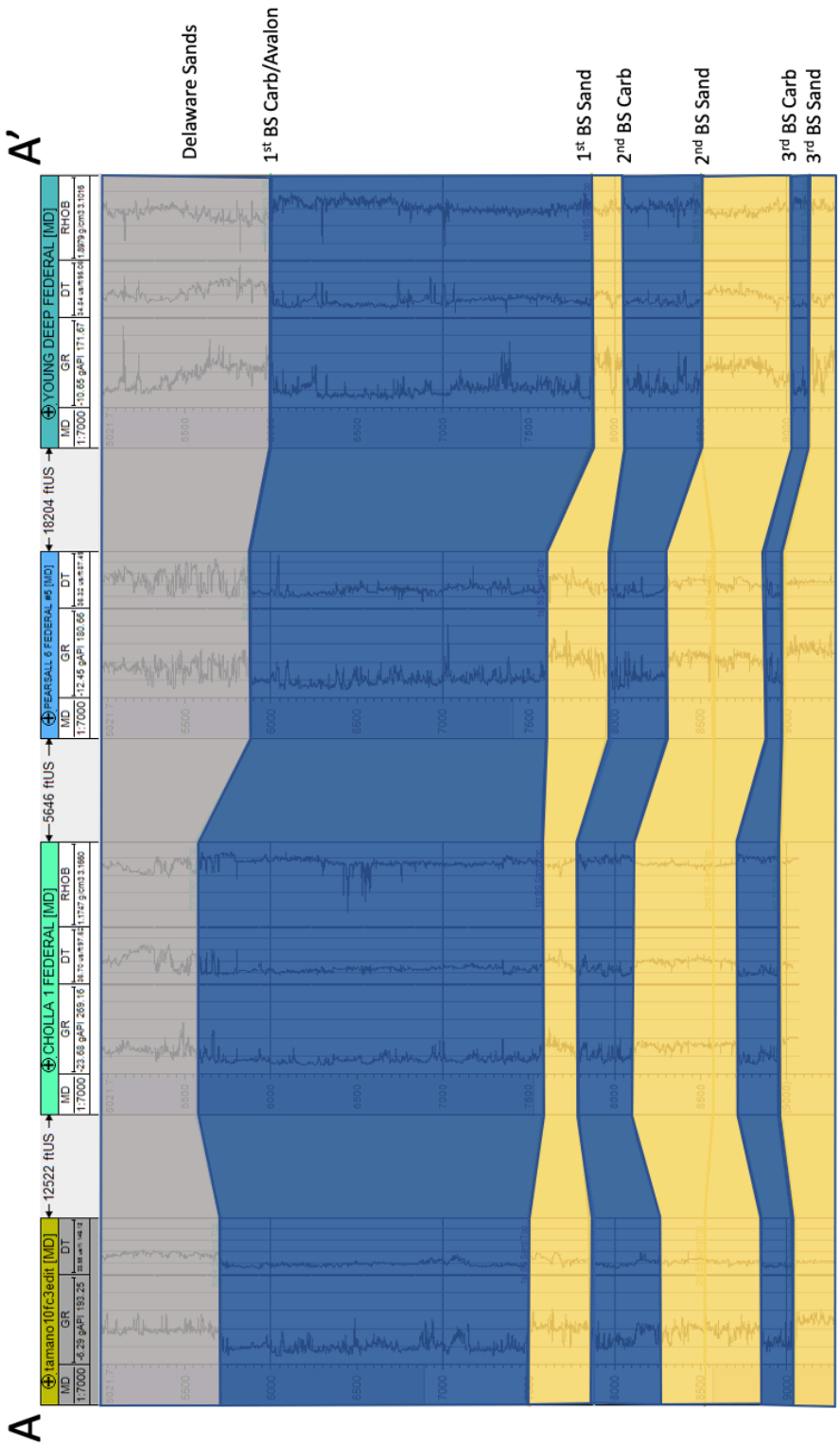

Figure 27: Cross section A – A' showing depositional strike. Highlighting the Bone Spring intervals, color coordinated for yellow to represent sand intervals and blue for carbonates. This figure illustrates the difference in interval thicknesses across the depositional strike.

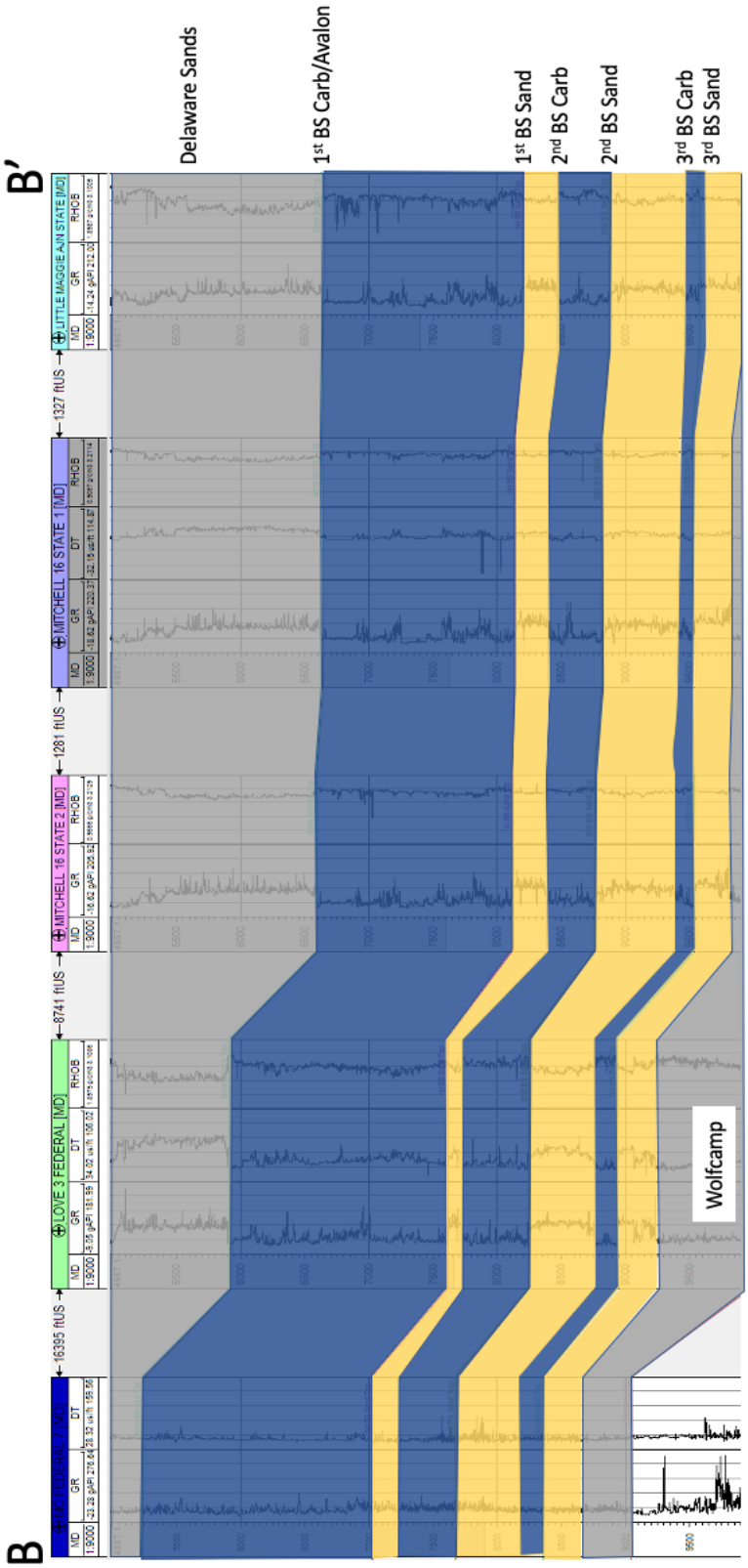

Figure 28: Cross section B – B' showing depositional dip, with the same color coordination as cross section A – A'. This figure illustrates the difference in interval thicknesses across the depositional dip.

Seismic Analysis

Following the petrophysical analysis and application of the Galloway motifs, the well logs were tied to the seismic and were imported into Petrel. Major faults were picked, and formation tops were mapped out. Figures 29 through 35 reveal some of the formations that were mapped out, the Wolfcamp, the 3rd Bone Springs, 2nd Bone Springs, and the 1st Bone Springs. Time structure, and isochron maps were then constructed as are shown in Figures 39 through 45.

Structure Maps

The importance of depositional topography is an integral part of the deposition of the subsequent formations owing to the accommodation, angle of relief, and both transportation barriers and pathways. The top of the Wolfcamp is this foundational control for the Bone Spring Formation and has been mapped in Figure 31 and includes a fault zone that trends North to South that provides another direction of relief that sediments likely were transported down. This fault zone has also been mapped in both cross sectional view in Figure 30 and in map view in Figure 29. This is a compressional fault that has a significantly larger displacement on the eastern block of the fault that controls deposition into the Bone Spring. These two figures display the extent of this fault and why it is influential on sediment transportation. The fault provides considerable accommodation space, however has waning effects on deposition throughout the Bone Spring.

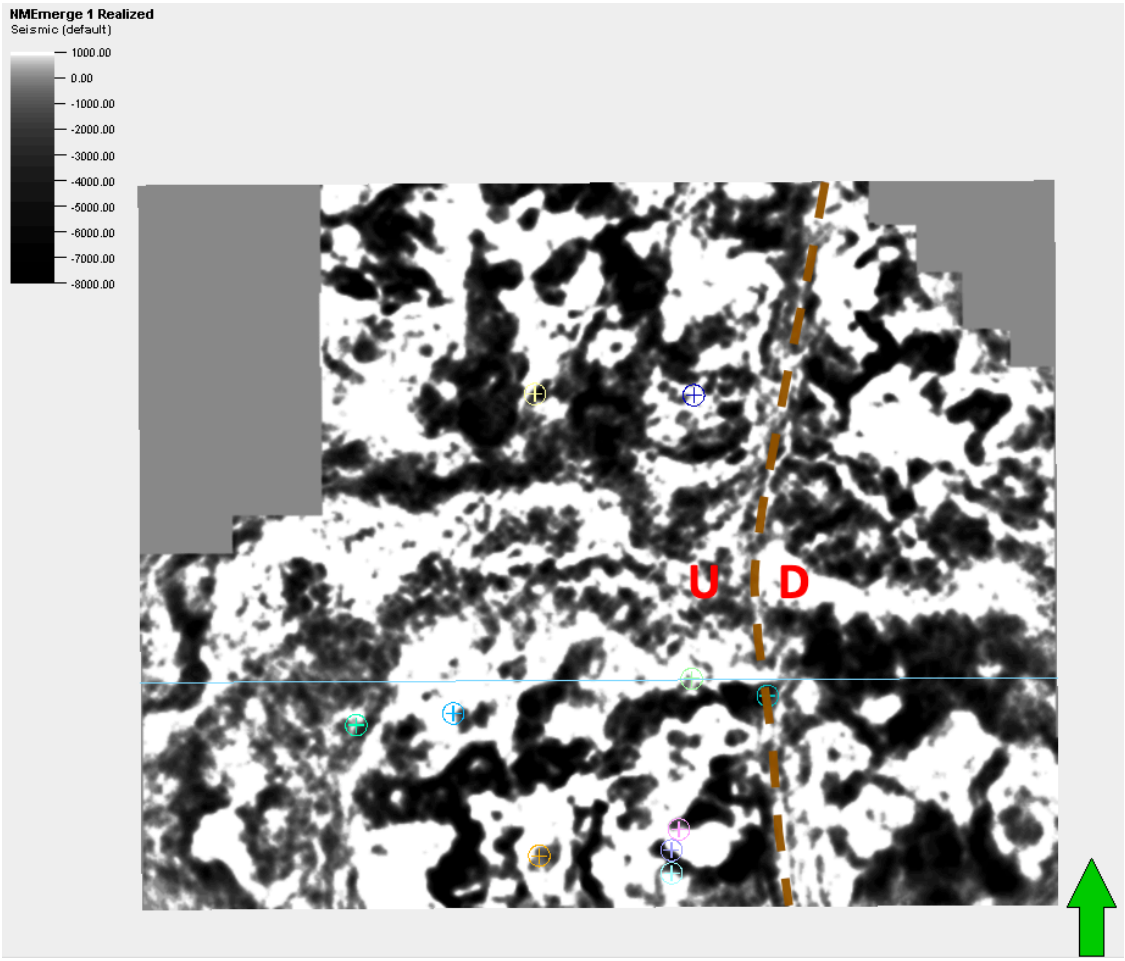

Figure 29: Seismic map view below the Wolfcamp top displaying a large fault zone passing through the entirety of study area. The East side is the downthrown block and provides significant accommodation space. The color scale was clipped to highlight contrast.

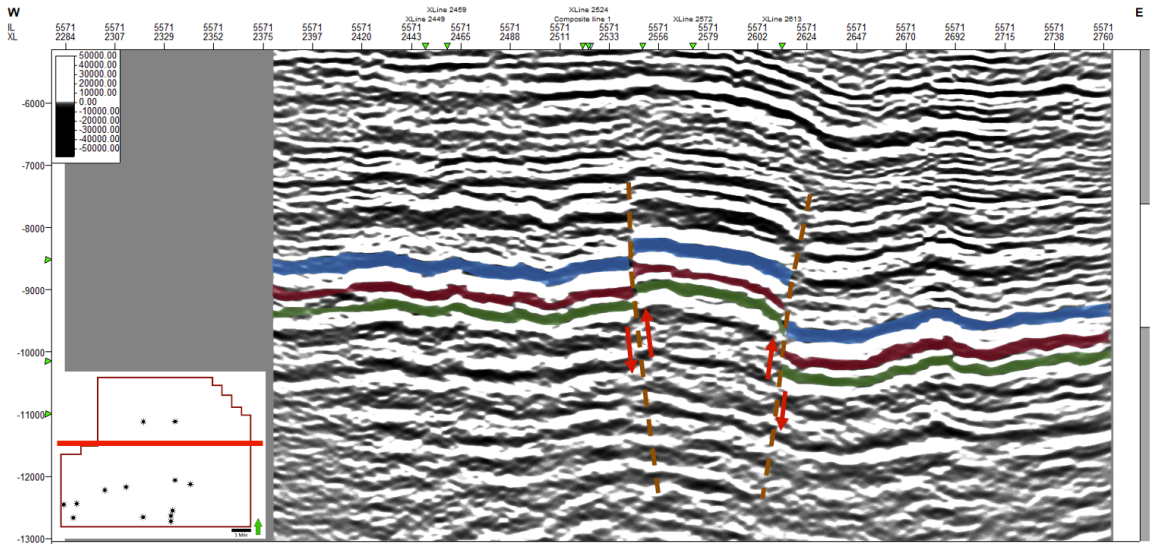

Figure 30: Cross section view of large compressional fault zone that continues into the Wolfcamp Formation. The fault on the eastern section has significantly more displacement. Three reflectors have been colored to highlight the fault displacement.

The general direction of dip of the area is southward as the shelf transitions into the basin with a strike trending approximately East west, thus sediment was likely transported nearly due south with some limbs falling to the east before ultimately heading south as well. It is important to note that once a deepwater fan is on the basin floor, especially for carbonates, the concept of depositional dip is at most idealized, as the fan itself resembles a pancake with depositional strike being in all directions (Pigott, unpublished Carbonate Geology Notes). However, as this volume is on the proximal slope, sediment gravity flow processes are especially dramatic. A few of these possible sediment dispersal routes have been mapped and are shown on Figures 31 through 37 marked by red arrows.

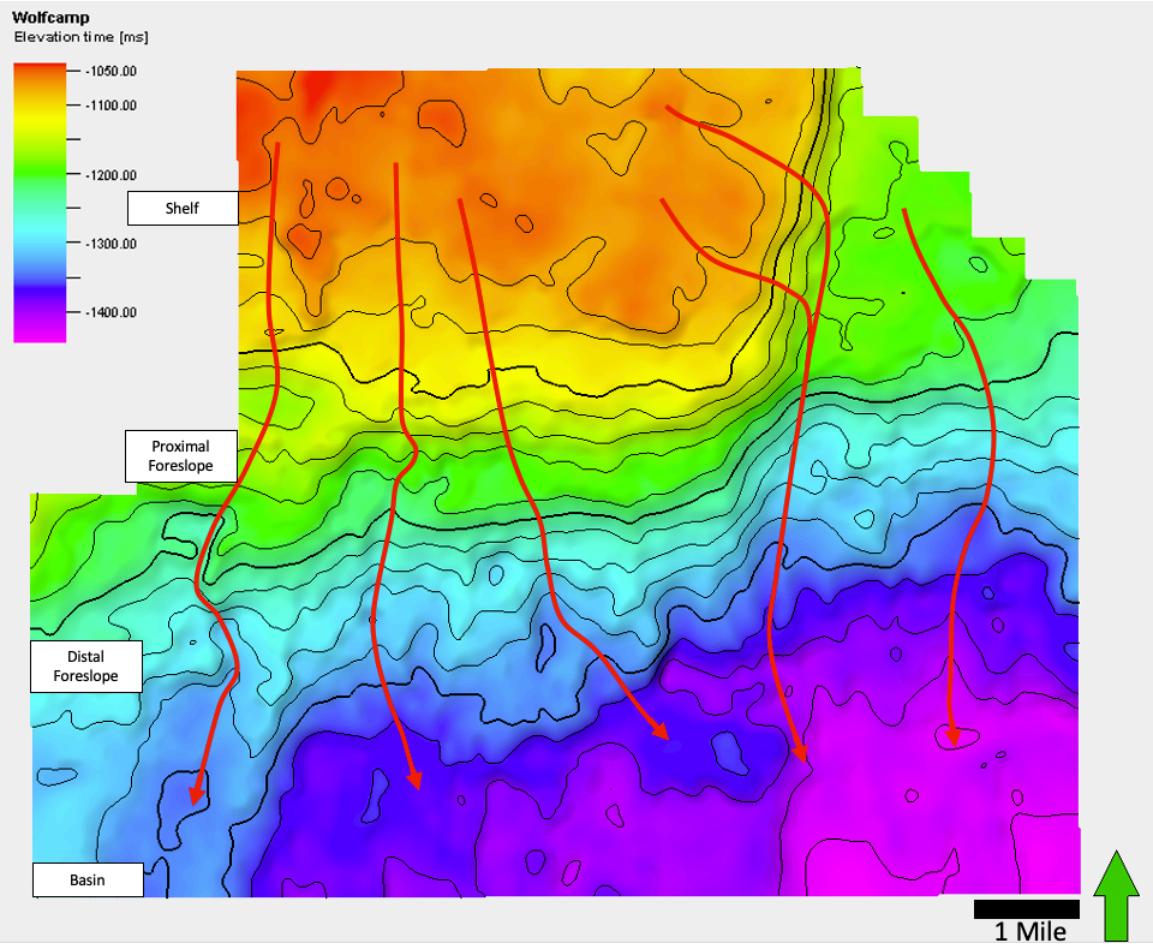

Figure 31: TWT structure map of the top of the Wolfcamp showing structure and deepening to the South-Southeast. TWT values range from -1040 to -1475 across the study area. This surface importantly reveals the effect of inherited topography for the overlying Bone Spring deposition. The arrows represent paths of possible sediment transportation trajectories as curved contours which point shelfward and broaden basinward. The average shelf slope angle is 18°. The different sections of the shelf are also labeled.

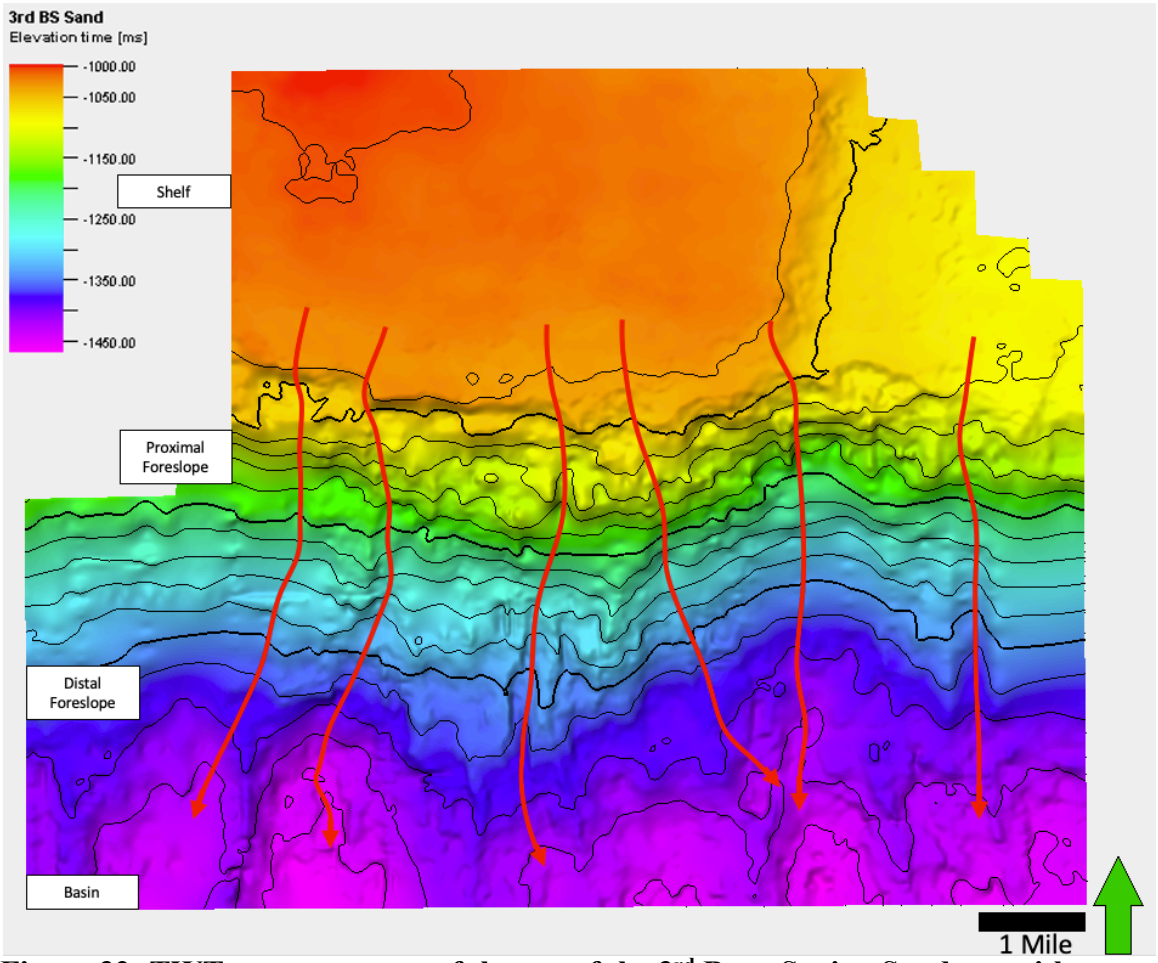

Figure 32: TWT structure map of the top of the 3rd Bone Spring Sand top with values ranging from -1000 to -1460. Displays a slight steepening compared to the Wolfcamp top. The arrows represent paths of possible sediment transportation trajectories as curved contours which point shelfward and broaden basinward. The average shelf slope angle is 19°. The different sections of the shelf are also labeled.

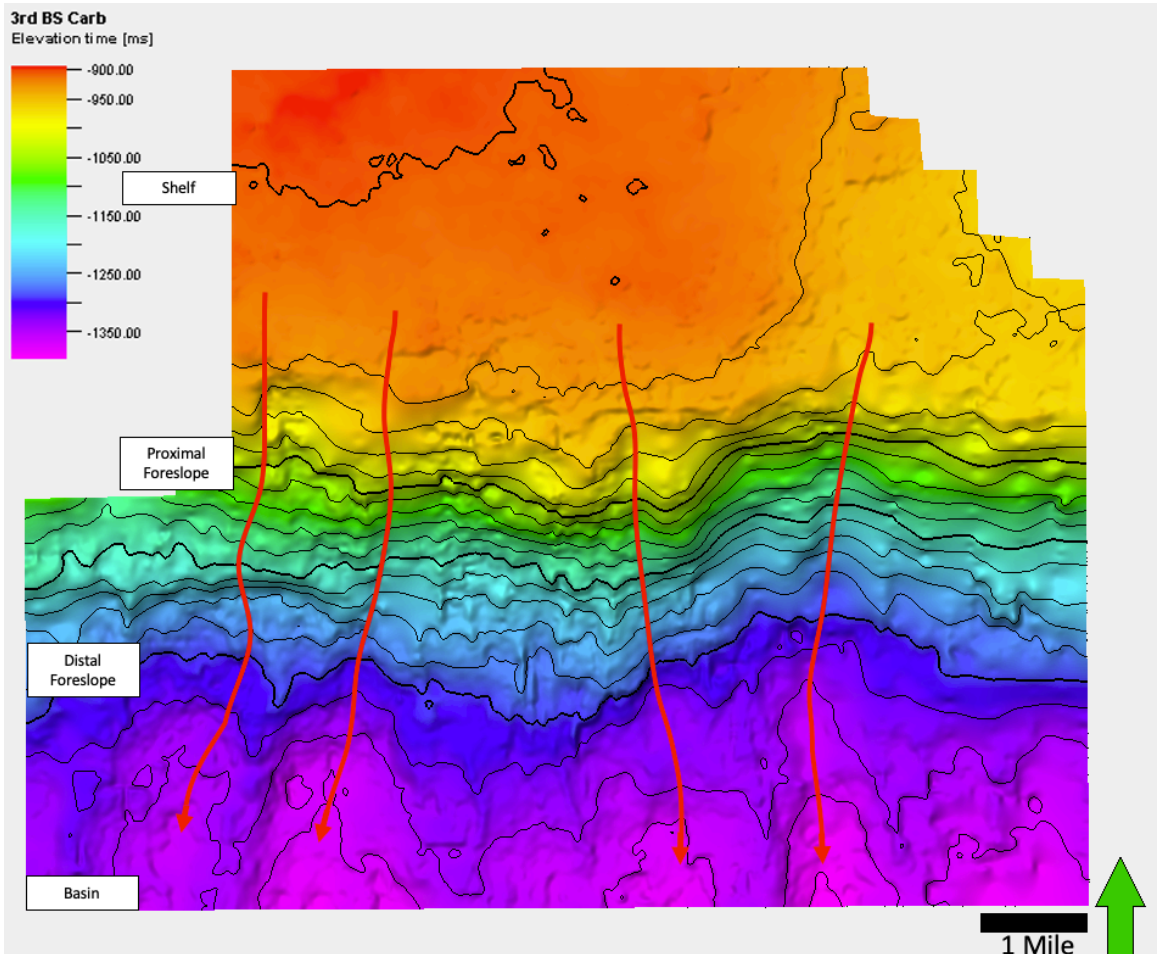

Figure 33: TWT structure map of the top of the 3rd Bone Spring Carbonate top with values ranging from -900 to -1450. The arrows represent paths of possible sediment transportation trajectories as curved contours which point shelfward broaden basinward. The average shelf slope angle is 19°. The different sections of the shelf are also labeled.

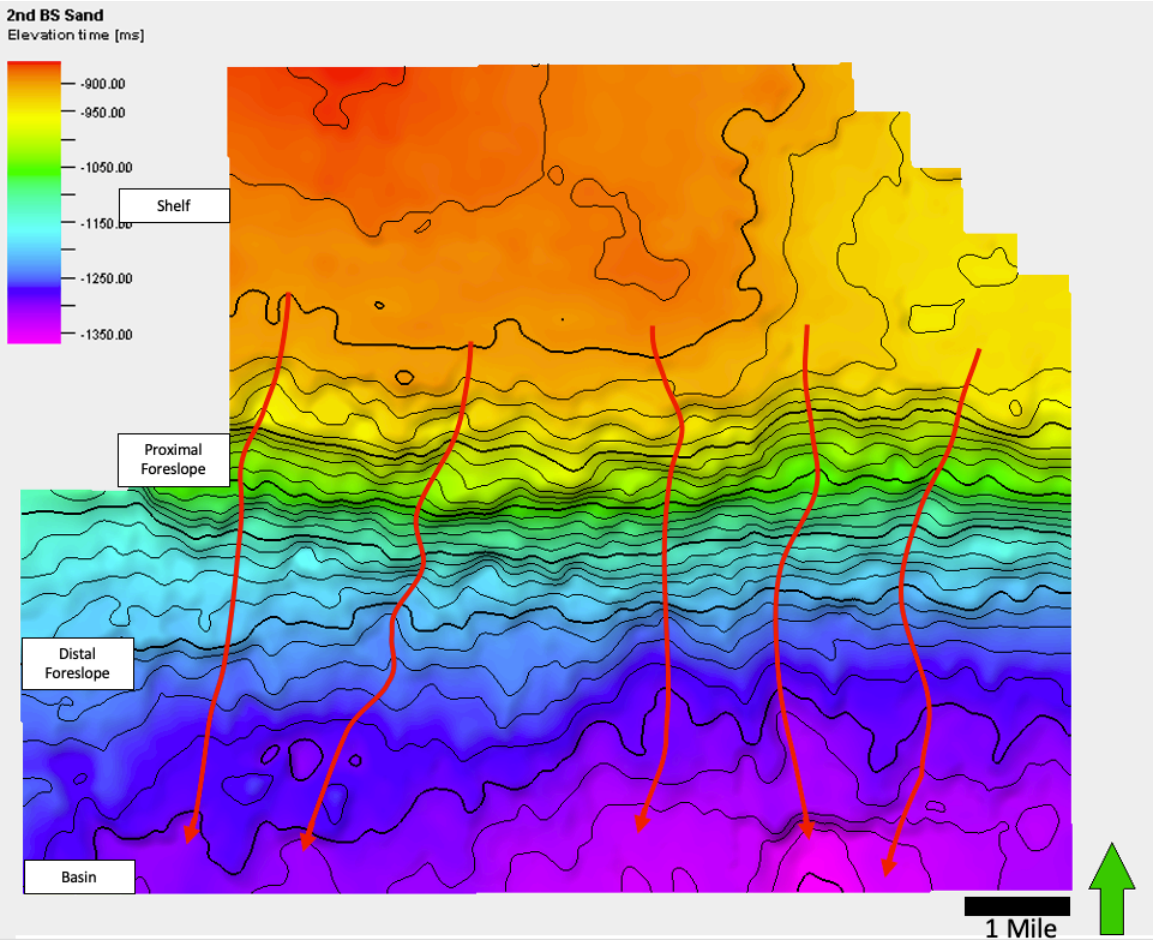

Figure 34: TWT structure map of the top of the 2nd Bone Spring Sand top with values ranging from -860 to -1360. The arrows represent paths of possible sediment transportation trajectories as curved contours which point shelfward broaden basinward. The average shelf slope angle is 21°. The different sections of the shelf are also labeled.

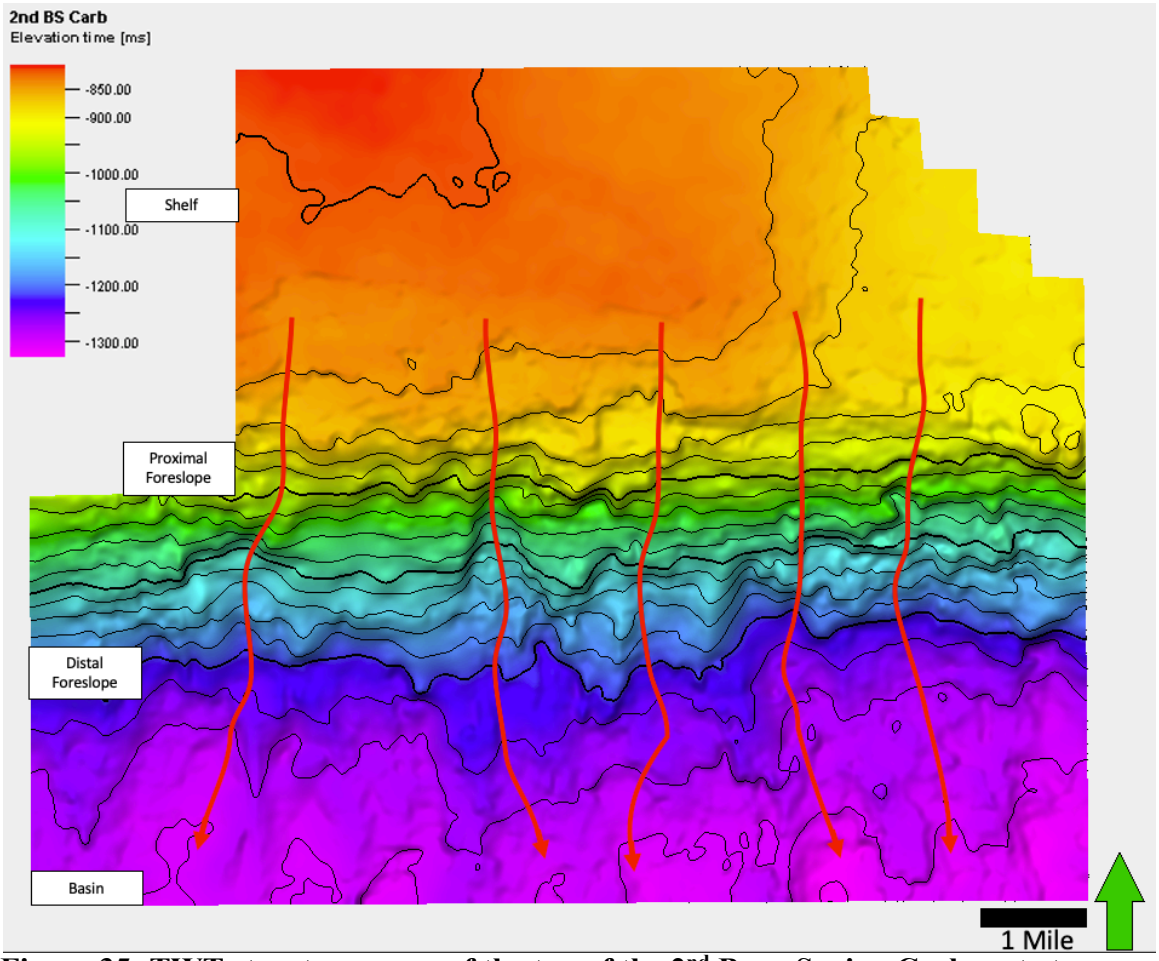

Figure 35: TWT structure maps of the top of the 2nd Bone Spring Carbonate top with values ranging from -810 to -1320. The arrows represent paths of possible sediment transportation trajectories as curved contours which point shelfward broaden basinward. The average shelf slope angle is 20°. The different sections of the shelf are also labeled.

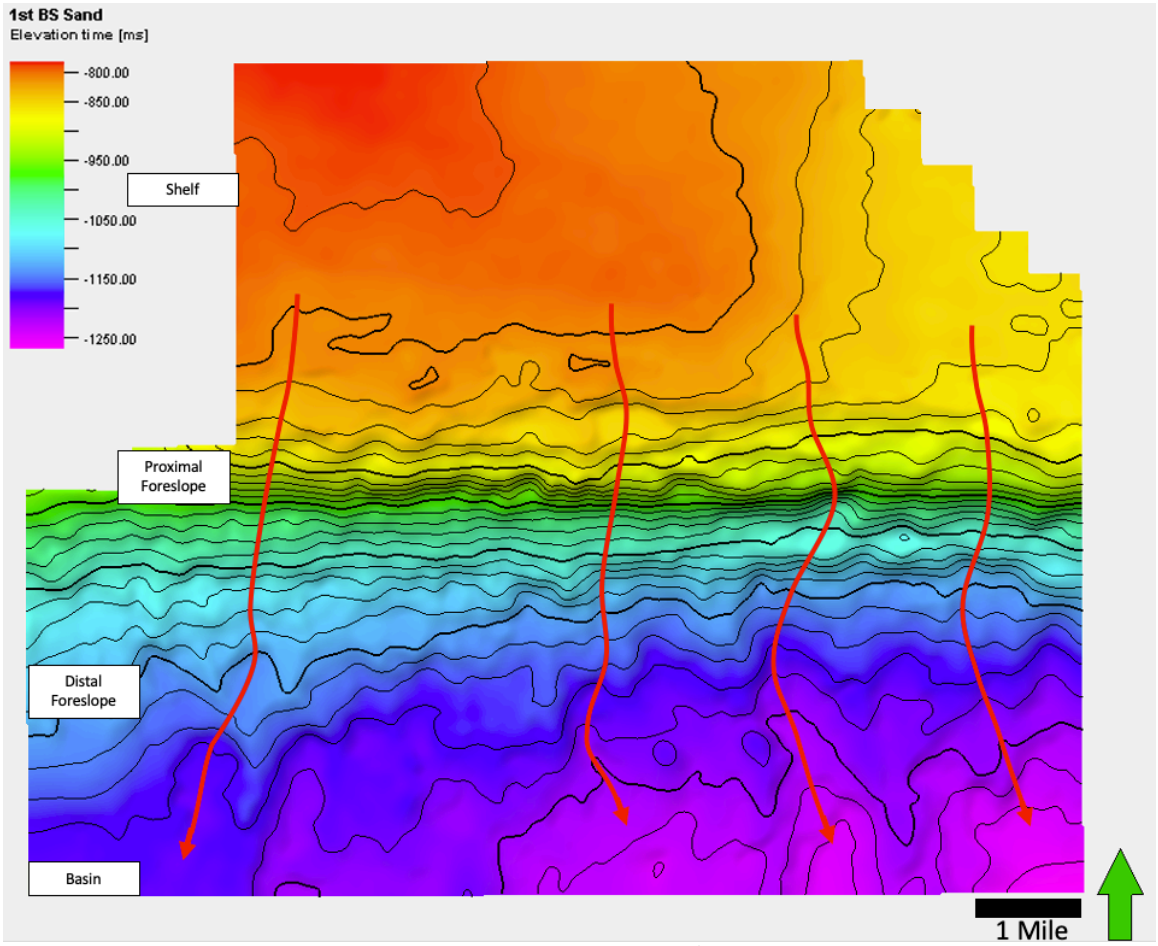

Figure 36: TWT structure maps of the top of the 1st Bone Spring Sand top with values ranging from -790 to -1270. The arrows represent paths of possible sediment transportation trajectories as curved contours which point shelfward broaden basinward. The average shelf slope angle is 22°. The different sections of the shelf are also labeled.

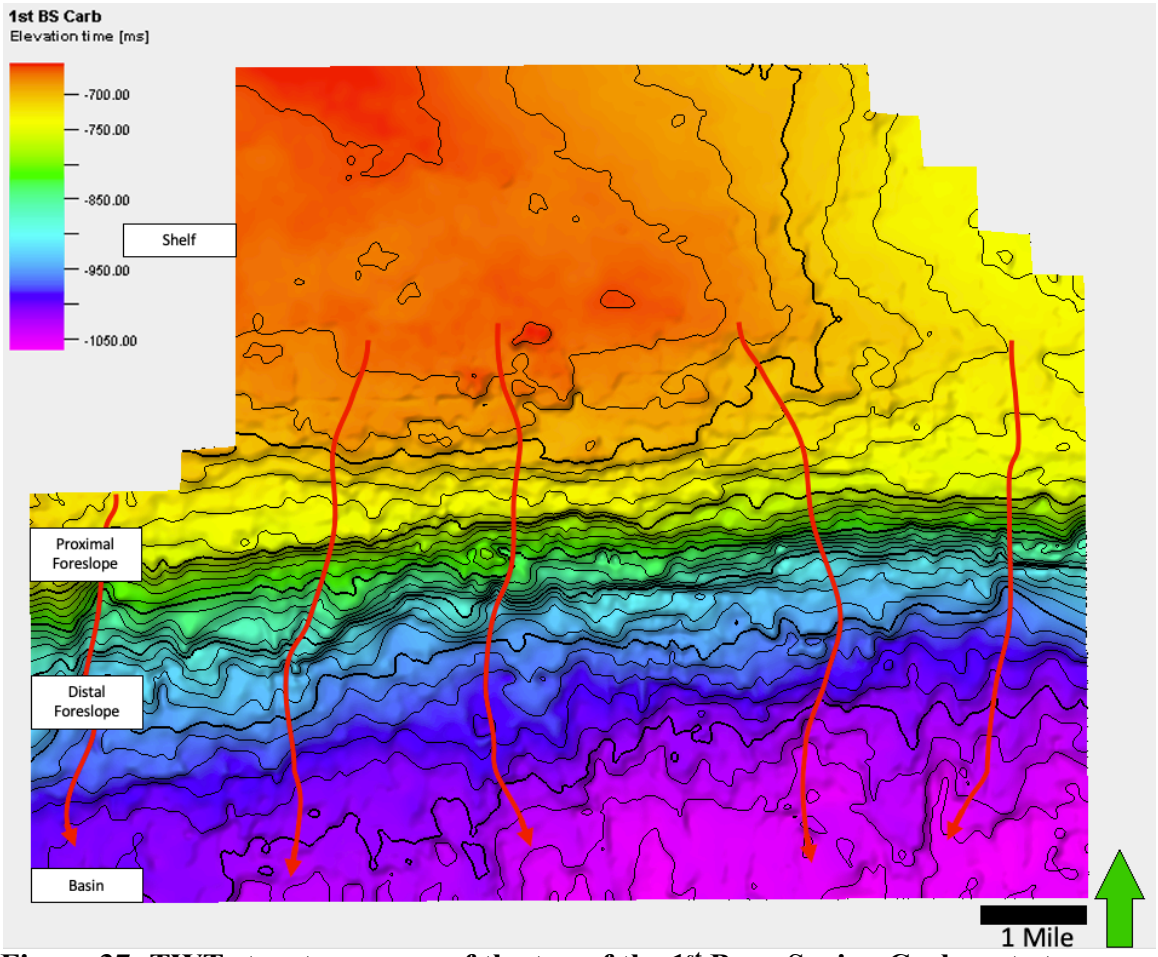

Figure 37: TWT structure maps of the top of the 1st Bone Spring Carbonate top with values ranging from -640 to -1060. The arrows represent paths of possible sediment transportation trajectories as curved contours which point shelfward broaden basinward. The average shelf slope angle is 20°. The different sections of the shelf are also labeled.

The structure maps demonstrate a steepening of the slope as carbonate production substantially increases from the Wolfcamp top (Figure 31) to the 1st Bone Spring top (Figure 37). Figure 36 compares the slope angles of these structure maps and reveals the effects of the carbonate buildup on the shelf. The Wolfcamp displays the lowest average slope angle of 18° and the highest angle slope is found on the 1st Bone Spring Sand at 22°.

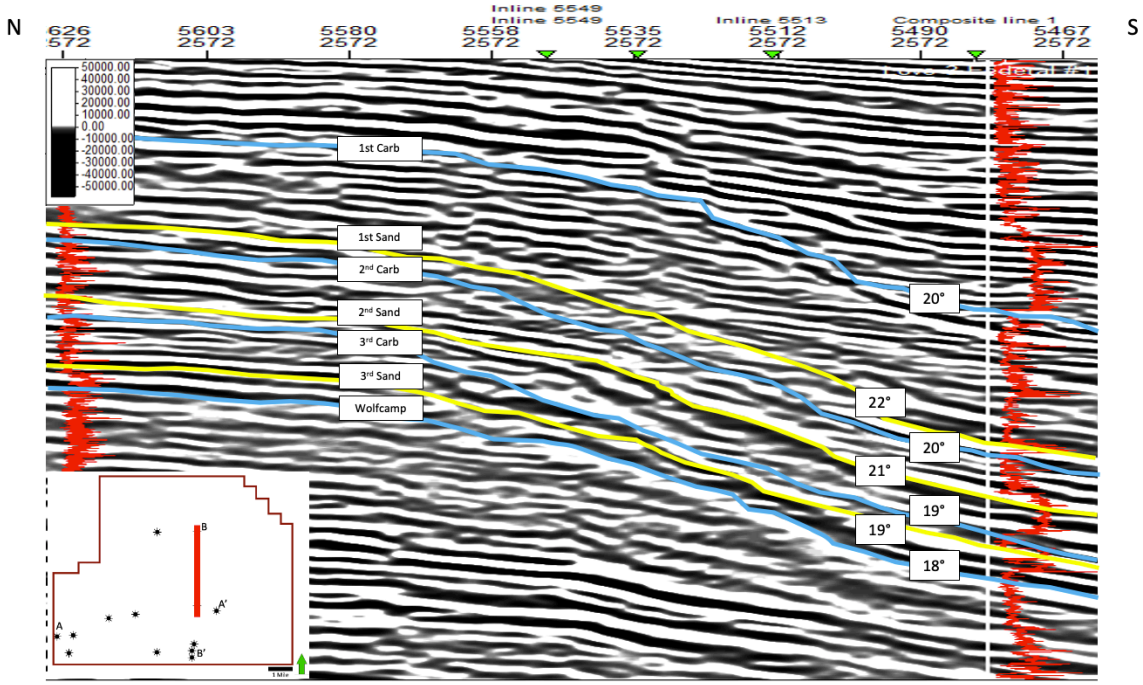

Figure 38: TWT structure maps of the top of the 1st Bone Spring Carbonate top with values ranging from -640 to -1060. The arrows represent paths of possible sediment transportation trajectories as curved contours which point shelfward broaden basinward. The average shelf slope angle is 20°.

Also, many of the evident channels or incised valleys that are displayed on the Wolfcamp top were filled in and leveled out to through the evolution of the Bone Spring Formation, which produces a much more uniform top. Figure 39 reveals how one of these massive valleys evolved by filling as the shelf prograded from the 3rd Bone Spring to the 1st Bone Spring. Figure 40 illustrates how a feeder system cuts through a carbonate shelf and a slope creating incised valleys, channel systems and submarine fan deposits. Such a model is consistent with this investigation which suggest suggests such a diagrammatic snapshot occurs during RST to LST times prior to shelf progradation during TST to HST times. As the feeder channels cut through previously continuous layers and create incised valleys the layers are eroded and broken up creating truncations. Subsequent filling of these channels causes younger sediments to be juxtaposed next to older existing layers.

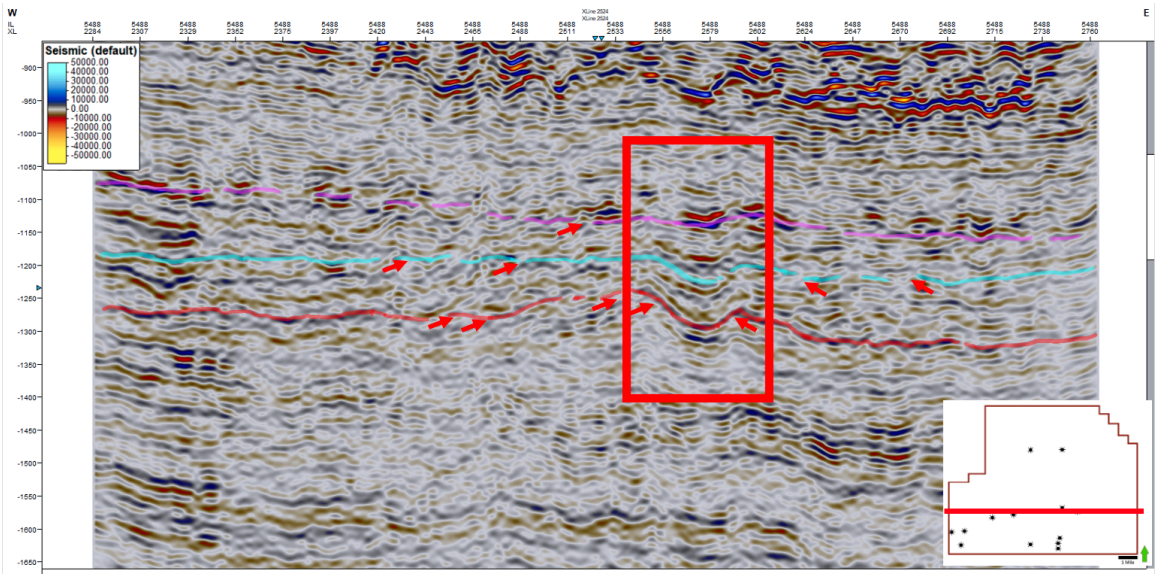

Figure 39: A crossline in the seismic that shows the filling and flattening of an incised valley of a feeder channel from the top of the 3rd Bone Spring Sand top to the 1st Bone Spring Sand top. Red horizon represents the 3rd Bone Spring Sand, cyan the 2nd Bone Spring sand, and pink the 1st Bone Spring Sand. Note the dramatic truncation of the reflectors beneath each sand top which represents an LST (see text for explanation).

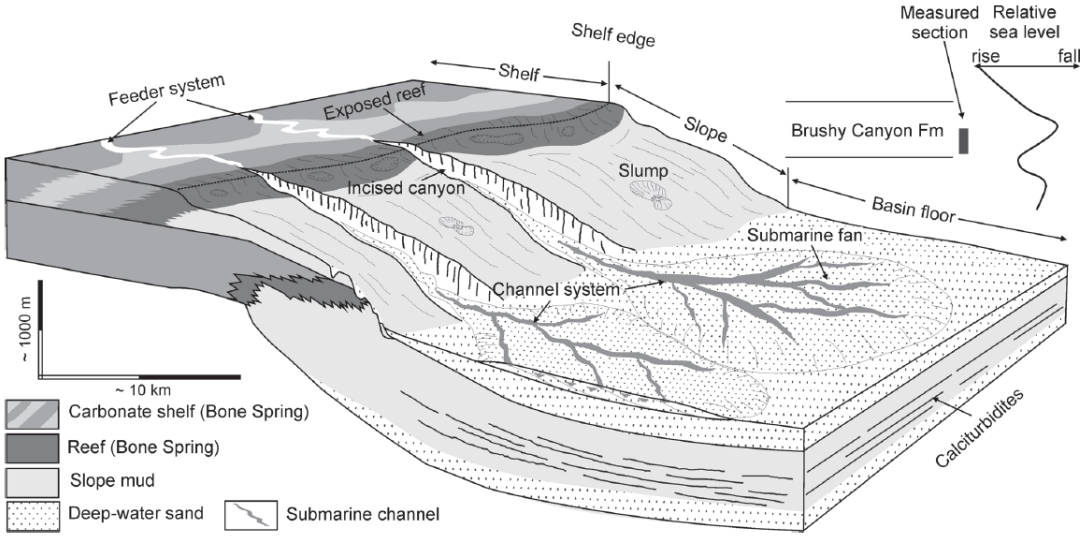

Figure 40: Model of incised valley creation and resulting deposition of submarine fan caused by a change of sea level in the Permian basin. Li et al. (2015), Bickley (2019).

Isopach Maps

After time structure maps were produced, the formation tops were then used to compute formation thickness, or isopach maps using the. Figure 41 shows the entire Bone Spring Formation thickness, from the top of the upper 1st Bone Spring Carbonate to the top of the Wolfcamp Formation. This thickness varies greatly from ~5,600 feet on the Northeast side of the study area on top of the shelf to ~3,400 feet along the southern boundary. Almost the entirety of this thickness variation is caused by the buildup of the carbonate shelf, while the previously mentioned fault zone (Figures 29 and 30) provided substantial accommodation that created the greatest area of thickness for the Bone Spring.

Figures 41 through 47 illustrate the thickness of each Bone Spring sand intervals. The 3rd Bone Spring Sand (Figure 42) exhibits thicknesses which range from ~50 feet to ~600 feet in the basin and the 3rd Bone Spring Carbonate (Figure 43) displays thickness ranging from ~100 feet to ~900 feet. The 2nd Bone Spring Sand (Figure 44) displays thickness ranging from ~100 to ~1100 feet and 2nd Bone Spring Carbonate (Figure 45) ranging from ~100 to ~1000 feet. The 1st Bone Spring Sand (Figure 46) with thickness ranging from ~100 to ~700 feet and 1st Bone Spring Carbonate (Figure 47) displaying the thickest interval ranging from ~1100 to ~2200. Through each of these sections, thickness is greatest more proximal to the slope found in relative low areas left from channels that eroded the underlying layer. In general, the sand layers of the Bone Spring are thickest proximal to the slope in the basin and the carbonate layers are the opposite, with the thickest areas on top of the shelf and diminishes towards the basin.

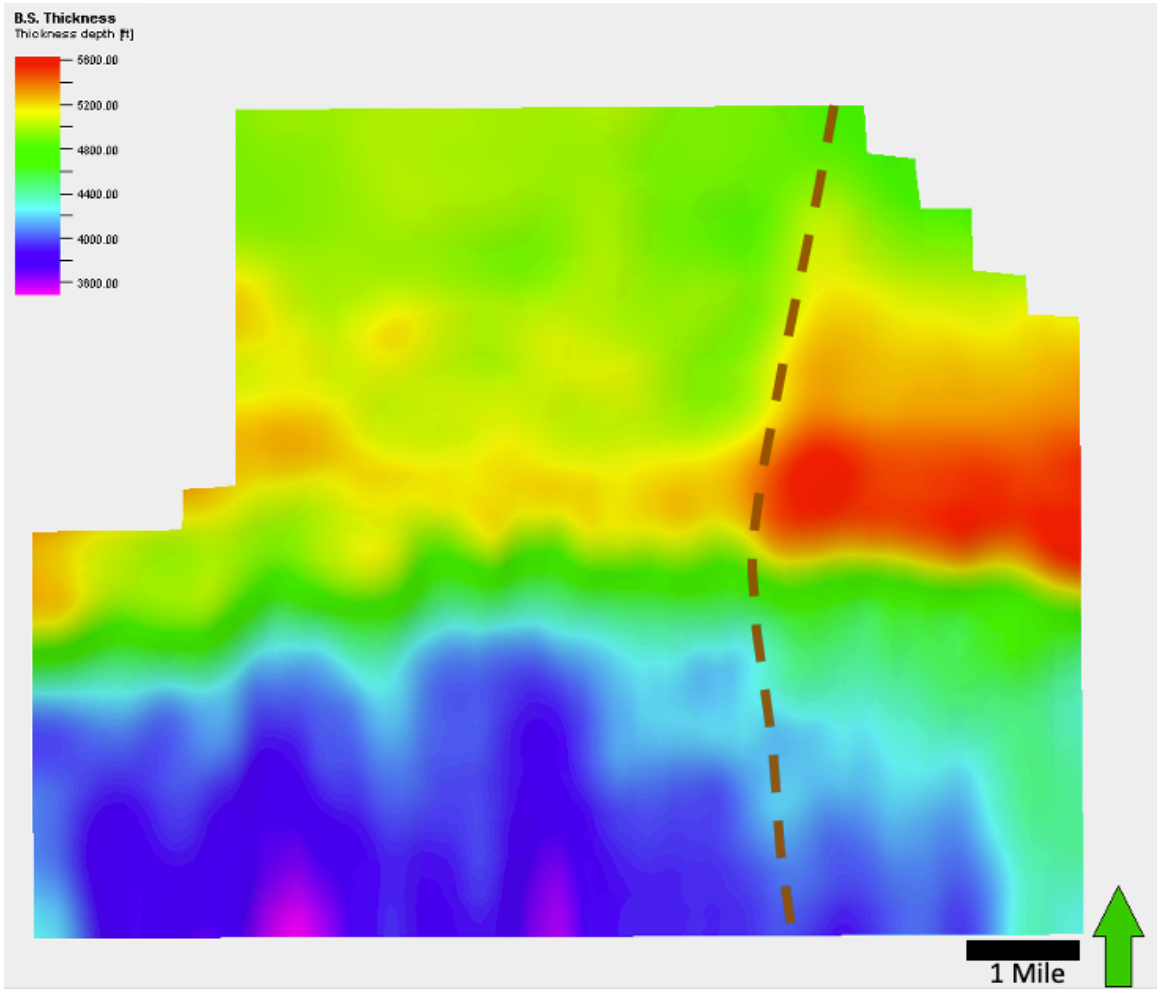

Figure 41: Gross Isopach map of the entire Bone Spring Formation interval from the top of the Bone Spring to the top of the Wolfcamp. Thickness is greatest over the faulted area seen on the Wolfcamp and thins drastically to the southern edge.

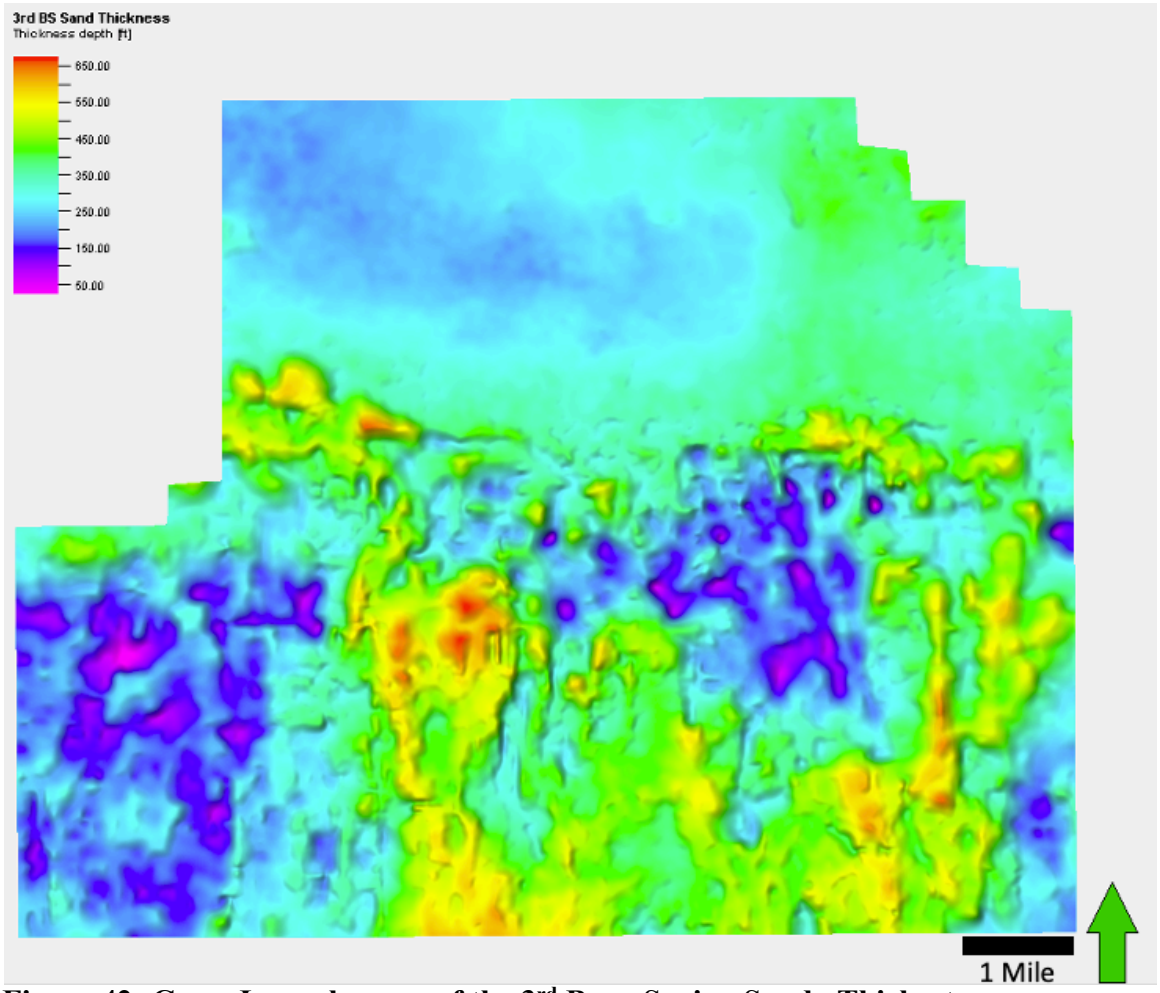

Figure 42: Gross Isopach maps of the 3rd Bone Spring Sand. Thickest areas are proximal to the slope in the basin with depths ranging from ~50 to ~600 feet.

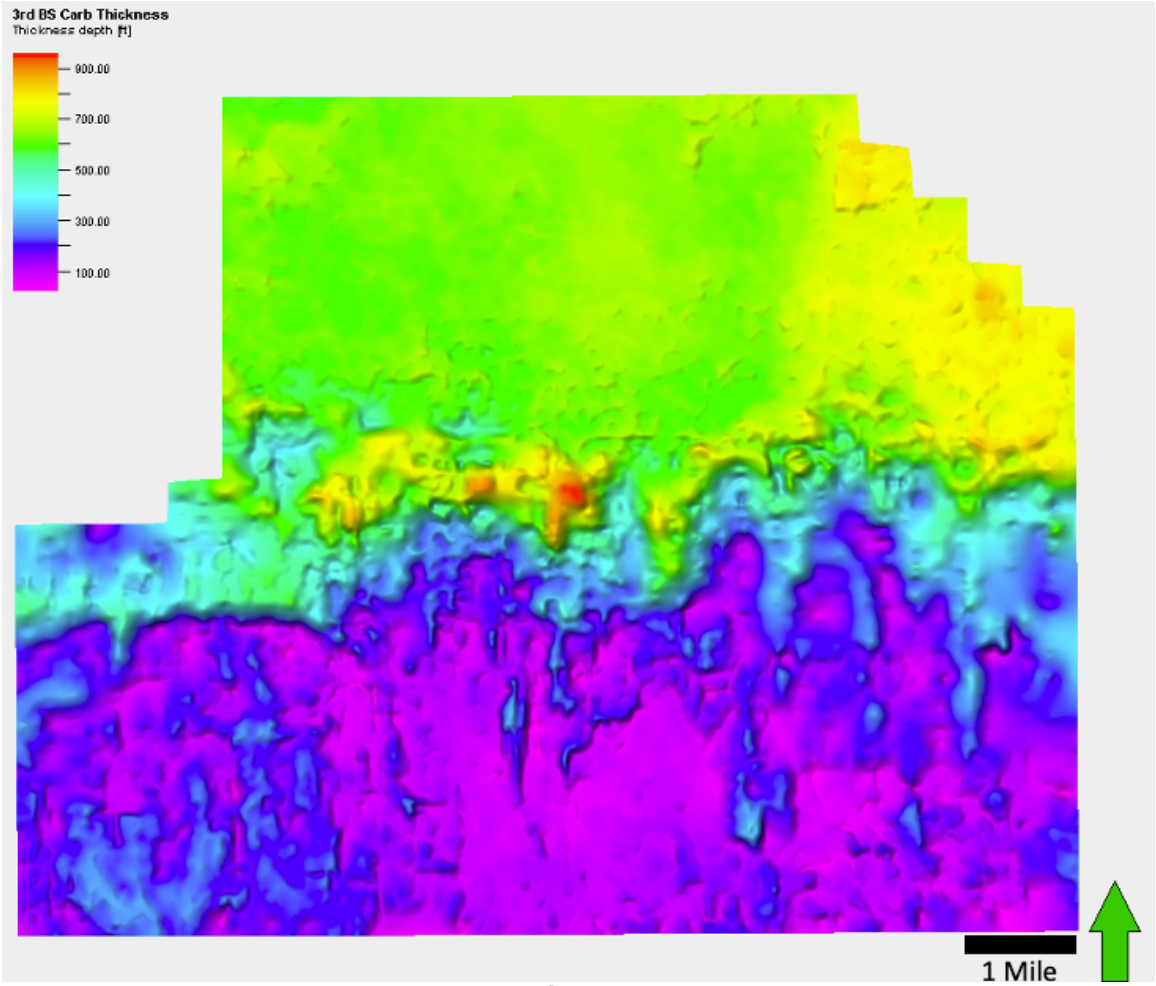

Figure 43: Gross Isopach maps of the 3rd Bone Spring Carbonate. Thickest areas are on top of the shelf with thicknesses ranging from ~100 to ~900 feet.

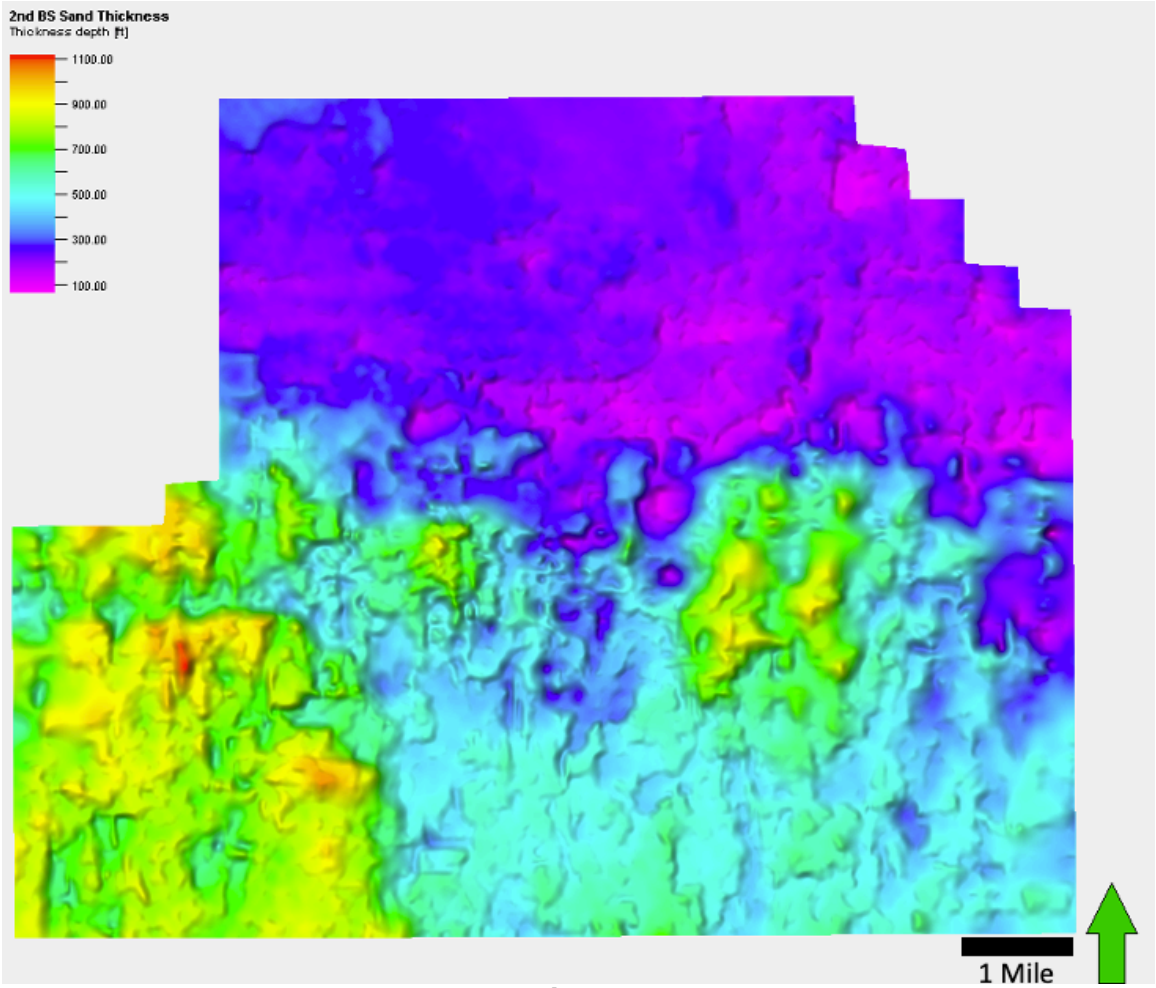

Figure 44: Gross Isopach maps of the 2nd Bone Spring Sand. Thickest areas are proximal to the shelf in the basin with thicknesses ranging from ~100 to ~1100 feet and the 2nd Bone Spring Sand is by far the thickest sand interval.

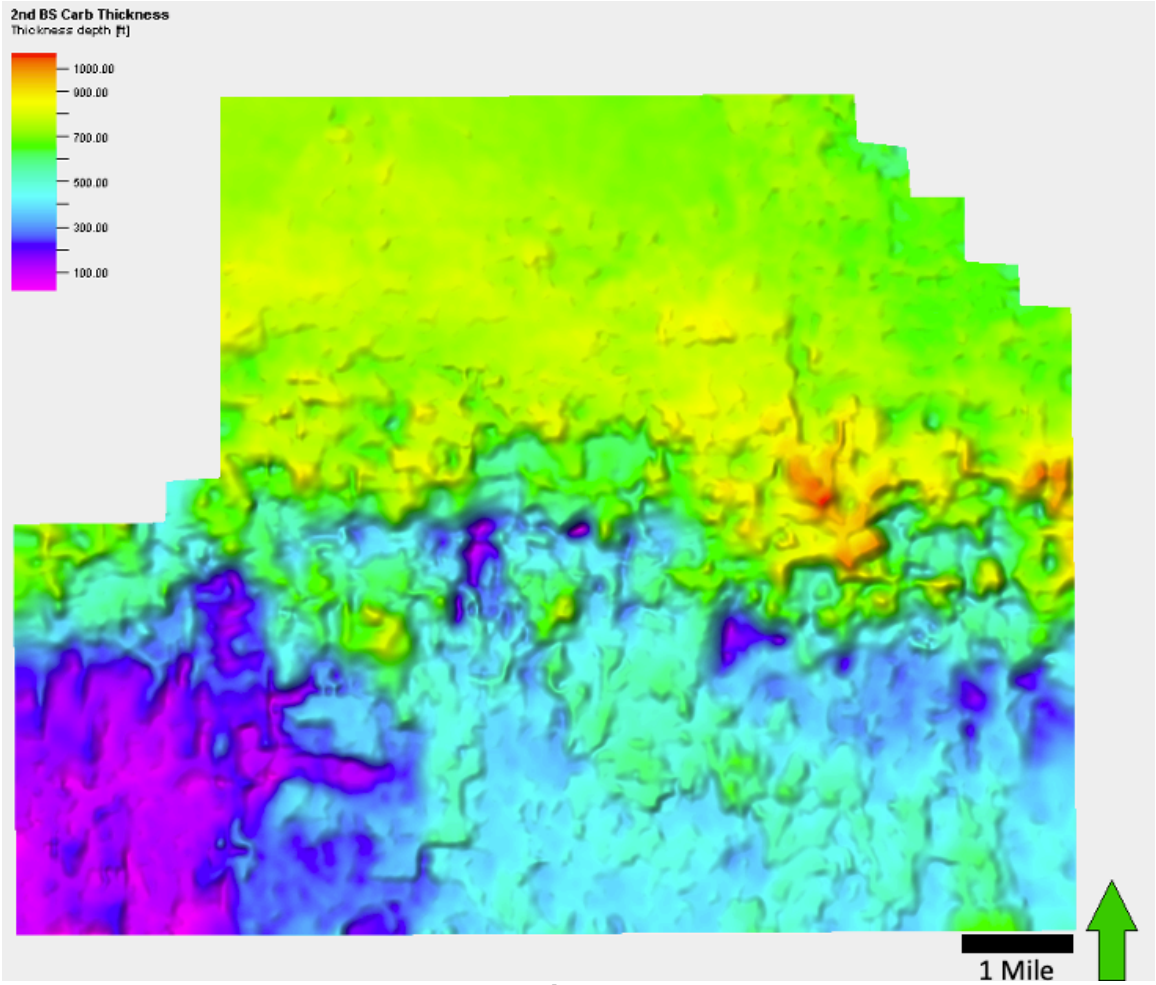

Figure 45: Gross Isopach maps of the 2nd Bone Spring Carbonate. Thickest sections are on top of the shelf with thicknesses ranging from ~100 to ~1000 feet.

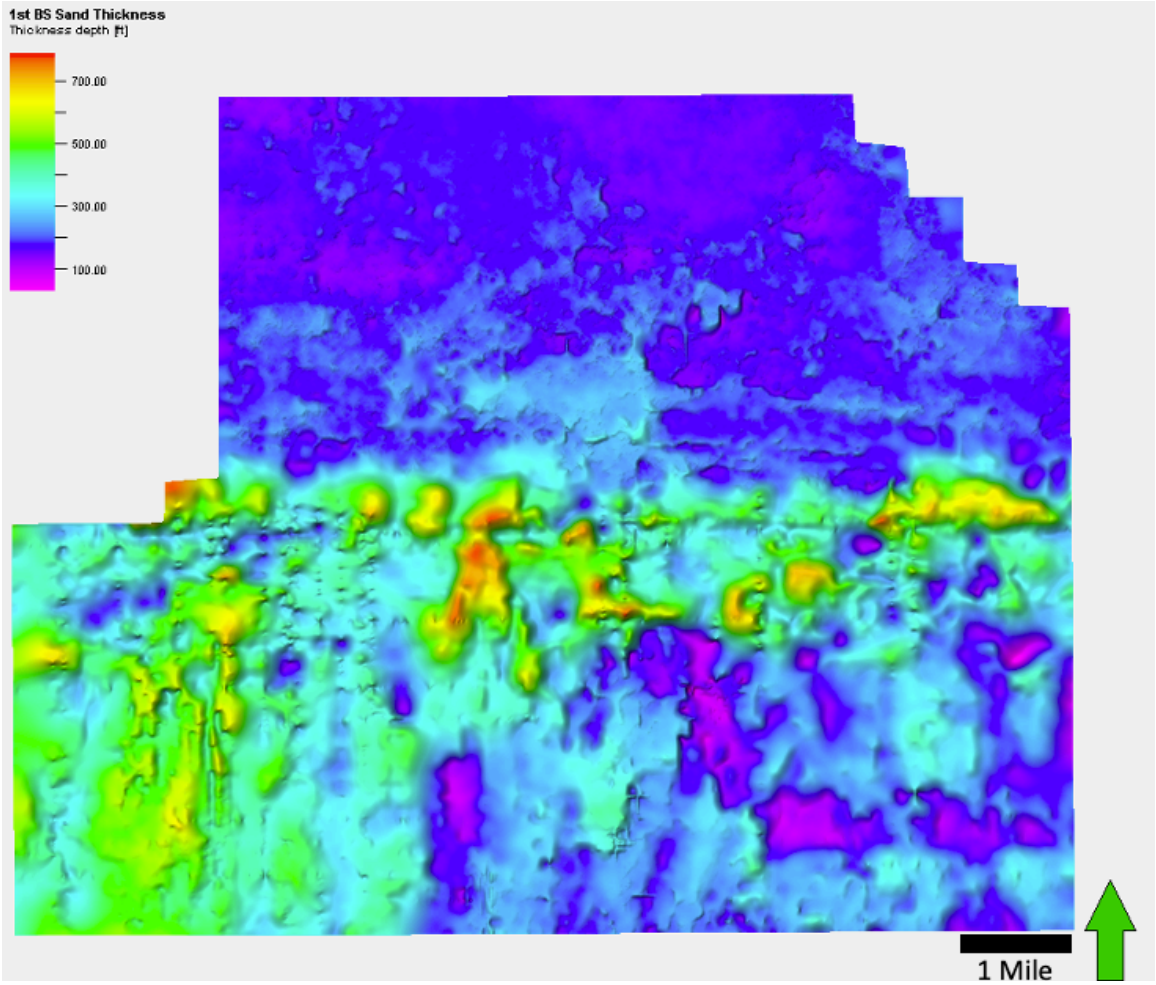

Figure 46: Gross Isopach maps of the 1st Bone Spring Sand. Thickest areas are proximal to the shelf in the basin with thicknesses ranging from ~100 to ~700 feet.

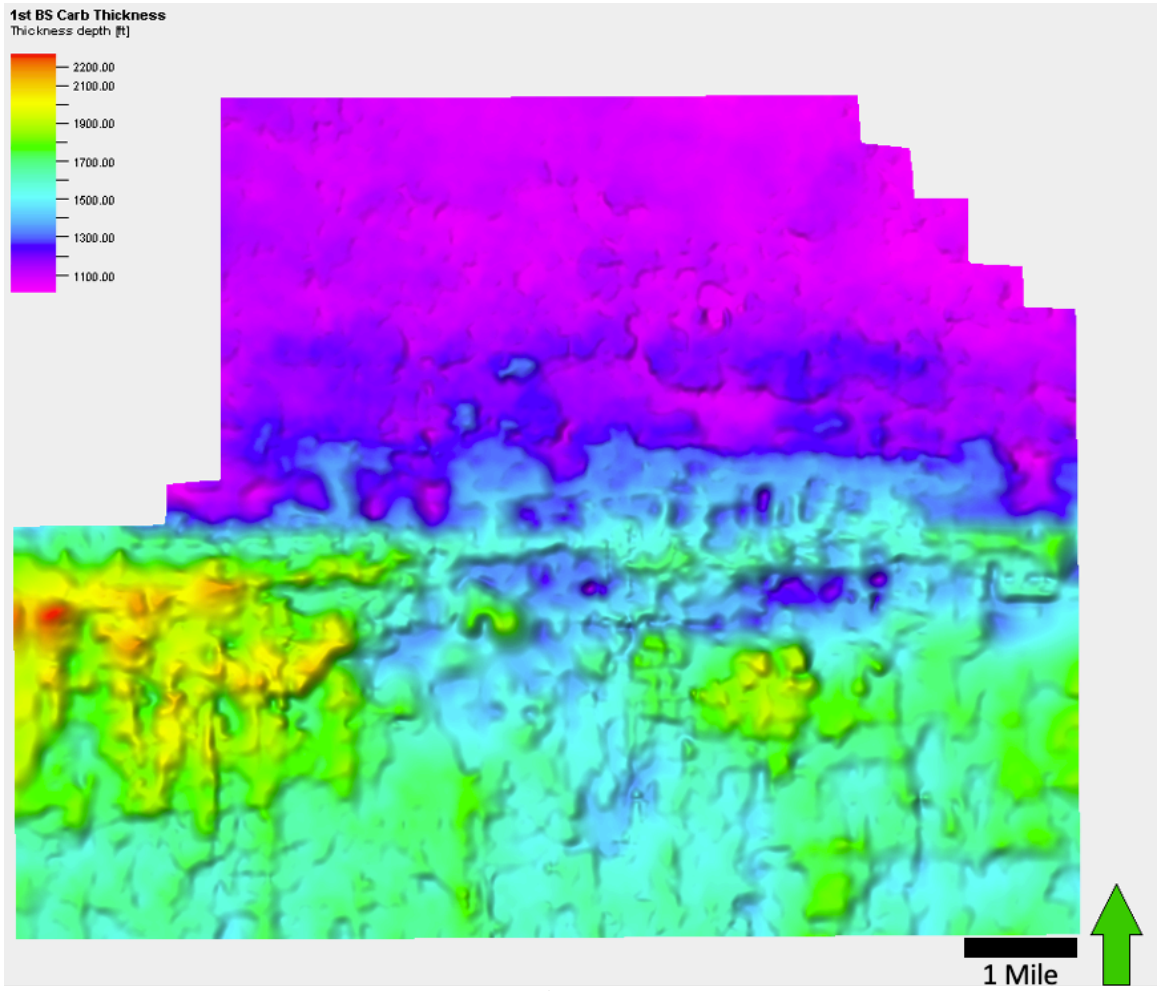

Figure 47: Gross Isopach maps of the 1st Bone Spring Carbonate. Thickest sections are on top of the shelf with thicknesses ranging from ~1100 to ~2200 feet and is the thickest carbonate interval in the Bone Springs.

Seismic Sequence Stratigraphy

After interval tops were mapped through the study area using well tied seismic, and isopach maps were produced, and compared through all the wells for accuracy, the Vail seismic sequence stratigraphy was implemented (Vail, 1987). First, inline cross sections of the seismic were produced that intersected previously interpreted wells. Seismic cross sections were picked to intersect wells and integrated into the volume. The first cross section (Figure 48) passes through the Mitchell 1 well, which is near the

southern boundary of the study area and offers a view of the most distal deposits in the area. The second cross section (Figure 49) goes through the Pearsall where on the western side of the study area the 3D seismic volume provides the most complete view. As mentioned in the previous chapter, the western side exhibits a thicker 1st Bone Spring Sand. This well is more proximal and is positioned at the base of the slope. Terminations were then mapped out on seismic-cross sections which were oriented along depositional dip (North to South).

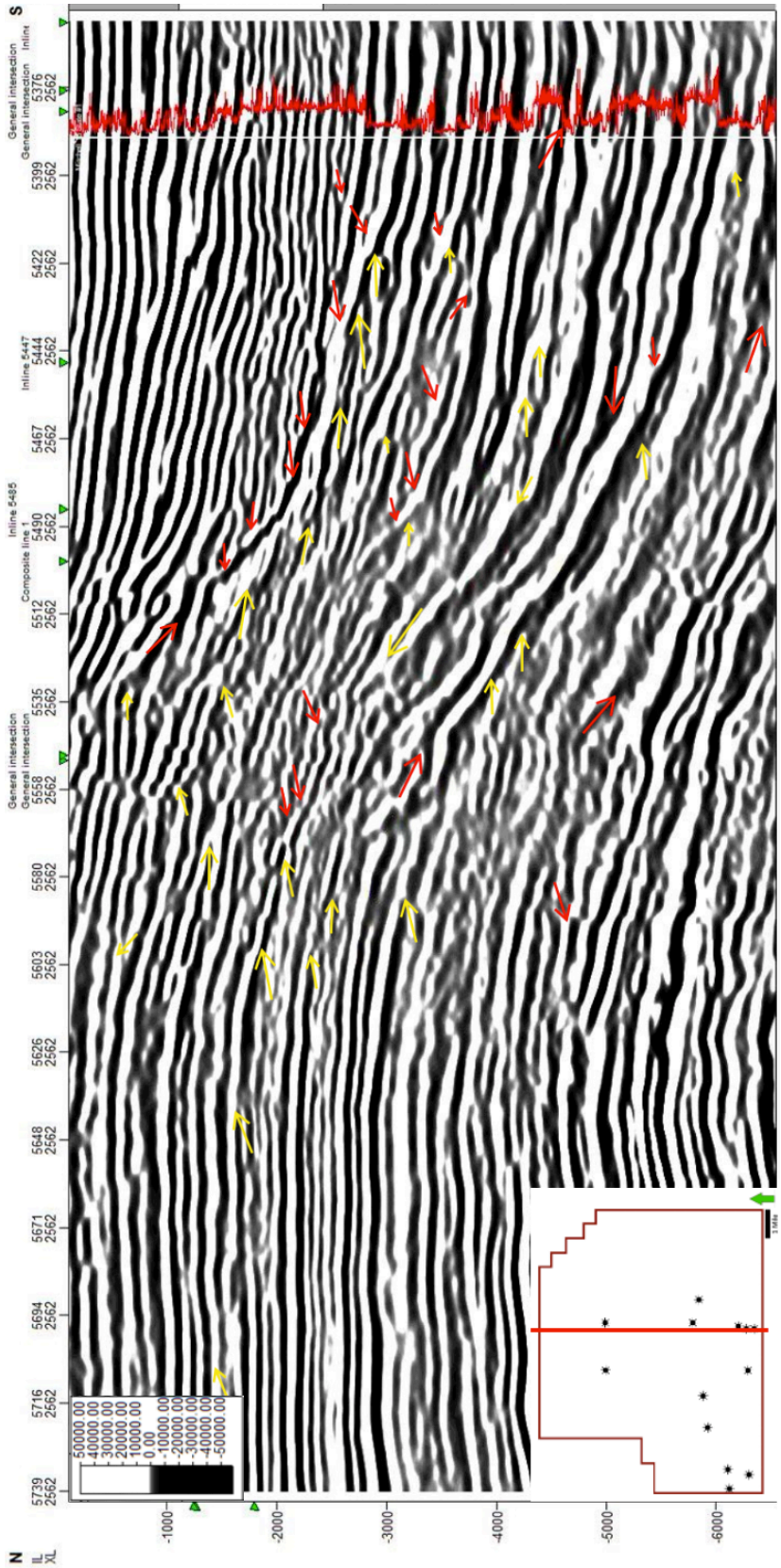

Figure 48: Seismic cross section number 1 going through the Mitchell 1 well with terminations displayed.

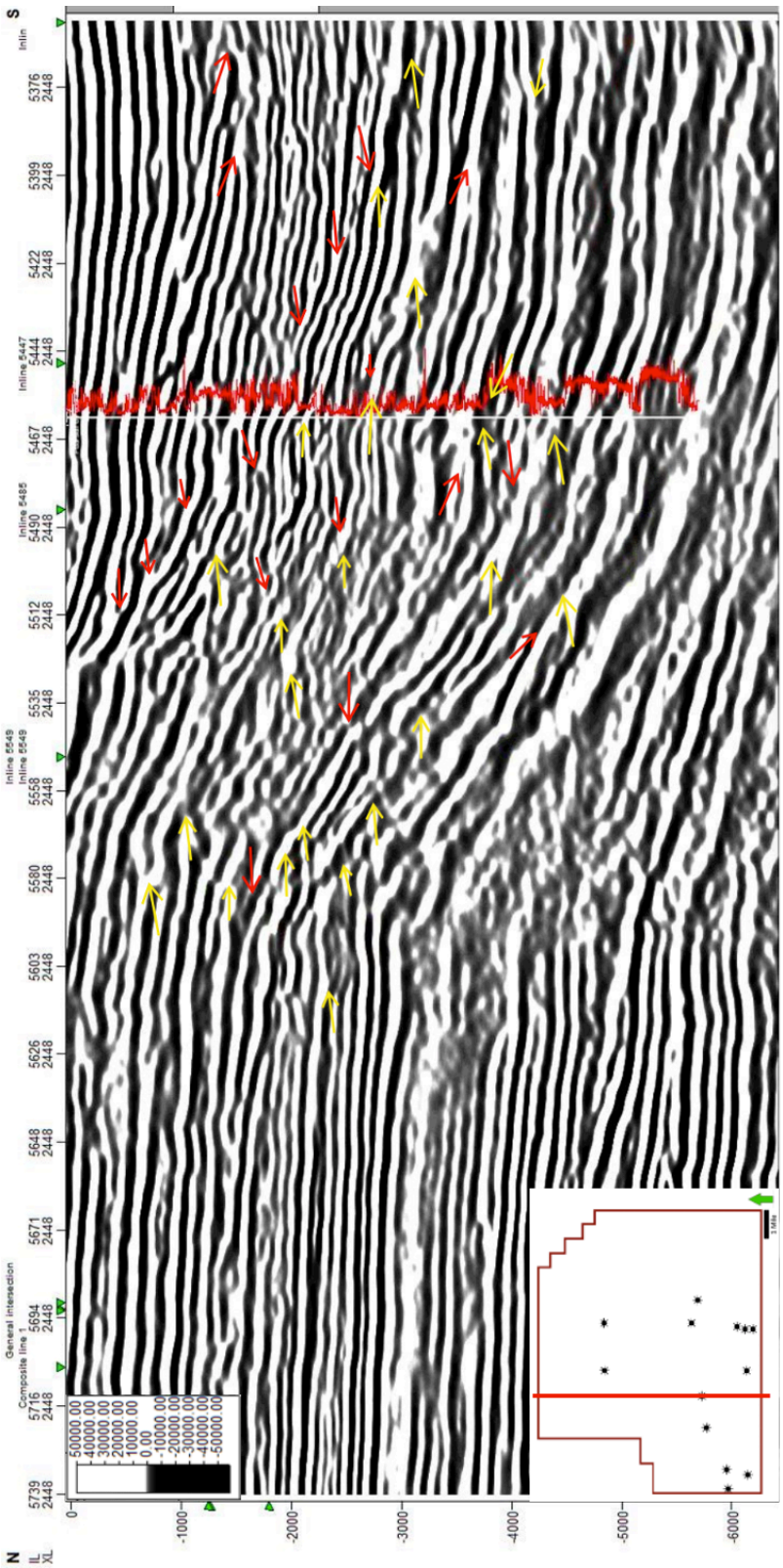

Figure 49: Seismic cross section number 2 going through the Pearsall 6 well with terminations displayed.

Once these terminations were applied on the cross sections, the petrophysical Galloway 3rd and 4th order sequence boundaries from the well logs were then superimposed adjacent to the gamma ray logs in the seismic (Figure 50 and 51). The 4th order sequences offer valuable insight into seismic reflectors that can appear discontinuous. However, seismic is not infallible, especially with the difficulties presented by the overlying evaporites in this area and the general uncertainty associated with seismic data. Because of this, not all sequences align, nonetheless many do match well. These confirmed reflectors can be correlated through many of the wells and makes for a more accurate and less complicated horizon mapping.

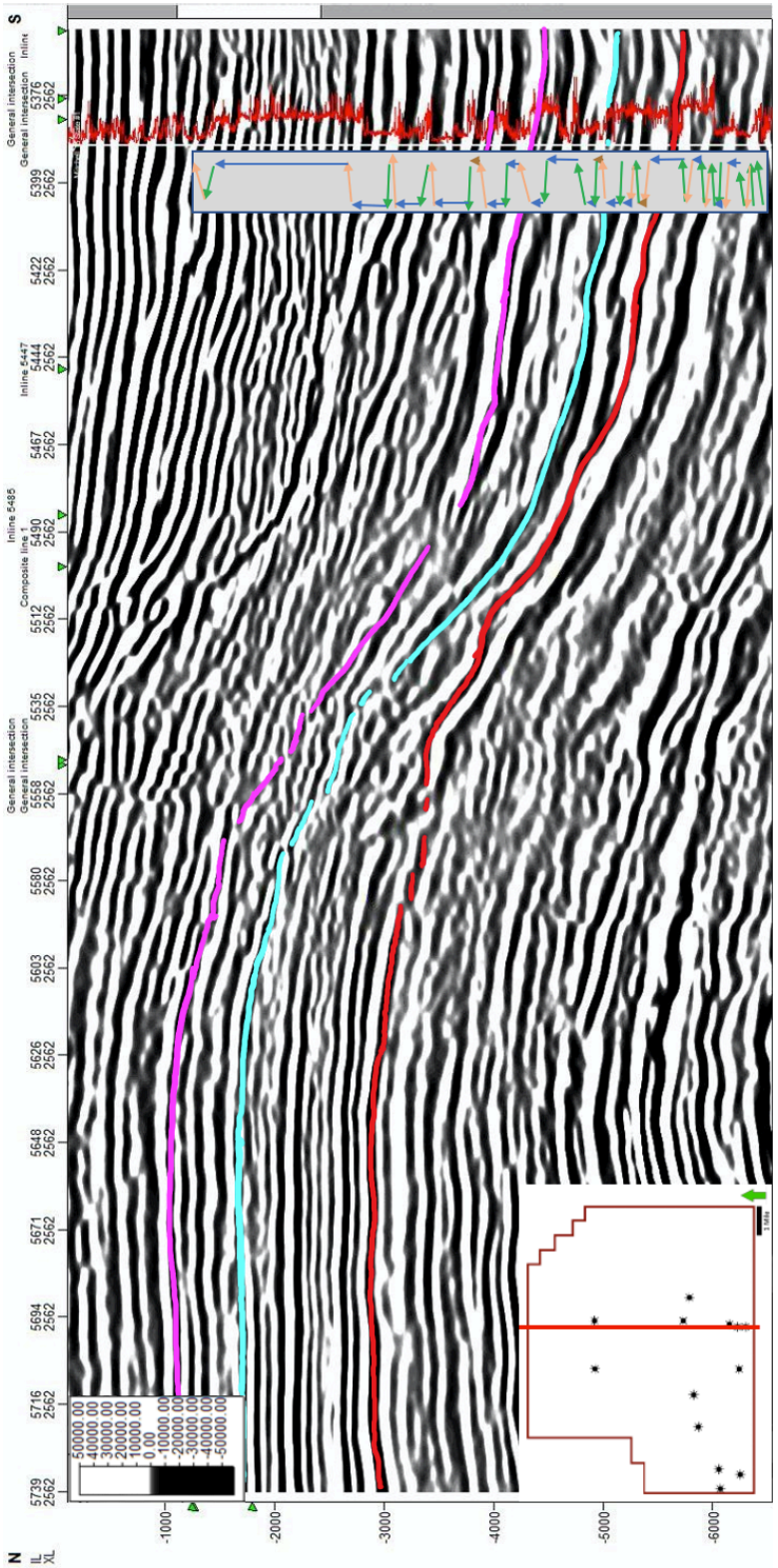

Figure 50: Seismic cross section 1 going through the Mitchell 1 well but showing the Bone Spring Sand tops and Galloway motifs superimposed, where blue arrows represent HST's, orange RST's, red LST's and green TST's (see text for explanation).

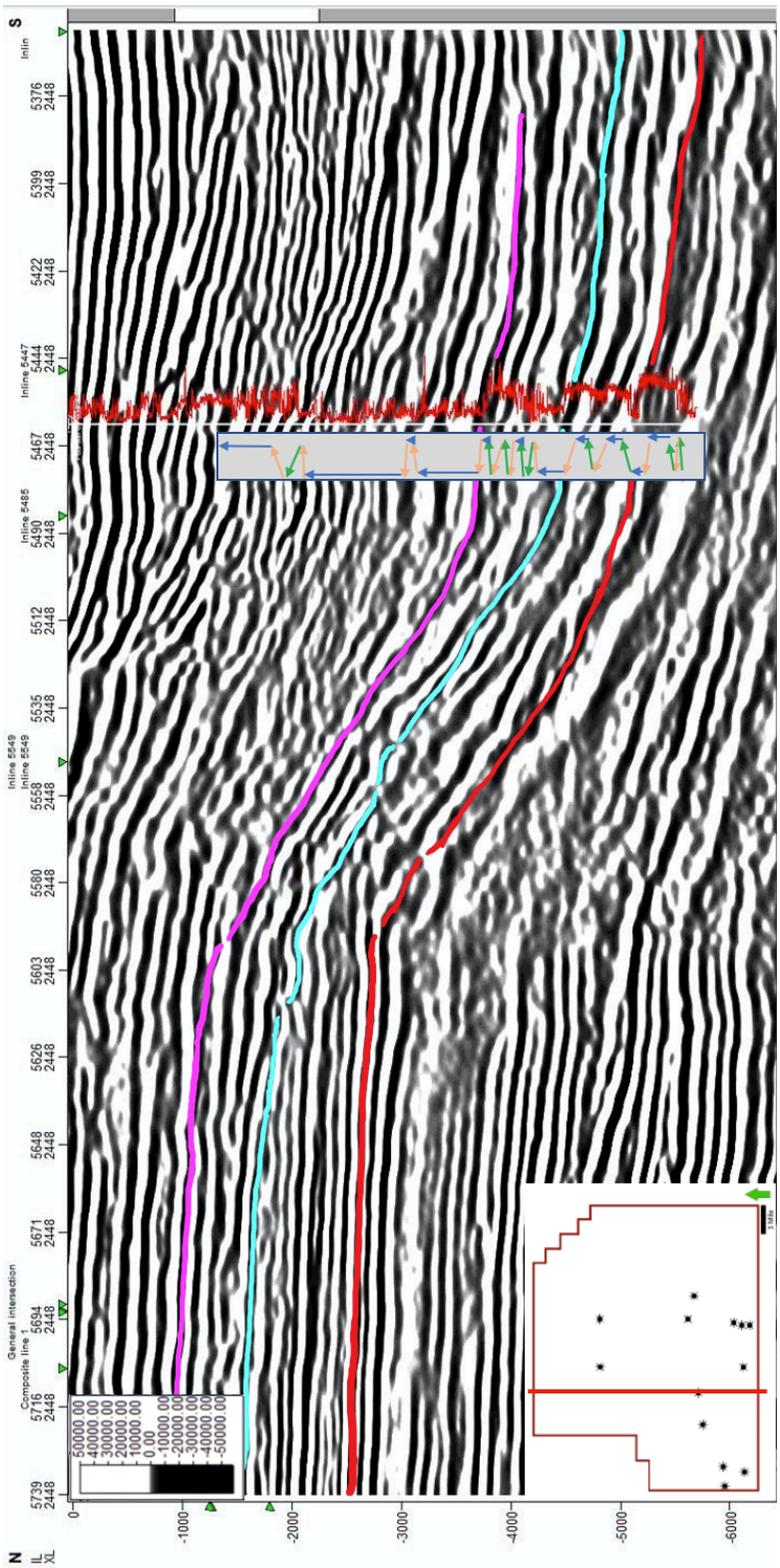

Figure 51: Seismic cross section 2 going through the Pearsall 6 well showing the Bone Spring Sand tops and Galloway motifs superimposed where blue arrows represent HST's, orange RST's, red LST's, and green TST's (see text for explanation)

Figure 52 shows a cross section along depositional strike through the Love Federal to highlight one major and one minor channel complex that can be observed to extend through the entirety of the Bone Spring in this volume. The 2nd Bone Spring Sand LST shows the largest amount off channel cutting, and then as subsequent layers are deposited on top the channel begins to level and fill in. The channel flattening out is likely a product of increased carbonate production during high stand times that choked the clastic channels. This is also supported by the decreasing clastic input seen in well logs after the thick 2nd Bone Spring Sand and is a dramatic example of reciprocal compensation stacking when the HST carbonate factory on the shelf is operating.

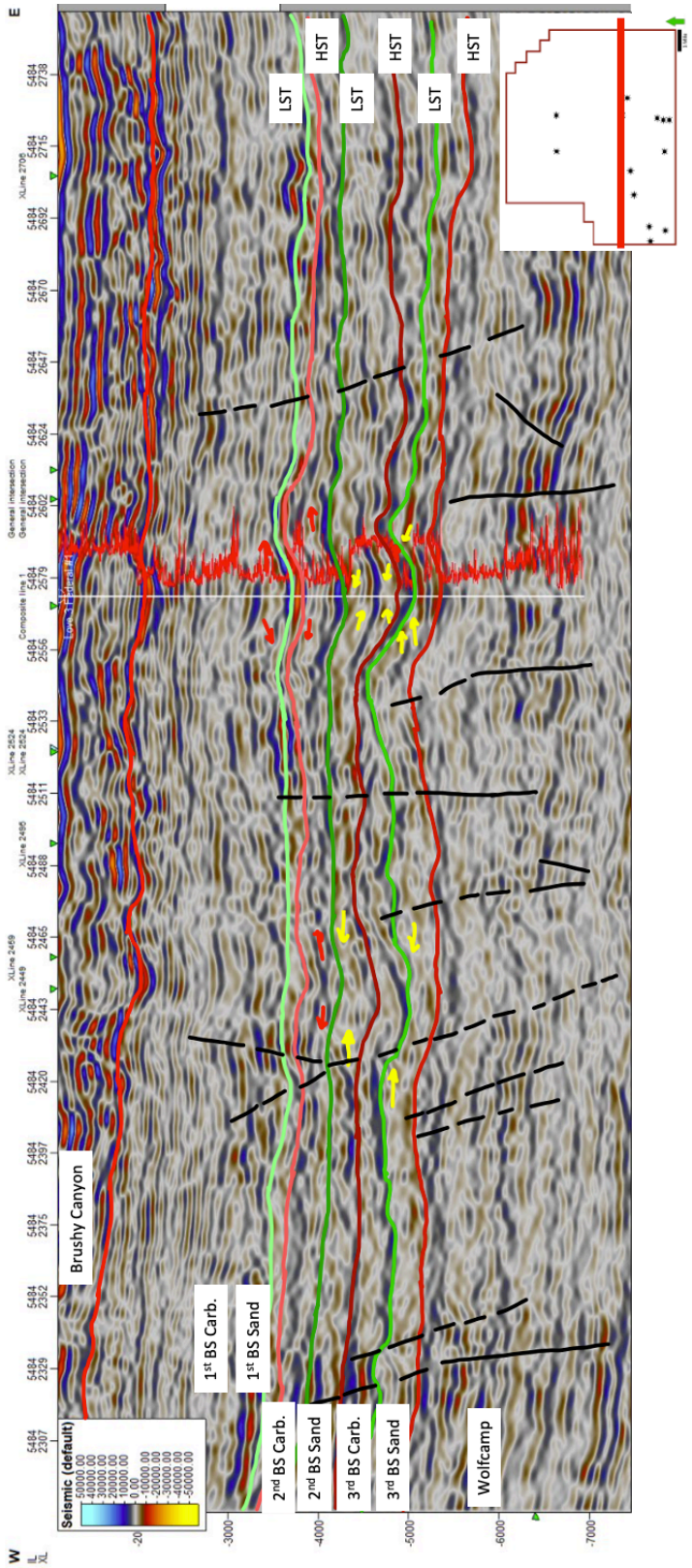

Figure 52: Seismic cross section in strike direction through Love Federal well, displaying formations, HST and LST systems tracts, terminations in yellow and red, and faults designated by dashed black lines.

Figure 53 and 54 both use the terminations and 4th order sequence to break out the seismic sequences through the whole area of study, which offers a visual display of the history of the Bone Spring deposition.

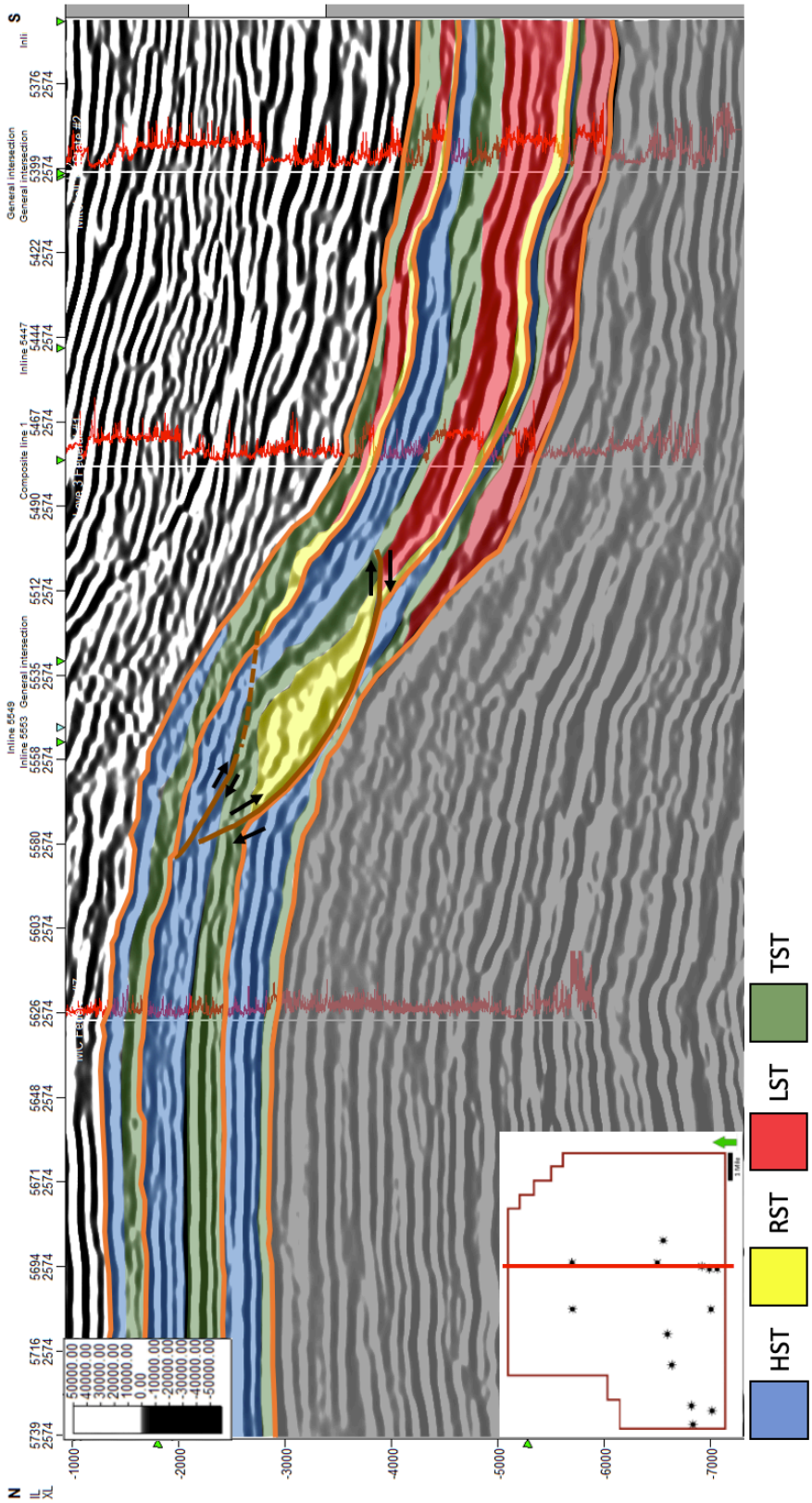

Figure 53: Seismic cross section 1 going through the Mitchell 2, Love and MC Federal wells and displaying seismic stratigraphic parasequence sets.

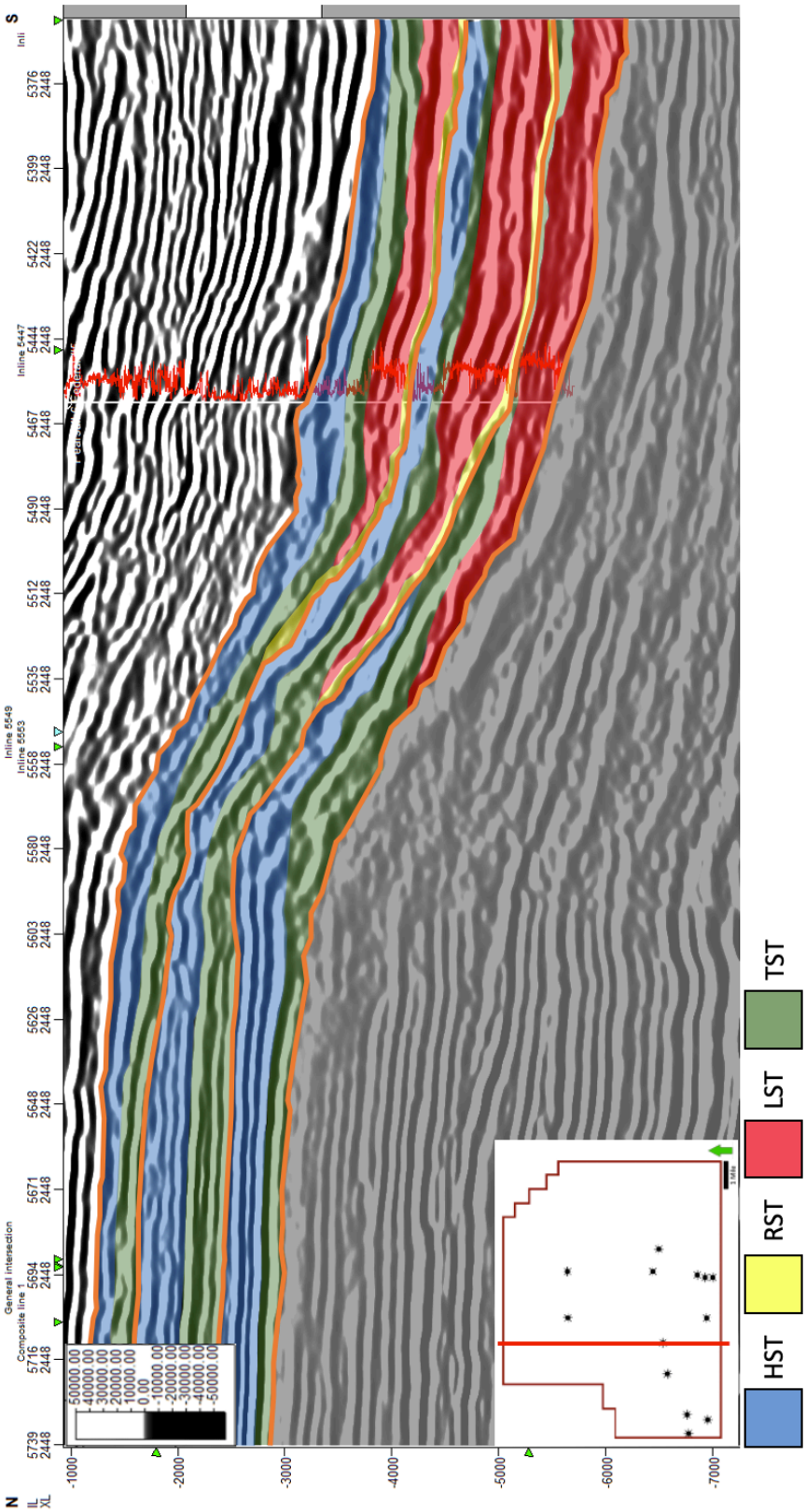

Figure 54: Seismic cross section 2 passing through the Pearsall and displaying the seismic the stratigraphic parasequence sets.

The adapted Galloway sequences were used to break out seismic horizon surfaces of sequence systems tracts through the deposition of the Bone Spring (Figure 55, 57, 59, and 61). Figure 56 displays a Highstand System Tract (HST) in the 3rd Bone Spring, Figure 58 a Lowstand Systems Tract (LST) in the 3rd Bone Spring, Figure 60 is a Transgressive Systems Tract (TST), and Figure 62 shows a Regressive Systems Tract (RST) or Falling Stage Systems Tract (FSST) in the 1st Bone Spring. The effects of massive channeling are present on all of these horizons, but are most clear on the LST, and RST surfaces. Figures 55, 57, 59, and 61 display a cross section of each sequence system tracts that were used to pick the corresponding horizons in Figures 56, 58, 60, and 62.

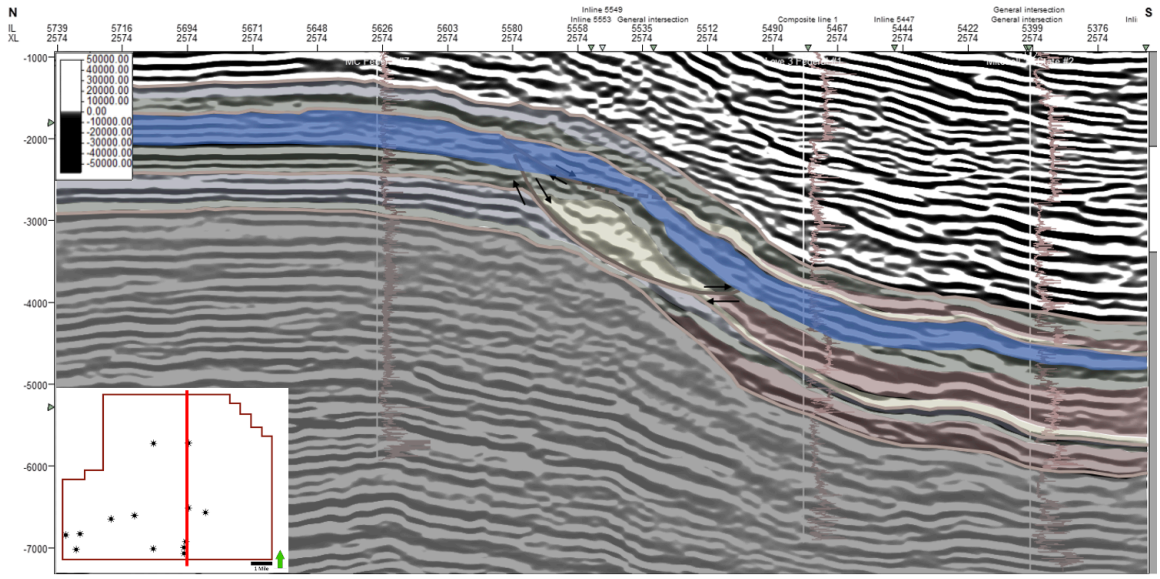

Figure 55: Seismic cross section of 3rd Bone Spring Carbonate Highstand Systems Tract (HST) highlighted in blue.

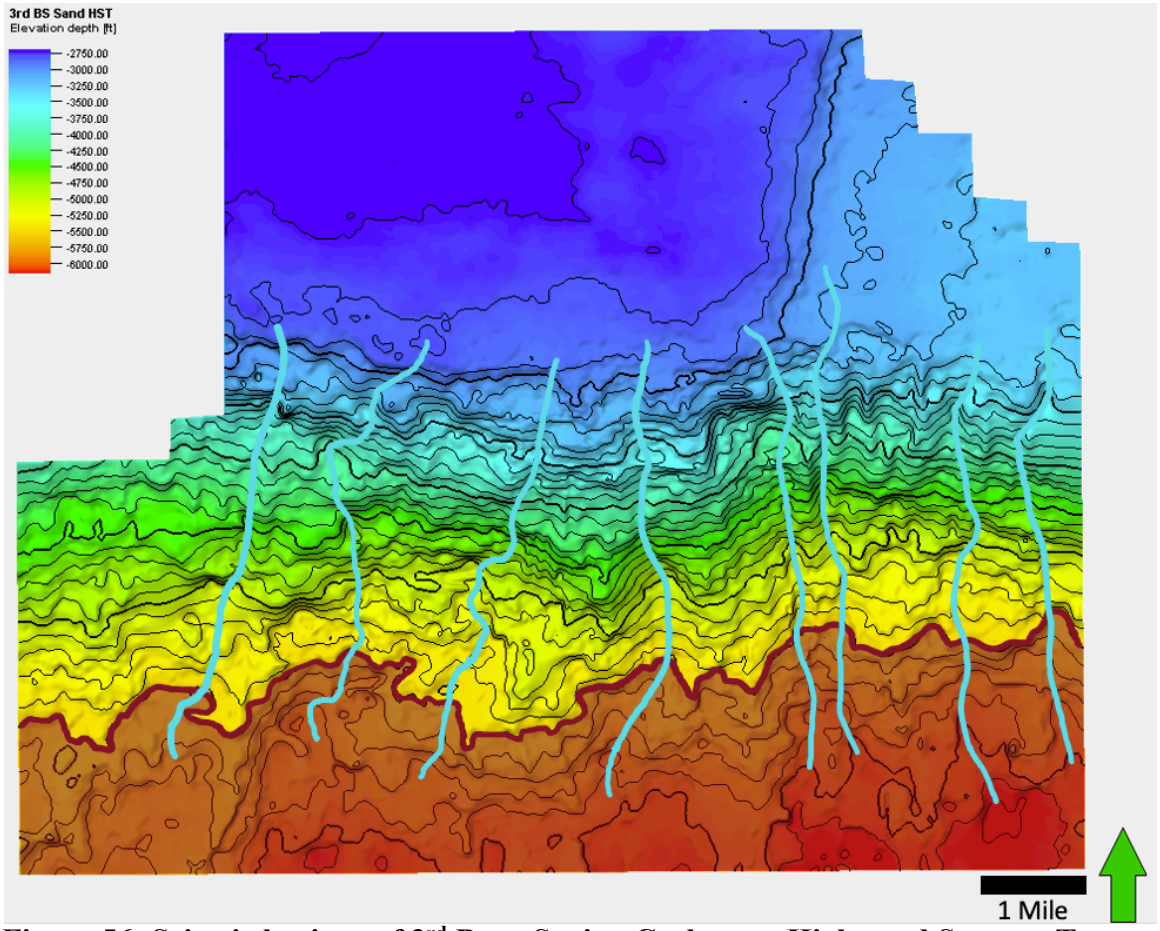

Figure 56: Seismic horizon of 3rd Bone Spring Carbonate Highstand Systems Tract (HST). The dark red area shows the carbonate apron fan deposit and the blue lines show interpreted channel paths.

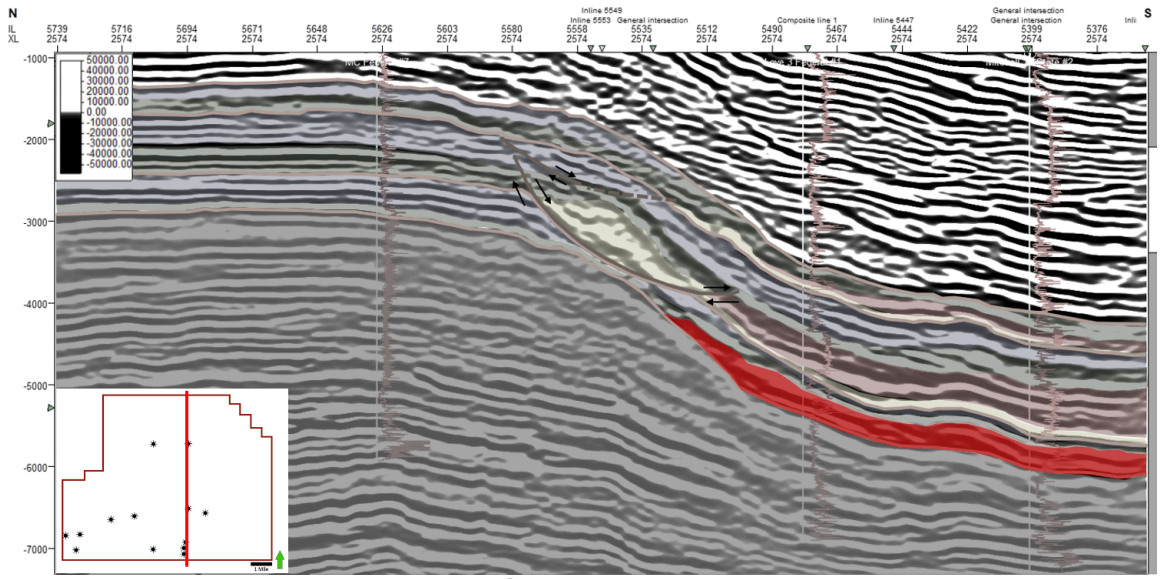

Figure 57: Seismic cross section of 3rd Bone Spring Sand Lowstand Systems Tract (LST) highlighted in red.

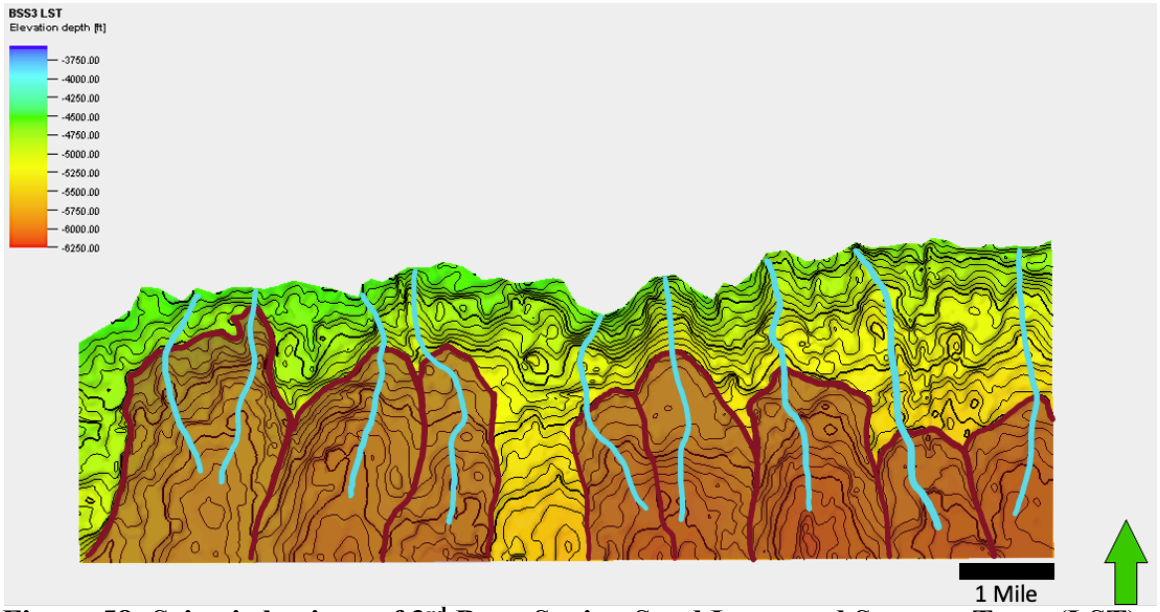

Figure 58: Seismic horizon of 3rd Bone Spring Sand Lowstand Systems Tract (LST). The dark red area shows the deposition of the sand fan deposits and the blue lines show interpreted channel paths.

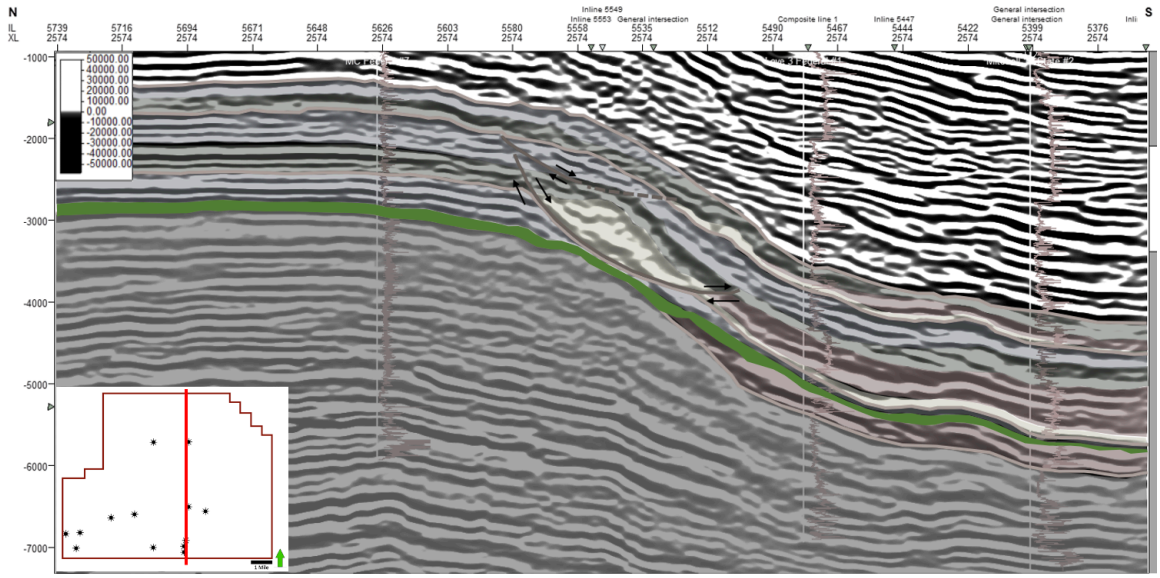

Figure 59: Seismic cross section of 3rd Bone Spring Carbonate Transgressive Systems Tract (TST) highlighted in green.

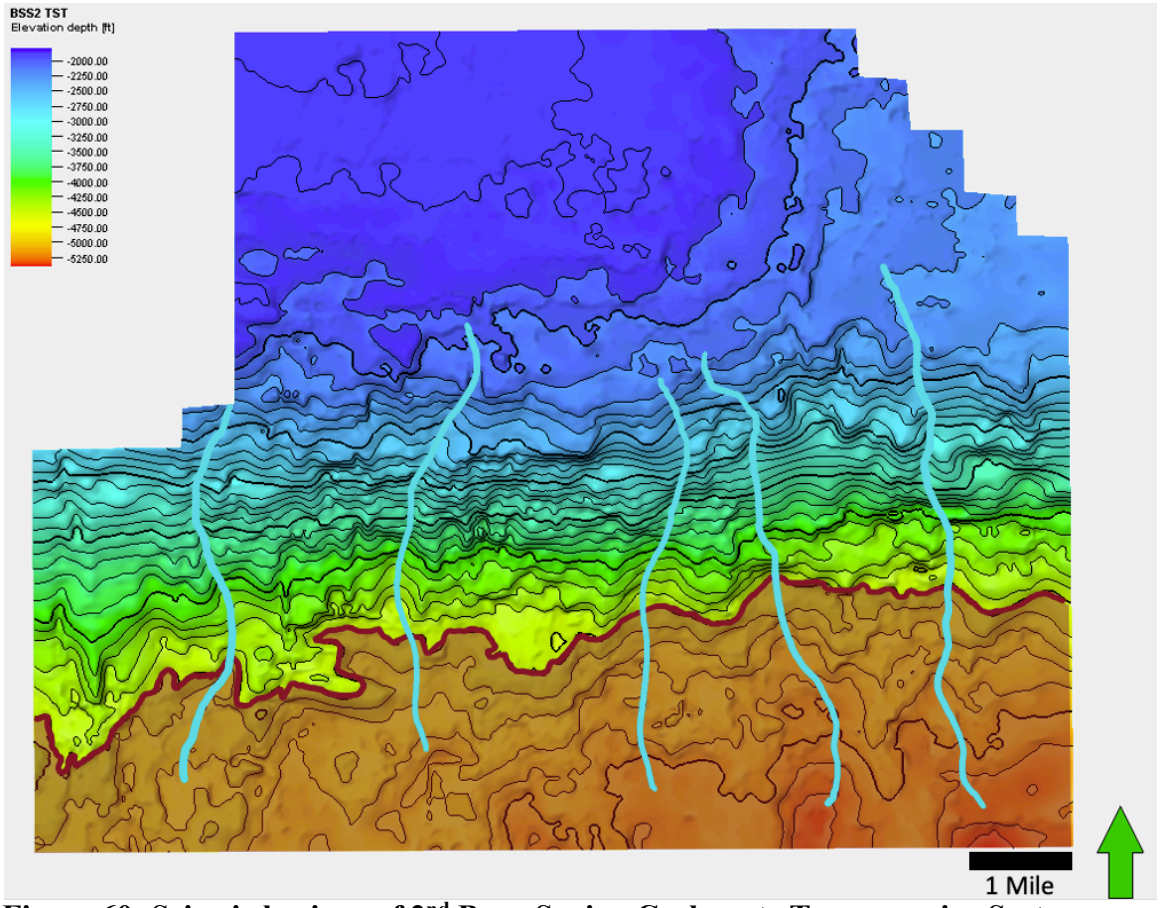

Figure 60: Seismic horizon of 2nd Bone Spring Carbonate Transgressive Systems Tract (TST). The dark red area shows the carbonate apron fan deposits and the blue lines show interpreted channel paths.

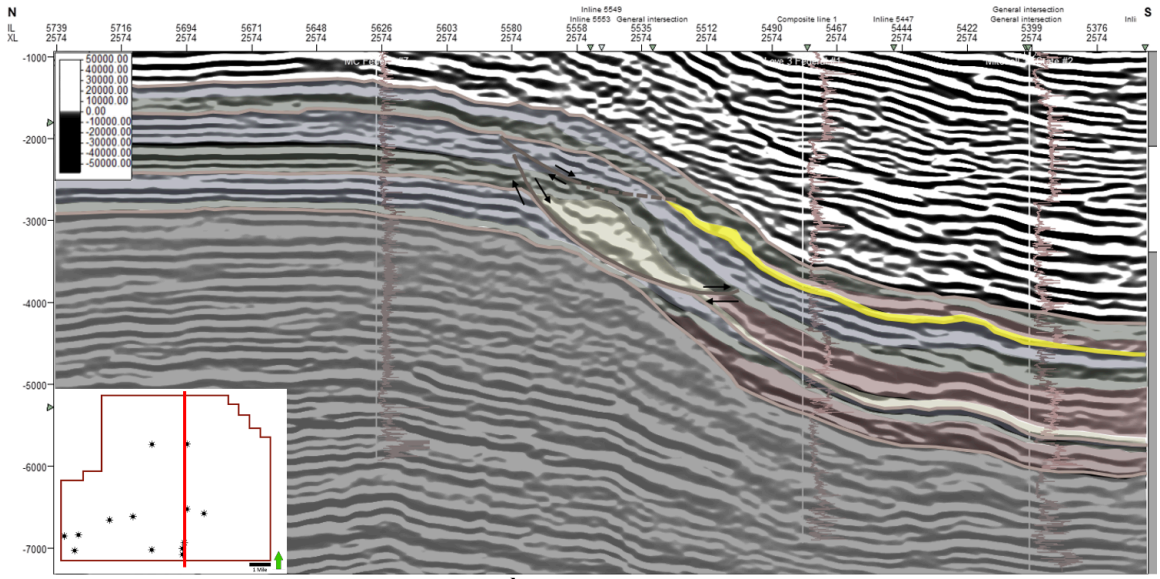

Figure 61: Seismic cross section of 2nd Bone Spring Sand Regressive Systems Tract (RST) highlighted in yellow.

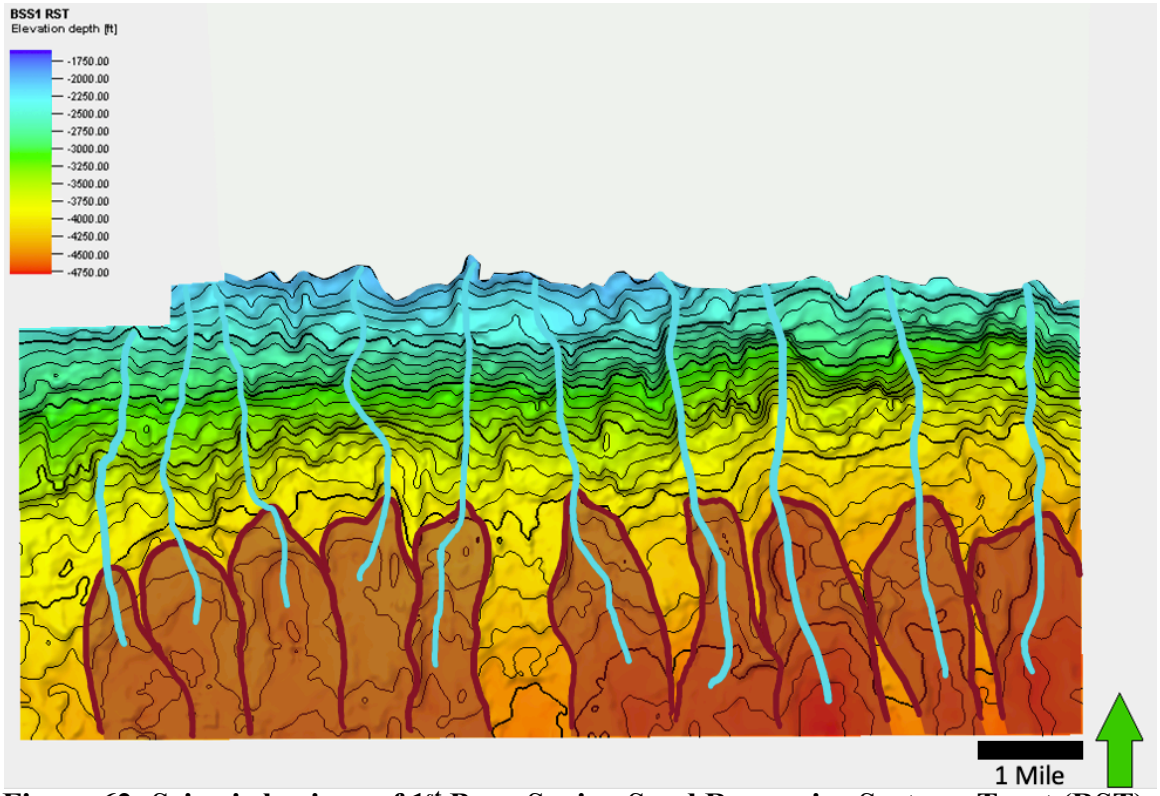

Figure 62: Seismic horizon of 1st Bone Spring Sand Regressive Systems Tract (RST) or Falling Stage Systems Tract (FSST). The dark red area represents sand fan deposits and the blue lines show interpreted channel paths.

The seismic horizons were measured to calculate the slopes of the different systems tracts. Figures 63-66 show the maximum slope angle of each of the systems tracts. The Transgressive Systems Tract (TST) shows the lowest angle slope with the maximum reaching only 19°. The Lowstand Systems Tract (LST) and the Highstand Systems Tract (HST) show a similar slope with the LST being 28° and the HST being 27°, however if the LST were to continue up the slope it is probable that it would show a higher angle than this. Predictably the Regressive Systems Tract (RST) shows the highest slope angle at 40°, which would explain why the slump failure occurred in the RST section.

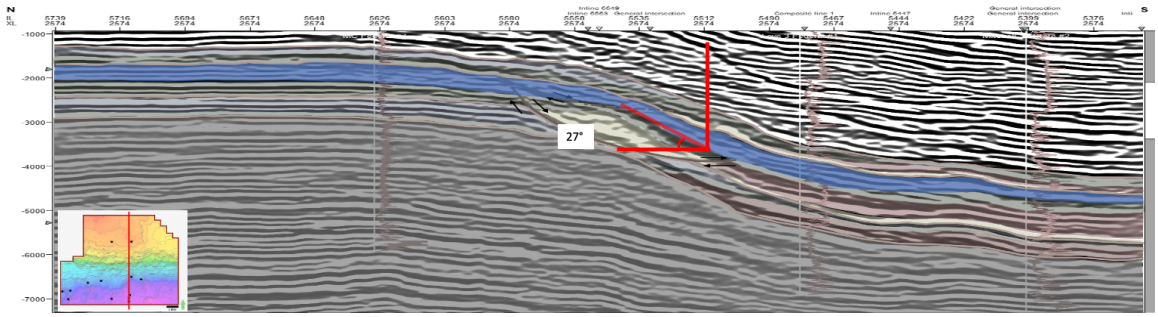

Figure 63: Seismic cross section of Highstand Systems Tract (HST) showing maximum slope angle of 27°.

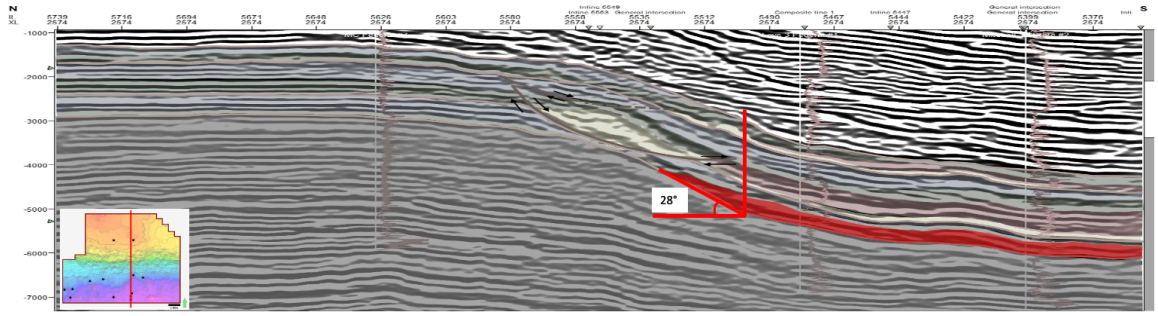

Figure 64: Seismic cross section of Lowstand Systems Tract (LST) showing maximum slope angle of 28°.

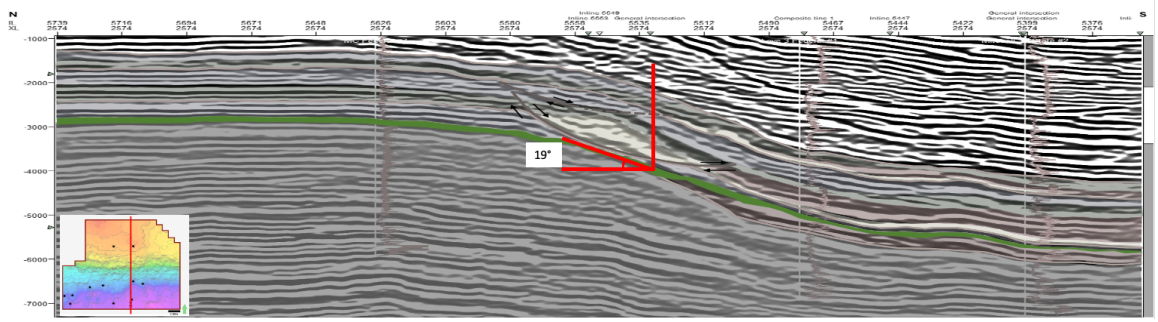

Figure 65: Seismic cross section of Transgressive Systems Tract (TST) showing maximum slope angle of 19°.

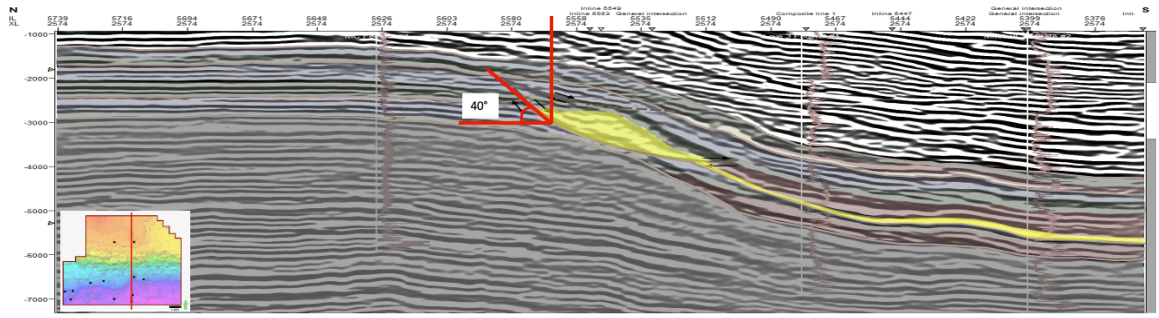

Figure 66: Seismic cross section of Regressive Systems Tract (RST) or Falling Stage Systems Tract (FSST) showing maximum slope angle of 40°. This high angle produces a slump to form at the top of the slope.

Discussion

The methods used throughout the seismic analysis give a clearer picture into the complexities of the Bone Spring Formation. Seismic analysis provides the ability to study a large area with the sacrifice of detail. Well logs however, show great detail, but are very localized and many times it is difficult to correlate across wells that are not close or in complex areas. Each of the methods used alone carry merit, but when used in conjunction the methods are able to fill in the gaps left by each alone. Figure 67 shows the Love 3 well with the Permian sea-level curve where LST's correspond to 3rd order sand intervals and HST's to carbonates. These correlations demonstrate that allocyclic controls influence 3rd order sequences. Therefore, the higher (4th order and higher) sequences observed in the well must be caused by autocyclic processes which correspond to changes in vertical and horizontal accommodation space, shelf progradation when the carbonate factory is active which fill reciprocally and compensationally the underlying LST channels with carbonates, and LST times of channel and love switching.

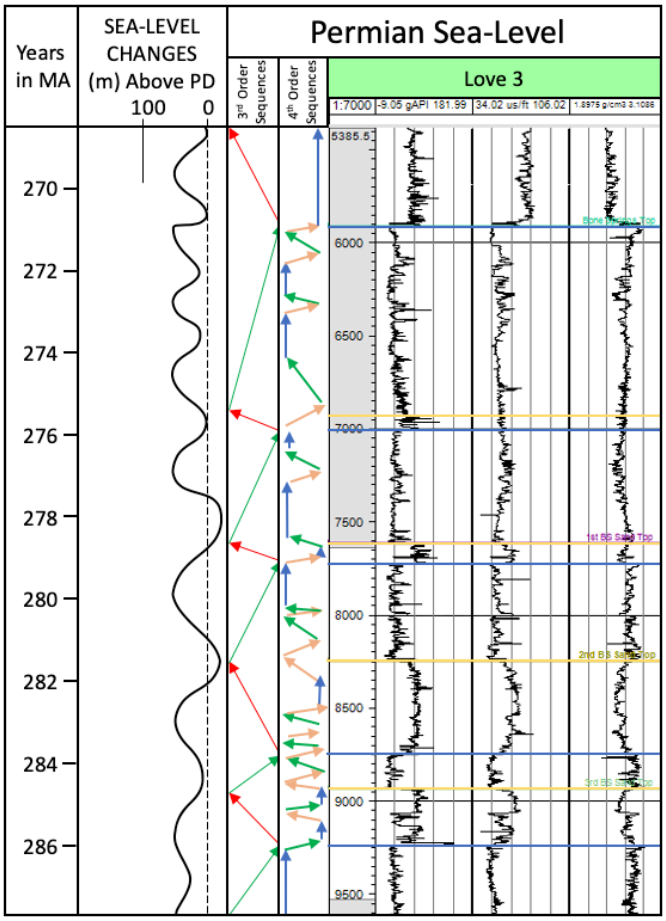

Figure 67: Love 3 well with 3rd and 4th order sequences correlated to global sea level curve for the Permian from Haq and Schutter (2008).

Figures 68 through 70 illustrate Bone Spring Sand interval isopach maps with overlayed channel paths from TWT structure maps. Erosion during sediment transport caused a reduction of thickness in some of the channels, but promising explorational areas are found where the channels and greater thicknesses correlate. These sections of overlap are likely deposits of clean sand channel fill and fans that would be high pay zones comprised of quartz rich sands and would be exceptionally frackable. Also, many of the thickest areas are adjacent to the channels and are presumably spill over that would also contain high pay zones.

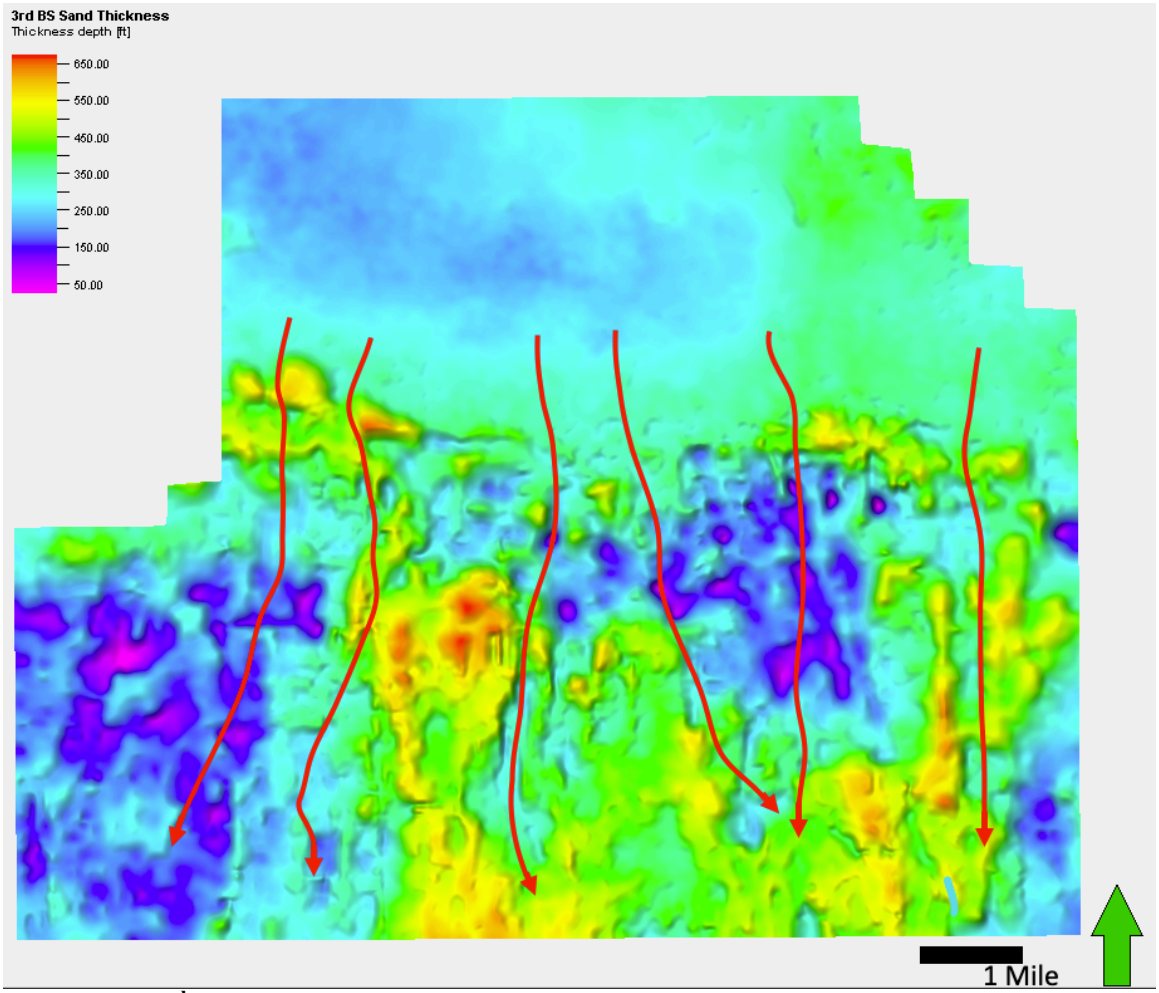

Figure 68: 3rd Bone Spring Sand isopach map with channel interpretations from TWT structure map of top of the 3rd Bone Spring Sand. Displays higher correlations of the channels and thicknesses in the Southeast area of the study.

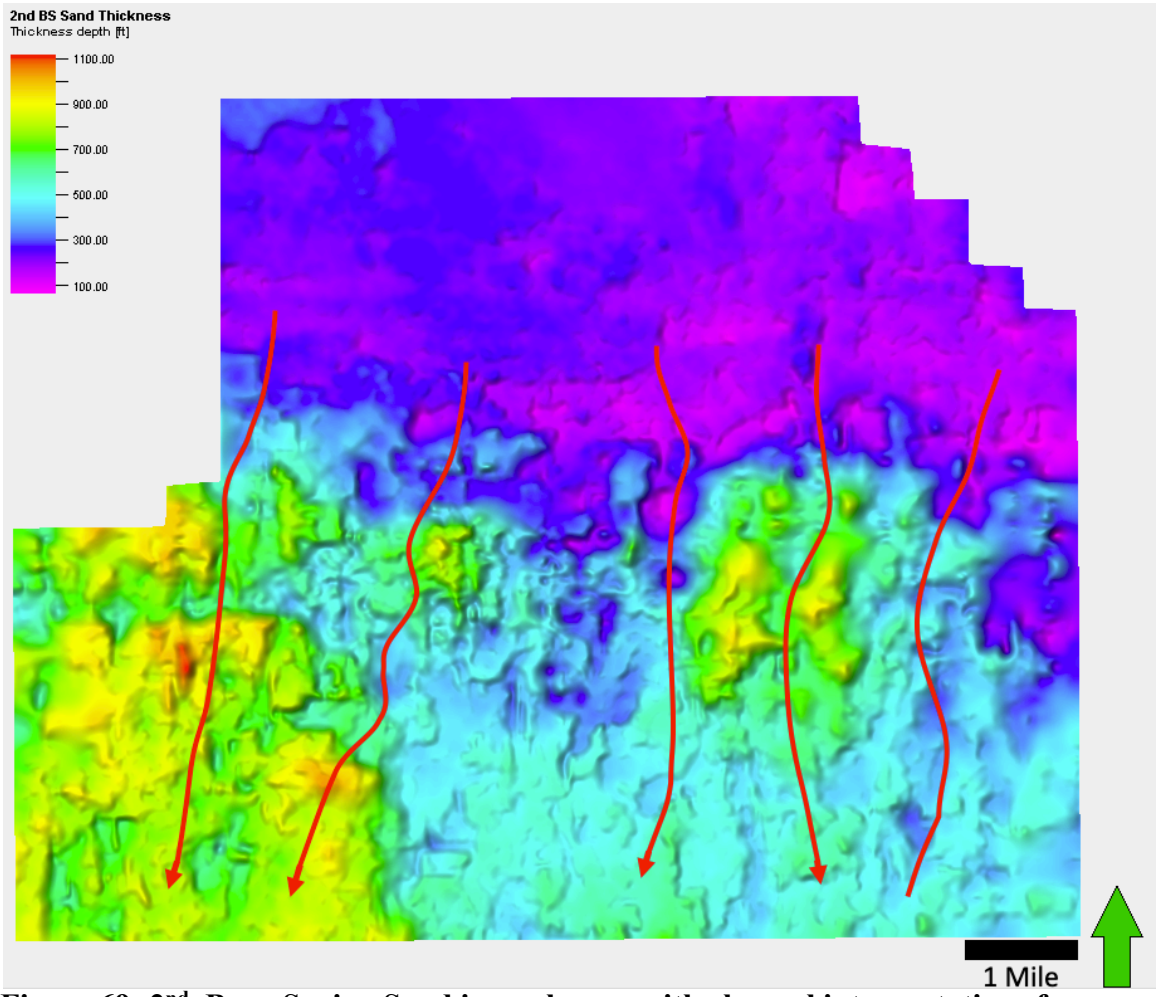

Figure 69: 2nd Bone Spring Sand isopach map with channel interpretations from TWT structure map of top of the 2nd Bone Spring Sand. Higher correlations of channel deposits and greater thicknesses are displayed in the Southwest area of the study.

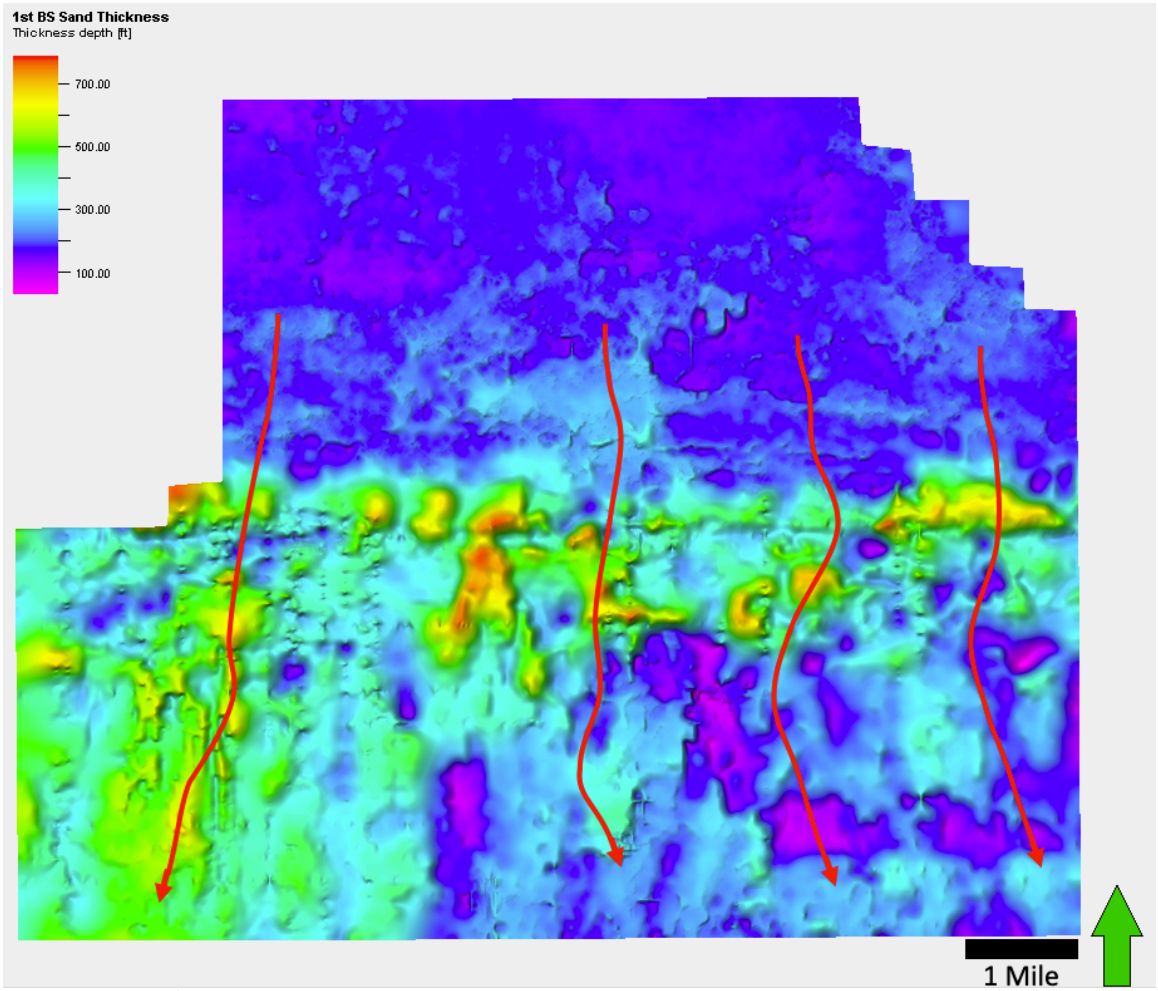

Figure 70: 1st Bone Spring Sand isopach map with channel interpretations from TWT structure map of top of the 1st Bone Spring Sand. Higher area of channel deposits and greater thicknesses are displayed in the Southwest area of the study.

For the all of the preceding seismic figures there is a theoretical and pragmatic importance for all of the interpretations. For example, each of the different parasequence sets affect:

- shelf slope
- number of channels,
- what is being transported down the channels (HST carbonates, RST sloughing, LST sands, TST shales for seals, and MTC owing to slope instability of the preceding parasequence sets)

However, there is a pragmatic meaning, for conventional production such as:

- faults acting as migration pathways from deeper organic shales of the Wolfcamp
- channels as charged higher porosity reservoirs which finger downdip into organic shales of the basin floor fans and are sealed at the shelf break as the TST pinches out
- shelf edge carbonates acting as potential updip reservoirs

As well as pragmatic meaning for unconventional production:

- channels containing the most quartz for fracking channels
- shales produced during LST times are most rich in organics (Crosby, 2015)

Future studies, particularly ones that have a greater number and dispersion of wells that meet the required specifications and in other areas could employ this method

for expanding a detailed analysis for the Leonardian Bone Spring Formation of the Delaware Basin.

Chapter 7: Conclusions

Conclusions

This study was a continuation of the previous work from Crosby (2015), Bickley (2019), and Frazier (2019). Crosby and Bickley both used high resolution sequence stratigraphy in different areas of the Bone Spring Formation to relate parasequence sets to inferred changes in sea level and construct a seismic stratigraphic model. Frazier focused on the same area seen in this study and used sequence stratigraphy to derive insights into relative sea level change. This study was able to continue their investigation of the Bone Spring Formation by using seismic sequence stratigraphy to examine the effects of channeling. Owing to the complexity of the Bone Spring Formation, study of this area will likely never be completely finished, but together these works begin to provide more holistic insight in the complicated depositional history of the Leonardian Bone Spring Formation.

The reciprocal sedimentation that produced the Bone Spring Formation caused an intricate stratigraphic history that requires methodology capable of fine scale analysis in order to understand. Through this study, an integration of both an adapted Galloway well log and a seismic sequence stratigraphy were useful tools that allowed for an in-depth investigation of the events that resulted in the formation of the Bone Spring.

Well log sequence stratigraphy provided a framework by first breaking the Bone Spring into five 3rd order sequences that indicate relatively large-scale sea-level changes. Approximately sixteen 4th order sequences were then selected using the Galloway motifs that allow for accurate representation of the clean carbonate intervals. The 3rd order

sequences were then integrated by synthetic well ties to the seismic, where they matched with reflectors indictive of the changes between carbonate and siliciclastic intervals. Structure and Isopach maps were then produced using well tops verified by well log sequences. Lastly the 4th order sequences from the well log analysis were then superimposed against the gamma ray logs in the seismic in order to pick out the seismic sequence stratigraphy. Using this approach allowed for the following.

- Applied sequence stratigraphy allows for five 3rd order sequences to be transferred to seismic and mapped to produce more similar well scale accuracy to seismic.
- In areas of reciprocal sedimentation 3rd order lowstand sequences to produce sand dominated intervals and highstands to produce carbonate dominated intervals, which these dissimilar intervals mark clear 3rd order boundaries in both well logs and seismic.
- Denoting smaller changes in the gamma ray profile result in sixteen 4th order sequences that are also correlative to seismic and give significance to seemingly irrelevant reflectors which greatly increases interpretation accuracy.
- The appreciated accuracy leads to more accurate structure, isochron, and seismic sequence stratigraphy, which could all produce significant economic advantages for exploration.
- Using this method of well log and seismic analysis to break out systems tracts across the study area, allows for the effects of channeling complexes to be clearly seen throughout the entirety of the Bone Spring Formation.

- Channel and fan mapping provide insight into areas that potentially contain large pay zones.

Taking advantage of the methods seen in this investigation allows for an understanding of the regional deposition of the Bone Spring. Using seismic sequence stratigraphy affords the ability to study the impact of sea-level change, reciprocal sedimentation, slope angles, slump failures, channeling and their relationships to changing systems tracts. Commingling channel mapping with formation thicknesses provides insight to areas that potentially contain large pay zones and are directly relevant to oil and gas exploration.

This study builds off of the substantial works of many great geologist and geophysicist to put many of their well-researched tools together to provide a more accurate depositional model to a complex area than any one of the tools alone. Because of the rich organic nature of this area, the economic impact of having a more extensive understanding in this area would be immense.

Recommendations for Future Work

With almost every large operator producing in the Permian Basin, there is naturally a lot of focused research, however there is far from a complete picture of each facet of the Bone Spring Formation. Some future work could focus towards:

- If access to more wells were available that were spread out through the study area, a more expansive investigation could be performed using a similar technique displaying in this study, more well control will on result in higher accuracy.

- Similarly, each independent interval warrants its own investigation and could be analyzed on a much finer scale.
- More advance geophysical analysis could also be done in the area, like deploying machine learning to predict and model facies between wells, or reservoir modeling utilizing the quality seismic.

Coda

Four questions in the problem definition were proposed, regarding interpreting the theoretical and pragmatic causes of the Bone Spring depositional process-response to changes in accommodation space. The answers to the posed questions are:

1. The three dimensional geometry reveals shelfs progradation during HST times and basin ward sediment gravity flows to have the gentlest slope as mainly carbonates are transported. In contrast, during LST times the shelf edge is steeper and incised channels transport sand from which are cutting through the exposed shelf. During RST times, Mass Transport Complexes dominate with shelf calving and TST times are recorded as backfilling.

2. The nature of the channeling, abandonment, and fill is one of reciprocal compensation. During TST and HST times, the inherited LST channels tend to heal with carbonate fill. On the other hand, during RST and LST times, channeling and downcutting up the slope predominates and active fan lobe switching occurs downdip.

3. The Mass Transport Complex observed appears to be an RST phenomenon which was likely due to oversteepening of the carbonate bank and sea level fell became unstable.

4. The exploration aspects of this study are profound. Conventionally, migration pathway filled channels would be excellent targets. Unconventionally, these same channels on the basin on the basin floor would have the greatest quartz content and frackability.

References

Adams, J.E., 1965, Stratigraphic-Tectonic Development of Delaware Basin: Bulletin of the American Association of Petroleum Geologists, v. 49.11, p. 2140-2148.

Bachmann, Joseph, Philip Stuart, Brian Corales, Blake Fernandez, Peter Kissel, Holly Stewart, David Amoss, Blaise Angelico, Alonso Guerra-Garcia, K. Blake Hancock, Richard Roberts, and Bill Sanchez, 2014, The "New" Horizontal Permian Basin. < *https://docplayer.net/15628065-The-new-horizontal-permian-basin.html*> Accessed June 21, 2019.

Brown, A. R., 2011, Interpretation of Three-Dimensional Seismic Data Seventh Edition: AAPG Memoir 42, p. 48.

Catuneanu, O., W.E. Galloway, C.G.St.C Kendall, A.D. Miall, H.W. Posamentier, A. Strasser, and M.E. Tucker, 2011, Sequence Stratigraphy: Methodology and Nomenclature: Newletters on Stratigraphy, v. 44/3, p. 173-245.

Catuneanu, O., V. Abreu, J.P. Bhattacharya, M.D. Blum, R.W. Dalrymple, P.G. Eriksson, C.R. Fielding, W.L. Fisher, W.E. Galloway, M.R. Gibling, K.A. Giles, J.M. Holbrook, R. Jordan, C.G.St.C. Kendall, B. Macurda, O.J. Martinsen, A.D. Miall, J.E. Neal, D. Nummedal, L. Pomar, H.W. Posamentier, B.R. Pratt, J.F. Sarg, K.W. Shanley, R.J. Steel, A. Strasser, M.E. Tucker, and C. Winker, 2009, Towards the Standardization of Sequence Stratigraphy: Earth-Science Reviews, v. 92.1-2, p. 1-33.

Crosby, Charles. B., 2015, Depositional History and High Resolution Sequence Stratigraphy of the Leonardian Bone Spring Formation, Northern Delaware Basin, Eddy and Lea Counties, New Mexico. University of Oklahoma Master's Thesis.

Crosby, Charles B., Pigott, John D., and Pigott, Kulwadee L., 2017, Bone Spring Formation High Resolution Sequence Stratigraphy, Northern Delaware Basin, Eddy and Lea Counties, New Mexico, AAPG Annual Convention & Exhibition, Houston, TX.

Frazier, Cyril S., High Resolution Integrated Vail-Galloway Sequence Stratigraphy of the Leonardian Bone Spring Fm., N. Delaware Basin, Southeast New Mexico. University of Oklahoma Master's Thesis.

Galloway, W., E., 1989, Genetic stratigraphic sequences in basin analysis; 1, Architecture and genesis of flooding-surface bounded depositional units, AAPG bulletin, 73,125-142.

Haq, B. U., and S. R. Schutter, 2008, A Chronology of Paleozoic Sea-Level Changes: Science, v. 322, p. 64-68.

Hardage, B. A., J. L. Simmons, V. M. Pendleton, B. A. Stubbs, and B. J. Uszynski, 1998, 3-D Seismic Imaging and Interpretation of Brushy Canyon Slope and Basin Thin-bed Teservoirs: Geophysics, v. 63.5, p. 1507.

Hart, B.S., 1997, New Targets in the Bone Spring Formation, Permian Basin: Oil & Gas Journal, p. 85-88.

Henderson, C. M., V. I. Davydov, B. R. Wardlaw, and O. M. Hammer, 2012, Chapter 24: The Permian Period, in F.M. Gradstein, ed., The Geologic Time Scale 2012: 1st ed. Oxford: Elsevier, 2012. P. 654-677.

Hill, C.A., 1996, Geology of the Delaware Basin, Guadalupe, Apache, and Glass Mountains, New Mexico and West Texas: Society for Sedimentary Geology, Albuquerque, New Mexico, v. 96-39.

Hills, J.M., 1984, Sedimentation, Tectonism, and Hydrocarbon Generation in Delaware Basin, West Texas and Southeastern New Mexico: AAPG Bulletin, v. 68.3, p. 250-267.

Huang, Yanqing, 2018, Sedimentary Characteristics of Turbidite Fan and its Implications for Hydrocarbon Exploration in Lower Congo Basin: Petroleum Research 3, p. 189-196.

Keller, G.R., J.M. Hills, and R. Djeddi, 1980, A Regional Geological and Geophysical Study of the Delaware Basin, New Mexico and West Texas: New Mexico Geological Society Guidebook, p. 105-111.

Kocurek, G. and B.L. Kirkland, 1998, Getting to the Source: Aaeolian Influx to the Permian Delaware Basin Region: Sedimentary Geology, v. 117.3-4, p. 143-149.

Li, Shunli, 2015, The Role of Sea Level Change in Deep Water Deposition Along a Carbonate Shelf Margin, Early and Middle Permian, Delaware Basin: Geologica Carpathica, p. 99-116.

May, Jeff, 2018, Well Log Sequence Stratigraphy: Applications to Exploration and Production. 2018. Unpublished Nautilus Lecture Notes

Mazzullo, S.J., 1995, Permian Stratigraphy and Facies, Permian Basin (Texas-New Mexico) and Adjoining Areas in the Midcontinent United States *in* P.A. Scholle, T.M. Peryt, and D.S. Ulmer-Scholle, eds., The Permian of Northern Pangea, Berlin: Springer-Verlag, v. 2, p. 41 58.

Mccullough, B.J., 2014, Sequence-Stratigraphic Framework and Characterization of the Woodford Shale on the Southern Cherokee Platform of Central Oklahoma: Master's thesis, University of Oklahoma, Norman, Oklahoma, 210 p.

Montgomery, S.L., 1998, The Permian Bone Spring Formation, Delaware Basin: Petroleum Frontiers, v. 14.3, p. 1-89.

Mullins, H.T., and H.E. Cook, 1986, Carbonate Apron Models: Alternatives to the Submarine Fan Model for Paleoenvironmental Analysis and Hydrocarbon Exploration: Sedimentary Geology, v. 48.1-2, p. 37-79.

Mutti, E., and Sonnino, M., 1981: Compensation cycles: A diagnostic feature of turbidite sandstone lobes; Abstracts Volume, 2nd European Regional Meeting of International Association of Sedimentologists, Bologna, Italy, p. 120-123.

Pigott, John D., 2019, GPHY 5613: Introduction to Seismic Stratigraphy. Spring 2019. Unpublished Lecture Notes.

Pigott, John D., 2017, GEOL 5363: Carbonate Geology. Fall 2017. Unpublished Lecture Notes.

Pigott, John D. and Bradley, Bryant W., 2014, Application of Production Decline Curve Analysis to Clastic Reservoir Facies Characterization within a Sequence Stratigraphic Framework: Example- Frio Formation, South Texas, GCAGS Journal, Vol 3, p. 112-133.

Pigott, John D., Yalcin, Esra, Pigott, Kulwadee L., and Michael Williams, 2015, 3D Delaware Basin Model: Insight into its Heterogeneous Petroleum System Evolution as a Guide to New Exploration, West Texas Geological Society Convention, Midland, Tx.

Plemons, Travis O., Pigott, John D., Brown, Andrew L., Pigott, Kulwadee, Pigott L., and Carpenter, Brett, 2019, Multidisciplinary Geomechanical Analysis of the Leonardian Bone Spring Outcrop, Bone Canyon, Texas: West Texas Geological Society Fall

Radivojevic, Dejan and John D. Pigott, 2010, Seismic Stratigraphic Based Chronostratigraphy (SSBC) of the Serbian Banat Region of the Basin (Pannonian Basin), Central European Journal of Geosciences, 2(4), p 481-500.

Ross, C.A. and J.R.P. Ross, 1995, Permian Sequence Stratigraphy in P.A. Scholle, T.M. Peryt, and D.S. Ulmer-Scholle, eds., The Permian of Northern Pangea: Berlin: Springer-Verlag, v. 1, p. 98-113.

Ruppel, Stephen C., and W. Bruce Ward, 2013, Outcrop-based Characterization of the Leonardian Carbonate Platform in West Texas: Implications for Sequence-stratigraphic Styles in the Lower Permian: AAPG Bulletin, v. 97.2, p. 223-250. Symposium, Midland, Texas.

Saller, A.H., J.W. Barton, and R.E. Barton, 1989, Slope Sedimentation Associated with a Vertically Building Shelf, Bone Spring Formation, Mescalero Escarpe Field, Southeastern New Mexico: SEPM Special Publication, v. 44, p. 275-288.

Silver, B.A. and R.G. Todd, 1969, Permian Cyclic Strata, Northern Midland and Delaware Basins, West Texas and Southeastern New Mexico: AAPG Bulletin, v. 53.11, p. 2223-2251.

Shumaker, R.C., 1992, Paleozoic Structure of the Central Basin Uplift and Adjacent Delaware Basin, West Texas: AAPG Bulletin, v. 76.11, p. 1804-1824.

Slatt, R.M., 2013 GEOL 5970: Reservoir Characterization I. Fall 2016. Unpublished Lecture Notes.

Slatt, R. M., 2006, Stratigraphic Reservoir Characterization for Petroleum Geologists, Geophysicists, and Engineers, v. 10, Elsevier.

Sloss, L.L., 1963, Sequences in the Cratonic Interior of North America: Geological Society of America Bulletin, v. 74.2, p. 93-113.

Sloss, L.L., 1988, Chapter 3: Tectonic Evolution of the Craton in Phaerozoic Time, in L.L. Sloss, ed., Sedimentary Cover – North American Craton: U.S.: The Geology of North America: The Geological Society of America, p. 25-41.

Stevenson, Christopher J., Jackson, Christopher A.-L., Hodgson, Davis M., Hubbard, Stephen M., Eggenhuisen, Joris T., 2015, Deep-Water Sediment Bypass: Journal of Sedimentary Research, v. 85, p. 1058-1081.

Straub, K. M., Paola, C., Mohrig, D., Wolinsky, M. A., & George, T., 2009, Compensational Stacking of Channelized Sedimentary Deposits: Journal of Sedimentary Research, 79(10), p. 673-688. https://doi.org/10.2110/jsr.2009.070

USGS, 2018, USGS Announces Larges Continuous Oil Assessment in Texas and New Mexico: <https://www.usgs.gov/news/usgs-announces-largest-continuous-oil-assessment-texas-and-new-mexico> Accessed June 21, 2019.

Vail, P. R., 1987, Seismic Stratigraphy Interpretation Using Sequence Stratigraphy: AAPG Studies in Geology 27, volume 1:Atlas of Seismic Stratigraphy.

Vail, P. R., and Posamentier, H. W., 1988 Eustatic Controls on Clastic Deposition II – Sequence and System Tract Models: Sea-Level Changes, p. 125-154.

Veevers, J. J., and C.M. Powell, 1987, Late Paleozoic Glacial Episodes in Gondwanaland Reflected in Transgressive-regressive Depositional Sequences in Euramerica: Geological Society of America Bulletin, v. 98.4, p. 475-487.

Williams, Michael T., John D. Pigott, and Kulwadee L. Pigott, 2014, Delaware Basin Evolution: Preliminary Integrated 1D,2D, And 3D Basin Model for Petroleum System Analysis, 2014, AAPG Annual Convention & Exhibition, Houston, Tx.

Wilson J. L., 1967, Cyclic and Reciprocal Sedimentation in Virgilian Strata of Southern New Mexico: Geological Society of American Bulletin, v. 78 (7), p. 805-818.

Xu, Chenxi, Zhuobo Wang, Pigott, John D., Pigott, Kulwadee L., Frazier, Cyril S, and Zhou, Yuqi, 2018, Lidar-Xrf constrained seismic model of McKittrick Canyon Shelf Edge Outcrop: Insight into Subsurface Capitanian Shelf Edge Sequence Stratigraphy and Paleo Oceanic Environments, West Texas Geological Society Fall Symposium, Midland, Texas.

Yang, K.M. and S.L. Dorobek, 1995, The Permian Basin of West Texas and New Mexico: Tectonic History of a “Composite” Foreland Basin and Its Effects on Stratigraphic Development: SEPM Special Publication, v. 52, p. 149-174

Zhou, Y., 2014, High Resolution Spectral Gamma Ray Sequence Stratigraphy of Shelf Edge to Basin Floor Upper Capitan Permian Carbonates, Guadalupe Mountains, Texas and Delaware Basin, New Mexico: Master’s thesis, University of Oklahoma, Norman, Oklahoma, 131 p.